THESIS

A COMPARISON OF THE DEMOGRAPHY, BODY CONDITION AND RESOURCE USE OF EMPEROR GEESE (*ANSER CANAGICUS*) AT THE GEOGRAPHIC EXTREMES OF THEIR WINTERING RANGE

Submitted by

Robyn M. Thomas

Department of Fish, Wildlife, and Conservation Biology

In partial fulfillment of the requirements

For the Degree of Master of Science

Colorado State University

Fort Collins, Colorado

Summer 2026

Master's Committee:

Advisor: Lise M. Aubry

William L. Kendall
Cory T. Williams
Tyler L. Lewis

ABSTRACT

A COMPARISON OF THE DEMOGRAPHY, BODY CONDITION AND RESOURCE USE OF EMPEROR GEESE (*ANSER CANAGICUS*) AT THE GEOGRAPHIC EXTREMES OF THEIR WINTERING RANGE

Emperor geese (*Anser canagicus*) are a Bering Sea endemic species that have experienced long-term population declines and a recent harvest closure, prompting interest in the factors influencing their population dynamics. Understanding how environmental variation across the annual cycle affects demographic performance is therefore important for effective management. Emperor geese spend a large portion of their year on their winter grounds where they occupy geographically distinct regions that differ substantially in environmental conditions, yet the consequences of this spatial variation for survival, recruitment, and individual performance remain poorly understood. To address this, I evaluated variation in survival and productivity across two locations at the geographic extremes of the species' winter range (Shemya Island in the western Aleutians and Women's Bay in the Kodiak Archipelago) and examined differences in resource use and body condition among these same populations. From 2024 to 2026, I estimated age ratios as a proxy to productivity, and from 2020 to 2026, I used mark–resight data to estimate annual apparent survival. I also assessed the influence of regional climate conditions using the Aleutian Low–Beaufort Sea Anticyclone (ALBSA) index. I then used stable isotope analysis and morphometric data to quantify diet, isotopic niche structure, and body condition at each winter location during the winters of 2024 and 2025.

Apparent survival and juvenile-to-adult ratios were consistently lower on Shemya than on Kodiak, with juveniles exhibiting reduced survival relative to adults, particularly on Shemya. Survival at both sites was related to seasonal climatic conditions, although the seasonal drivers differed between regions. Patterns of resource use and body condition also varied across wintering areas, with birds on Kodiak exhibiting a diet enriched in $\delta^{13}C$ and $\delta^{15}N$ signaling more marine based and protein rich resources and generally had higher body condition, while birds on Shemya appeared to rely on lower quality resources and exhibited lower body condition. Isotopic niche width differed between sites and years, with limited overlap between populations. These findings indicate that wintering location is an important source of variation in survival, recruitment, and individual performance in emperor geese. Spatial heterogeneity in winter environments may therefore influence population dynamics not only through movement and shifting distribution, but also through differences in demographic contribution among wintering regions. This work highlights the importance of winter ecology in shaping population processes and provides insight relevant to emperor geese management decisions.

ACKNOWLEDGEMENTS

I would like to sincerely thank my advisor, Dr. Lise Aubry, for her guidance, support, and mentorship throughout this project. Her encouragement and thoughtful feedback were instrumental in shaping this work and in my development as a researcher. I am also deeply grateful to Dr. Tyler Lewis for his collaboration and mentorship and for trusting me to take this project on. I have really enjoyed working with and learning from him over the past three years. Because of Lise and Tyler, I was able to pursue this research and develop a thesis that I am excited about and proud of. I would also like to thank my committee members, Dr. Cory Williams and Dr. Bill Kendall, for their valuable feedback and support throughout my graduate program. I am also grateful to Kim Samsel, Melinda Neiblum, and Dr. Jennifer Boyd for their support at CSU, as well as the Fish, Wildlife, and Conservation graduate student body. I would like to thank the Aubry and Koons labs for fostering a collaborative and supportive research environment, including Dr. Dave Koons, Jordan Thompson, Mairin Murphy, James Golden, Galen Burrell, and Alex Badeaux. I would also like to thank my fellow graduate students Sam Radosevich, Nöel Clark, Lisa Roerk, and Travis Rainey for their support and friendship during my time at CSU.

I thank the Alaska Department of Fish and Game for funding my graduate work, and Colorado State University for additional support. I was humbled to receive the Dennis Raveling Scholarship, the Douglas L. Gilbert Memorial Scholarship, the North American Wetlands and Migratory Waterbird Fellowship, the North American Arctic Goose Conference travel award and Best Master's Oral Presentation Award, the Thomas Posey Travel Award, and the Van Riper

travel award. I am grateful to the organizations and donors who made this work possible and supported my research during my masters.

This work would also not have been possible without strong partnerships and inter-organizational collaborations. I would like to thank the U.S. Fish and Wildlife Service Migratory Bird Program, Kodiak National Wildlife Refuge, the Alaska Department of Fish and Game on Kodiak, the U.S. Coast Guard Base on Kodiak, and Eareckson Air Station for providing logistical support, field access, and housing for our crews. I would also like to thank Daniel Smith with the Sun'aq tribe of Kodiak, Brian Uher-Koch at USGS Alaska Science center, and Zak Pohlen at USFWS Migratory Birds program for contributing data to this project.

I am incredibly grateful to the dozens of field technicians and volunteers who contributed to this project over the past 6 years. I would especially like to thank Zak Pohlen, Tasha DiMarzio for their dedication collecting data for this project since 2020. On Kodiak, I thank Denise and James Link, and their kids Sammy, Wesley, and Chloe for their extraordinary support, including boat access, re-sighting efforts, net-drying space, and countless acts of generosity that made fieldwork on Kodiak possible. On Shemya, I thank Brodie Hicks and Jen Cooper for their enthusiasm and for providing valuable re-sight data.

Lastly, I would like to thank my friends and family in both Alaska and Colorado for their support while I balanced time between these two places during graduate school. I am especially grateful to my partner, Lalo, and to my parents for their constant encouragement and support throughout this journey. Having the opportunity to return to Colorado during this project and spend more time with my family made this experience especially meaningful.

DEDICATION

This thesis is dedicated to Shiloh Schulte, a dear friend and an incredible ornithologist that we lost too soon. He helped instill in me a love for birds and science during a formative time in my life. I will always be grateful to him for the joy he brought to fieldwork and the impact he had on everyone he met.

TABLE OF CONTENTS

ABSTRACT……..……...……..…….. ii
ACKNOWLEDGEMENTS…....…….……..…...iv
DEDICATION ……..…….……..…vi

CHAPTER 1: A COMPARISON OF EMPEROR GOOSE DEMOGRAPHY AT THE GEOGRAPHIC EXTREMES OF THEIR WINTERING RANGE……...……1
Introduction……1
Methods ……..…….5
Study Area ….……5
Sampling and Data Acquisition ……..…….……...6
Statistical Analysis…..……..8
Results ……..11
Age Ratios…….…….……11
Survival Analysis…...…….…….……11
Regional climate effects on apparent survival……...……13
Discussion …...…….15
Management Implications…....……23
Tables and Figures…..…..…...……...……..24
References ……..…...……47

CHAPTER 2: DIET, RESOURCE USE AND BODY CONDITION OF EMPEROR GEESE AT THE GEOGRAPHIC EXTREMES OF THEIR WINTER RANGE…….……53
Introduction ….…..……..……..53
Methods ……..……...……56
Study Area ……56
Sampling ……..…….…58
Statistical Analysis...……..…60
Results ...…..……..……64
Tissue differences and baseline correction……..……..64
Isotopic Niche Width and Overlap...……...…….…..65
Stable Isotope Mixing Model……..…….…...66
Body Condition...…..…….……..…….…….67
Discussion ……..…….…….……68
Figures and Tables …...…….……76
References ……..…….…….……90

CONCLUSION …...…….……..…….96
APPENDIX…...…….……..…….....98
Chapter 1 Supplementary Materials ….…..…..……98
Chapter 2 Supplementary Materials ….…....……105

CHAPTER 1: A COMPARISON OF EMPEROR GOOSE DEMOGRAPHY AT THE GEOGRAPHIC EXTREMES OF THEIR WINTERING RANGE

Introduction

Demographic rates, particularly adult survival, reflect the cumulative influence of environmental conditions and anthropogenic pressures acting across the annual cycle, and can therefore provide key insight into constraints on population growth (Lebreton et al., 1992). In long-lived species, population growth is typically most sensitive to adult survival, especially that of females (Heppell et al., 2000; Sæther & Bakke, 2000). Even small changes in adult survival can substantially alter population growth trajectories, particularly when recruitment is variable (Koons et al., 2014; Schmutz et al., 1997). For migratory birds, such as waterfowl, estimating survival is especially challenging because individuals occupy several geographically distinct habitats throughout their annual life cycle, where conditions encountered during migration or on wintering grounds can carry over to influence individual performance and population dynamics in the breeding season, and across subsequent seasons (Newton, 2004; Norris & Taylor, 2006; Rushing et al., 2017). Understanding how such spatial and environmental variability influences survival and other key demographic factors is therefore important for predicting population responses across the complete annual life cycle of migratory species.

Throughout the annual cycle, winter often presents the most challenging conditions and thus tends to have an outsized influence on survival (Sherry & Holmes, 1995). This is especially valid for waterfowl species wintering at northern latitudes, where challenging winter conditions may directly influence survival both directly through increased thermoregulatory costs (Root, 1988) and indirectly by restricting access to forage because of ice cover (Brêthes et al., 1994;

Ewanchuk & Bertness, 2003) and storm-driven disturbances (Carrington, 2002). Consequently, spatial heterogeneity in winter climate may generate geographic variation in survival within a species' wintering range.

The Emperor Goose (*Anser canagicus*) provides a compelling system to evaluate these dynamics. Endemic to the Bering Sea region, Emperor Geese breed primarily along coastal areas of western Alaska, with the largest concentration on the Yukon–Kuskokwim 'YK' Delta and smaller numbers breeding on the Seward Peninsula and in eastern Russia (Lewis et al., 2021; Schmutz, 1995; Schmutz et al., 2020; *Fig. 1.1*). Unlike most Arctic and sub–arctic nesting geese that migrate across continents for the winter and utilize agricultural subsidies (Pearce et al., 2022), Emperor Geese remain within the Bering Sea region year-round, wintering in coastal habitats spread along the Aleutian Islands, Alaska Peninsula, and Kodiak Archipelago (Eisenhauer & Kirkpatrick, 1977; Hupp et al., 2008b) where they rely heavily on intertidal marine resources.

Wintering regions of Emperor Geese differ substantially in migration distance, habitat structure, and environmental exposure (Eisenhauer & Kirkpatrick, 1977; Uher-Koch et al., 2021). Satellite telemetry data demonstrate substantial variation in Emperor Goose migration distance among wintering regions, with individuals wintering in the western Aleutian Islands traveling >2,500 km from breeding areas, compared to <1,000 km for birds wintering along the Alaska Peninsula and Kodiak Archipelago (Hupp et al., 2008b). These differences in migration strategies may influence energetic expenditure and survival chances of Emperor Geese, particularly because their wintering areas differ in regional storm exposure and oceanographic conditions, with westerly wintering populations generally more exposed to extreme storm events (Mesquita et al., 2010; Smith et al., 2019). In marine waterfowl, climate variability at different

wintering sites has been linked to substantial interannual variation in adult survival, with large-scale climate indices influencing overwinter energetics and demographic rates. For example, in Common Eider (*Somateria mollissima*), a circumpolar sea duck that spends summer and winter at high latitudes, changes in winter climatic conditions were shown to affect the survival of females, a pattern that was consistent across three geographically distinct populations in Canada, Svalbard, and mainland Norway (Guéry et al., 2017). For Emperor Geese, because their wintering regions span > 2000 km and differ widely in environmental conditions, over-winter survival may vary among wintering locations; however, survival estimates for this species have been limited to breeding areas and have never been estimated both within or across distinct wintering regions.

Emperor Geese are culturally and economically important in Alaska, making their population status a primary management concern (Alaska Department of Fish and Game, 2017; Naves et al., 2025). Their abundance declined from approximately 139,000 birds in 1964 to fewer than 42,000 by the mid-1980s (Fischer et al., 2018; Gill & Petersen, 1982; USFWS, 1989). prompting fall–winter harvest closures in 1986 and spring–summer subsistence closures in 1987 (Pacific Flyway Council, 2016). Although harvest reopened in 2017 after partial recovery of the population (Alaska Migratory Bird Co-Management Council, 2016), continued declines over the last several years have once again prompted the complete closure of both the sport and subsistence harvests as of 2025 (Frost et al., 2024a; USFWS, 2025).

Despite the cultural and economic importance of this species, contemporary survival estimates are still lacking. Because harvest regulations and population objectives are informed by demographic models, uncertainty in survival estimates limits the ability of waterfowl managers to evaluate harvest sustainability and anticipate population responses to environmental change

(Pacific Flyway Council, 2016). Previous estimates were derived between 1982–2004 and were largely restricted to adult females marked on the breeding grounds (Hupp et al., 2008a; Petersen, 1992; Schmutz et al., 1994). Obtaining updated survival estimates across sex, age class (i.e. with juveniles more vulnerable than adults), and wintering location has been identified as a conservation priority for the species (Mengak et al., 2022).

In this study, we compare two wintering regions that represent the geographic extremes of the Emperor Goose winter range and differ markedly in migration distance and winter environment. Shemya Island, in the western Aleutian Islands, is characterized by frequent winter storms, persistent high winds, and an exposed coastline where geese experience some of the most severe marine conditions within the species' range. In contrast, Kodiak Island, in the Gulf of Alaska, provides more sheltered bays and estuaries and is substantially closer to the primary breeding grounds on the Yukon–Kuskokwim Delta, resulting in shorter migration distances. These differences in environmental exposure and migration strategy provide a natural framework for evaluating how winter conditions influence annual productivity and survival (*Fig. 1.2*).

To determine whether demographic constraints differ between these contrasting winter environments, we estimated annual productivity and apparent survival of Emperor Geese wintering at Shemya and Kodiak. We used winter age ratios to index annual productivity because the proportion of juveniles observed during winter reflects variation in parental reproductive output and juvenile survival from hatch through winter migration (Hanson, 1963). Using leg-band resighting data collected between 2021 and 2026, we fit Cormack–Jolly–Seber models that account for imperfect detection (Lebreton et al., 1992) to estimate age-, sex-, and location-specific apparent survival from winter to winter for adults and from 6 to 18 months of

age for juveniles. We also evaluated whether apparent survival varied with location-specific and regional climatic indices for Emperor Geese wintering on Shemya and Kodiak.

We predict that (i) apparent survival and juvenile to adult ratios would be lower at Shemya than at Kodiak due to increased energetic costs associated with a longer winter migration and more frequent exposure to severe weather; (ii) juvenile survival would exhibit greater inter-annual variability and be lower than adult survival given their vulnerability to environmental heterogeneity; and (iii) frequent inclement weather, as summarized by the Aleutian Low - Beaufort Sea Anticyclone, 'ALBSA' index, would negatively impact annual productivity and survival, especially on Shemya where Emperor geese are more 'exposed to the elements'. By quantifying the impact of winter location and climatic drivers on annual productivity and apparent survival, this study addresses a key demographic knowledge gap, crucially relevant to Emperor Goose management and further informs harvest decisions under shifting climate conditions in the Bering Sea.

Methods

Study Area

Our study was conducted at two wintering areas representing the eastern and western extremes of the Emperor Goose's winter range: Shemya Island (52.7° N, 174.1° E) in the western Aleutian Islands and Kodiak Island (57.7° N, 152.5° W) in the Gulf of Alaska (*Fig. 1.2*). Shemya (15 km²) is a low-lying island characterized by exposed rocky shorelines, limited topographic relief, and frequent storm events during winter (Rodionov et al., 2007; Vermaire et al., 2013). The island's approximately 400 Emperor Geese are distributed along the island's coastline in the intertidal zone (*Fig. 1.3a*). In contrast, Kodiak Island is characterized by rocky

and sandy beaches, mudflats, and estuarine bays that provide sheltered habitats relative to the more exposed Aleutian coastline (*Fig. 1.3b*). Our research on Kodiak was conducted primarily in Chiniak Bay, which supports a wintering population of approximately 1,100 Emperor Geese (Wilson, 2016).

Sampling and Data Acquisition

Live captures and resight. We captured Emperor Geese using 10m x 15 m rocket nets on Shemya from 2022–2026 and on Kodiak from 2020–2026 with no birds marked in 2021. Depending on intertidal conditions, rockets were either dug into the ground or placed on angled tripod stanchions and rockets were fired over geese either foraging or roosting in the intertidal. Upon capture, we marked geese with uniquely coded alphanumeric yellow plastic leg bands on the left tarsus and stainless steel USGS bands on the right tarsus (*Supplementary Fig. 1.2*). Each year, geese were marked in January on Shemya (n = 238) and in February and March on Kodiak (n = 477). A concurrent study fitted a subset of marked birds (n = 67) with internally implanted satellite transmitters during winters of 2020-2024.

To populate mark-resight models with appropriate data for estimating survival, we re-sighted banded Emperor Geese from accessible viewing locales during January on Shemya and February or March on Kodiak using telephoto-cameras and spotting scopes (*Supplementary Table 1.1*). On Shemya, observers systematically surveyed coastal areas around the island for two to three weeks following the January capture period, repeatedly circling the island and scanning coastlines where Emperor Geese congregated (*Fig. 1.3a*). On Kodiak, resight surveys were conducted primarily around Women's Bay (*Fig. 1.3b*), with occasional searches in nearby Middle and Kalsin's Bay, during three-week periods in February and March following banding. Moreover, marked geese on Kodiak were opportunistically resighted by local citizens throughout

the entire winter period of habitation (Oct – Apr; *Supplementary Table 1.2*). For each group of birds encountered, observers repeatedly scanned the group for marked birds until all unique bands were detected.

Age ratios. We conducted age ratio counts, defined as the number of juveniles over the number of adults counted, at both winter sites from 2024 – 2026. For each flock encountered, we conducted a single scan and classified birds as juvenile or adult based on conspicuous plumage characteristics and leg coloration (*Supplementary Fig. 1.3*). Birds whose age could not be confidently determined because of distance, lighting, or body position were excluded from our counts.

Climate data acquisition and predictor variables. To evaluate the influence of regional climate variability on apparent survival, we used the Aleutian Low–Beaufort Sea Anticyclone (ALBSA) index as a regionally relevant large-scale atmospheric covariate. The ALBSA index describes the relative strength and position of the Aleutian Low and Beaufort Sea high-pressure systems, which influence atmospheric circulation across the Bering Sea and Aleutian region (Cox et al., 2019). Positive ALBSA values generally reflect warmer, wetter, and stormier conditions with greater maritime air transport, whereas negative values reflect cooler conditions associated with stronger high-pressure systems and reduced warm-air transport.

We summarized monthly ALBSA values into biologically relevant seasonal periods corresponding to emperor goose annual cycle and wintering locale (Hupp et al., 2008a; Naves et al., 2025). For Shemya, seasons were fall migration and staging (September–November), winter (December–March), spring migration and staging (April–May), and summer (June–August). For Kodiak, where geese overwinter for a longer period, seasons were classified as fall migration and staging (September), winter (October–April), spring migration and staging (May), and summer

(June–August). We also calculated an annual mean ALBSA value for each year of our study to represent broader climatic conditions across the full annual cycle. Seasonal and annual ALBSA values were standardized within each wintering site and across years (mean = 0, SD = 1). Thus, coefficients are scales to represent the effect of a one standard deviation change from average conditions at each site (*Supplementary Table 1.3*).

Statistical Analyses

Age ratios. To evaluate spatial and temporal variation in age ratios, we modeled counts of juveniles using generalized linear models (stats package; 'glm' function; R version 4.4.3; R Core Team., 2024) with a log-link (McCullagh & Nelder, 2019). We included the number of adults as a log-transformed offset so that juvenile counts were modeled relative to adult abundance, allowing estimation of juvenile to adult ratios while accounting for variation in flock size. Our candidate model set included all combinations of the following covariates: site (Shemya, Kodiak), year (categorical), and a site × year interaction (*Table 1.1*). Models were initially fit with a Poisson distribution and ranked using Akaike's Information Criterion corrected for small sample size (AICc). However, because the Poisson model exhibited substantial overdispersion (Pearson dispersion = 5.29), our final inference model was refit using a quasi-Poisson error distribution (O'Hara & Kotze, 2010).

Annual Survival. We used Cormack–Jolly–Seber (CJS) mark–recapture models to estimate apparent annual survival (Φ) and detection probability (p) from annual encounter histories spanning winter-to-winter (RMark package; 'mark' function; R version 4.4.3; Laake, 2013; R Core Team., 2024; Program MARK, White & Burnham, 1999), following a standard live-encounter modeling framework (Lebreton et al., 1992). The CJS model conditions the likelihood on first capture and estimates survival between sampling occasions while accounting

for imperfect detection. Because capture and resight years differed between our study sites, we conducted survival analyses separately for each site. We used observations of leg bands on wintering areas to construct encounter histories to estimate apparent survival (Φ) between winters, and detection (p) at each wintering sites (Burnham et al., 1987). We assumed the population to be closed within a winter period and that all marked birds had arrived in the wintering areas at the time of sampling. In the encounter histories, we interpreted the initial marking of an individual as the first encounter and classified geese in all subsequent winters as seen if they were located at least once in the survey area in any given winter. If a known death occurred, typically via band reports from hunters, we censored the individual to inform the model likelihood that the individual died after the last live encounter. To evaluate whether the inclusion of transmitter-equipment influenced detection and survival estimates, we conducted likelihood ratio tests to evaluate whether transmitter status improved model fit.

We first evaluated candidate model structures for p while holding an effect of age on Φ . p was modeled as constant, time-varying, or sex-specific (*Table 1.2*, *Table 1.3*). The best-supported detection structure was retained for subsequent analyses of Φ. Note that p cannot be estimated on the final occasion in a full time-varying model, because Φ and p are partially confounded in the final interval, when no subsequent encounter occasion exists to separate mortality from non-detection. To address this issue and improve model stability, detection probabilities for the final two sampling occasions were set equal and estimated as a single pooled parameter (White & Burnham, 1999). For each site, we then developed a candidate model set to evaluate variation in Φ among age classes (juvenile vs. adult), sex, and time (linear vs. categorical; *Table 1.4; Table 1.5*)

Impact of regional climate on apparent survival. We incorporated seasonal ALBSA covariates into the previously described CJS model framework to evaluate whether regional climate variability influenced apparent annual survival. For our CJS models, seasonal ALBSA covariates were aligned with the subsequent annual survival interval. For example, we used winter conditions during December 2024–March 2025 to model apparent annual survival for the 2025–2026 interval. We assigned ALBSA covariates to survival intervals by matching interval end years to the Φ design matrix in MARK. For each site, we allowed p to vary across years, while apparent survival was modeled as a function of ALBSA predictors. Candidate models included a null model, a demographic baseline model that included age and sex, models with the various ALBSA covariates, and additive models that included age, sex, and ALBSA covariates (*Table 1.6; Table 1.7*). Because seasonal ALBSA indices were occasionally correlated within sites (particularly at Kodiak; *Supplementary Table 1.4*), we evaluated the singular effect of each seasonal ALBSA covariate on apparent survival and never considered multiple ALBSA covariates simultaneously within the same model.

Model selection. Our inference was based on an information-theoretic approach where competing models that captured various hypotheses were ranked using Akaike's Information Criterion corrected for small sample sizes (AICc; Akaike, 1998; Burnham & Anderson, 1998). The model with the lowest AICc represents the most parsimonious model among the subset of possibles models ran, and models within two AICc units were generally considered to fit the data equally well. We also calculated an AICc weight for each model, as it provided a more intuitive way to weight the relative contribution of different models in explaining the data.

Results

Age ratios

Juvenile-to-adult ratios varied among sites and years (*Table 1.8*, *Fig. 1.4*). The top-supported model (AICc weight = 1) included a Site × Year interaction (analysis of deviance: $F_{2,55} = 9.26$, $p < 0.001$), indicating that temporal patterns in age ratios differed between wintering regions; no other models received support. Model-estimated juvenile-to-adult ratios were consistently higher at Kodiak than Shemya in all years. At Kodiak, ratios declined from 0.24 juveniles per adult (95% CI: 0.21–0.28) in 2024 to 0.17 (0.14–0.20) in 2025, then increased to 0.28 (0.24–0.33) in 2026. In contrast, ratios at Shemya increased steadily over time, from 0.03 juveniles per adult (0.02–0.05) in 2024 to 0.04 (0.03–0.07) in 2025 and 0.13 (0.09–0.19) in 2026. Despite this improvement, age ratios at Shemya remained substantially lower than those at Kodiak throughout the study period.

Survival Analysis

Detection. Initial model selection for recapture probability indicated strong support for time-varying detection at both wintering sites. At Shemya, the top-supported model similarly included age effects on survival and year-specific detection probability ($\Phi \sim$ Age, $p \sim$ Year; AICc weight = 0.55; *Table 1.2*), with a model including additional sex effects on detection also competitive (ΔAICc = 0.99, AICc weight = 0.34). At Kodiak, the top-supported detection model included year-specific variation in detection probability with constant survival ($\Phi \sim$ Null, $p \sim$ Year; AICc weight = 0.55; *Table 1.3*), with a model including age effects on survival also receiving some support (ΔAICc = 1.2, AICc weight = 0.30). These models retained year-specific detection probability in subsequent survival analyses. At both sites, estimated detection probability increased across years, on Shemya from 0.74 (95% CI: 0.62–0.83) in 2023 to 0.95

(0.85–0.98) in 2025 and on Kodiak from 0.71 (95% CI: 0.55–0.84) in 2021 to 0.97 (0.91–0.99) in 2025 (*Fig. 1.5*).

Transmitter effect. Survival models including transmitter as a covariate showed no improvement in fit relative to models without (LR = 0.16, p = 0.69). Similarly, models examining transmitter effect on detection probability had no significant reduction in deviance (LR = 2.57, p = 0.11; *Table 1.9*). At Shemya, apparent survival was 0.75 (95% CI: 0.64–0.84) for transmitter birds (n = 34) and 0.81 (95% CI: 0.76–0.85) for non-transmitter birds (n = 204), while detection probability was 0.92 (95% CI: 0.75–0.98) for transmitter birds and 0.83 (95% CI: 0.77–0.88) for non-transmitter birds. At Kodiak, apparent survival was 0.88 (95% CI: 0.80–0.93) for transmitter birds (n = 32) and 0.86 (95% CI: 0.82–0.89) for non-transmitter birds (n = 444), and detection probability was 0.92 (95% CI: 0.84–0.97) for transmitter birds and 0.90 (95% CI: 0.86–0.93) for non-transmitter birds. Because transmitter status did not meaningfully improve model fit for apparent survival or detection probability, we included transmitter-equipped birds in all subsequent analyses.

Shemya. Model selection indicated strongest support for models that included year and age effects on apparent survival and year-specific effects on detection probability (*Table 1.4*). A model including age and a linear temporal trend in survival received the most support ($\Phi \sim \text{Age} + \text{Year}_{\text{Linear}}$, $p \sim \text{Year}_{\text{Categorical}}$; AICc = 647.65, AICc weight = 0.41), although a simpler age-only model was also competitive (ΔAICc = 0.96, AICc weight = 0.26). Apparent annual survival differed substantially between age classes, with adults exhibiting consistently higher survival than juveniles (*Table 1.10*, *Fig. 1.6*). Adult survival progressively declined from 0.84 (95% CI: 0.77–0.90) during the 2022–2023 interval to 0.74 (95% CI: 0.65–0.81) during 2025–2026, while juvenile survival progressively declined from 0.49 (95% CI: 0.29–0.70) to 0.34 (95% CI: 0.16–

0.57) over the same period. Overall, this represents an average 10% decline in adult and 16% decline in juvenile apparent survival over the 4-year study period at Shemya.

Kodiak. Model selection indicated that apparent survival on Kodiak was best explained by year-specific detection probability (*Table 1.5*; $\Phi \sim \text{Year}_{\text{Categorical}}$, $p \sim \text{Year}_{\text{Categorical}}$; AICc = 831.54, weight = 0.27), although models including sex or age class also received some support (ΔAICc < 2). A model with a linear temporal trend was less supported, indicating survival fluctuated among years rather than changing linearly. Apparent annual survival (Φ) varied across intervals in the top-ranked model. Estimates were lowest in 2025–2026 (0.77, 95% CI: 0.70–0.83), similar in 2020–2021 (0.83, 95% CI: 0.68–0.92) and 2022–2023 (0.83, 95% CI: 0.73–0.90), and higher in 2023–2024 (0.86, 95% CI: 0.80–0.91) and 2024–2025 (0.89, 95% CI: 0.83–0.94). The 2021–2022 estimate was highest (0.98, 95% CI: 0.47–1.00), although the confidence interval was wide. (*Table 1.11*, *Fig. 1.6*). Although models including sex received some support (ΔAICc < 2), apparent survival was similar between males and females, with overlapping confidence intervals and comparable temporal trends (*Fig. 1.7*).

Regional climate effects on apparent survival

Shemya. Models including ALBSA climate predictors collectively received stronger support than models that did not include such predictors (*Table 1.6*). Model support was distributed among several competing seasonal climatic models. The top-supported model included age, sex, and prior summer ALBSA (AICc = 649.46, model weight = 0.24), although models including prior winter (weight = 0.21), prior fall (weight = 0.17), and prior spring ALBSA (weight = 0.16) were all within ΔAICc < 1 of the top model. The demographic baseline model without climate covariates also remained competitive (weight = 0.14).

Predicted relationships varied among seasons. Higher ALBSA values for the prior winter, spring, and fall—representing relatively warmer, wetter, and stormier regional conditions—were generally associated with higher apparent annual survival estimates, particularly for juveniles, whereas higher ALBSA values for the prior summer were associated with lower survival, particularly for juveniles (*Fig. 1.8*). Apparent annual survival tended to decrease with increasing prior summer ALBSA, with adult apparent annual survival ranging between approximately 0.73–0.85 across the observed standardized ALBSA index range (−1.38 to 1.00), with similar values for males (0.73–0.85) and females (0.75–0.86). In contrast, juvenile survival was substantially lower, ranging from 0.31–0.50 for males and 0.33–0.52 for females (*Table 1.12*). When considering prior winter ALBSA, apparent annual survival increased with increasing ALBSA values. Specifically, adult apparent annual survival ranged between 0.73–0.84 across the observed standardized ALBSA index range (-1.34–1.06) with similar estimates for males (0.73–0.83) and females (0.74–0.84). In contrast, juvenile survival was substantially lower, with estimates ranging from 0.33–0.47 for males and 0.35–0.49 for females (*Table 1.13*). Juvenile apparent survival remained much lower than adult survival across the full range of climatic conditions (*Table 1.14 and Table 1.15*).

Kodiak. On Kodiak, the top-ranked model included effects of age, sex, and prior winter ALBSA (AICc = 832.60, model weight = 0.67), whereas all alternative seasonal and annual ALBSA models received little support (ΔAICc > 3.7; Table *1.7*). Predicted annual survival increased with higher prior winter ALBSA values, where higher values reflect relatively warmer, wetter winter conditions. Adult apparent annual survival ranged from approximately 0.77–0.91 across the observed standardized ALBSA index range (−1.56 to 1.17), with similar values for males (0.77–0.88) and females (0.80–0.91), while juvenile survival was slightly lower, ranging

from 0.72–0.86 for males and 0.76–0.88 for females (*Table 1.16*). Although both age classes responded positively, adults consistently had slightly higher apparent survival than juveniles.

Discussion

This study provides new evidence that demographic rates of Emperor Geese vary across the geographic extremes of their winter range, a key insight given the general lack of understanding about the processes driving recent changes in their winter range and their repeated recurring population declines over the last several decades. Recent work by Uher-Koch et al., (2021) has shown that increasing numbers of Emperor Geese are wintering closer to their breeding grounds with fewer geese migrating out the Aleutian Island chain**.** Although such a pattern suggests a contemporary shift in winter distribution, the demographic processes underlying it remain unclear. Redistribution could reflect emperor geese actively selecting new winter locations due to changing habitat quality and altered climate conditions, or alternatively the redistribution could be driven by site-specific differences in survival and recruitment across their winter range. Our results support the latter hypothesis by demonstrating that multiple demographic parameters, including juvenile survival, age ratios, body condition, and climate-survival relationships, differ substantially between Kodiak and Shemya. Such patterns are consistent with broader work on migratory birds showing that conditions encountered outside the breeding season shape survival, reproduction, and subsequent population dynamics (Marra et al., 2015; Newton, 2007). Regional climate predictors were also associated with apparent annual survival, although impacts differed between wintering areas with geese on Shemya being sensitive to climate across all major seasons of the annual cycle, while those on Kodiak were primarily influenced by just winter conditions. Together, these findings suggest that wintering

regions contribute differently to population dynamics and provide a potential demographic explanation for ongoing changes in Emperor Goose winter distribution.

Ratios of juveniles-to-adults were approximately 3.8 times higher at Kodiak than at Shemya, although values at Shemya increased during the study period while Kodiak's were more variable and noticeably lower in 2025 than 2024 and 2026 (*Fig. 1.8*). Winter age ratios provide an index of productivity rather than a direct demographic estimate and require careful interpretation because they integrate several demographic processes, including nest success, breeding propensity, survival and migratory strategies (Rönkä et al., 2011; Sedinger et al., 2001). As such, several mechanisms could explain lower juvenile representation on Shemya, and these mechanisms could act solely or in unison. First, juvenile survival may be lower during migration or winter, reducing the number of young birds that successfully reach the more distant and environmentally exposed wintering area of Shemya (Gupte et al., 2019). Second, adults that wintered on Shemya may arrive to the breeding grounds in poorer condition, and therefore be less likely to initiate breeding, thereby lowering subsequent recruitment (i.e. carry-over effects of winter and migration; Ely et al., 2007). Breeding propensity in geese is often dependent on body condition, with individuals in poorer energetic states more likely to defer reproduction (Bearhop et al., 2005; Sedinger et al., 2008). Third, family groups with goslings may be less likely to undertake the long migration to Shemya, which is near the far reaches of their migratory range, instead wintering at closer sites such as Kodiak. This type of behavior has been documented in other goose species. For example, family groups of Brent Geese (*Branta bernicla hrota)* and Graylag Geese (*Anser anser*) often differ from nonbreeding adults in migration timing, habitat use, or winter distribution, with juveniles and adults accompanied by young more likely to use nearer or distinct wintering areas than 'unattached' adults (Black et al., 1992; Prevett &

MacInnes, 1980; Scheiber et al., 2005). In this scenario, the Shemya and the western Aleutians may function as a wintering area used disproportionately by adults capable of completing a longer migration, while family groups with juveniles may be underrepresented. Fourth, differences in juvenile ratios may reflect non-random distribution of individuals among wintering areas. If competition for winter habitat results in higher-quality or more socially dominant individuals preferentially occupying Kodiak, while competitively inferior individuals are displaced to the more distant Aleutian Islands, then adults wintering on Shemya may be intrinsically less likely to breed successfully regardless of winter conditions. Similar patterns have been documented in Pacific Black Brant (*Branta bernicla nigricans*), where winter location was associated with breeding probability, and individuals occupying higher-quality wintering areas exhibited greater reproductive success than those using lower-quality sites (Sedinger et al., 2011). Tracking breeding success and location of marked birds across the annual cycle would be helpful in explaining whether these differences arise primarily through differential juvenile survival, variation in breeding propensity, or selective migration.

The site-specific patterns we observed for annual survival further support the hypothesis that wintering region may be an important source of demographic heterogeneity within Emperor goose populations. Although Kodiak is located at a higher latitude, it likely provides a more sheltered and heterogeneous winter habitat than Shemya. The Kodiak Island study site of Women's Bay includes protected shorelines, expansive intertidal flats, estuarine ecosystems, and a broad range of foraging habitats and food sources (e.g. mussels, seaweed, intertidal grasses, macroalgae; Schmutz et al., 2020; Uher-Koch et al., 2021). In contrast, Shemya is a small and exposed island in the western Aleutians with limited topographic relief, few freshwater inputs, high exposure to frequent storm activity (*Fig. 1.2*). These differences likely influence resource

access, feeding opportunities, and energetic costs during winter, with potential consequences on annual survival. For Arctic and sub-Arctic waterfowl, increased thermoregulatory demands and reduced access to forage during severe weather can negatively affect body condition and survival (Root, 1988). For Emperor Geese, Uher-Koch et al., (2021) suggested that differences in their winter distribution and body condition may reflect spatial variation in winter habitat quality. Our observation of lower annual survival at Shemya may reflect repeated exposure of geese to harsher environmental conditions, coupled with fewer opportunities to offset these energetic costs through compensatory foraging and/or increased nutrient intake during a period when maintaining or accumulating body reserves is difficult (Clausen et al., 2015; Mason et al., 2006).

Lower juvenile survival relative to that of adults is common for a long-lived goose species, but the magnitude of detected difference on Shemya is significant (Sæther & Bakke, 2000). In long-lived species, life-history theory predicts that adult survival is often buffered against environmental variation, while demographic costs are more likely to appear through reduced breeding effort, recruitment, or delayed reproduction (Sæther & Bakke, 2000; Stearns, 1992). Unlike adults, juveniles (i.e. first-year birds) often show greater sensitivity to harsh conditions because of their inexperience, smaller size, lower energetic reserves, and inferior competitive ability relative to adults. As a result, juvenile survival is typically lower and more variable than adult survival, with increased susceptibility to predation, nutritional stress, severe weather, and the challenges of migration (Aubry et al., 2013; Schmutz et al., 1997). In our study, juvenile survival was substantially lower at Shemya than at Kodiak, suggesting that the harsher and more variable environmental conditions at Shemya may disproportionately affect first-year birds, and thereby amplify age-related differences in survival. Moreover, Shemya likely contributes far less recruitment into the future breeding population – by virtue of a consistently

lower juvenile survival alone – even though adult survival was within the range deemed sufficient by previous studies of Arctic-breeding geese (Hupp et al., 2008a; Schmutz et al., 1994, 1997).

For studies that use mark-resight of banded birds to estimate survival, such as ours, it is important to consider the limitations and assumptions of the survival estimation process. Foremost, apparent survival confounds true survival with permanent emigration; thus, lower estimates at a given wintering area, as we observed on Shemya, may partly reflect movement of marked individuals to unsampled wintering locations rather than mortality alone. Although emperor geese are generally thought to exhibit strong winter site fidelity (Hupp et al., 2008b; Uher-Koch et al., 2021), some movement among wintering areas cannot be ruled out. Nevertheless, we believe that emigration had little to no effect on our survival estimates. Preliminary analysis from a concurrent study of marked juvenile and adult emperor geese on Shemya (n = 19) and Kodiak (n = 27) that were equipped with transmitters collecting location data every 72 hours for 3–4 years found that both sites support high winter site fidelity, with only two birds not returning to the original banding area for each site.

Large-scale climate conditions were associated with changes in apparent annual survival at both sites, but the seasonal relationships between climate and survival differed between wintering sites. At both Kodiak and Shemya, survival tended to decrease with more negative ALBSA values from the prior winter, suggesting that colder and more extreme winters conditions may increase thermoregulatory costs while also limiting access to forage through intertidal icing, storm surges, or exposure to prolonged high winds (Newton, 2004). Such mechanisms may explain why winter conditions were the only seasonal index that showed a consistent relationship with apparent survival at both sites. Similar relationships between winter

climate and survival have been documented in other marine-associated birds; for example, survival of European shags (*Gulosus aristotelis*) declined during winters characterized by strong onshore winds and heavy rainfall due to large-scale mortality events (Frederiksen et al., 2008). Similarly, Laurenson et al., (2025) showed that overwinter survival of three sympatric seabird species declined during stormier winters, particularly when storms were frequent and intense.

At Shemya, however, our results indicate that apparent annual survival was associated with broad interannual climate variability rather than any single seasonal ALBSA index. Along with winter ALBSA effects, the best-supported model also included prior summer ALBSA as a strong predictor of apparent annual survival, with survival declining as summer ALBSA values became more positive. Because summer ALBSA reflects atmospheric conditions during the breeding season, our observed negative relationship with winter-to-winter survival may represent a carryover effect of summer conditions on survival (Cleasby et al., 2017). Positive summer ALBSA conditions are generally associated with warmer, wetter, and stormier weather in and around the Bering Sea (Cox et al., 2019), which could reduce reproductive success and/or adult body condition on their breeding grounds prior to fall migration. In geese, incubation is energetically demanding, and females often rely heavily on endogenous reserves while balancing nest attendance with recesses to forage (Afton & Paulus, 1992; Ankney & Macinnes, 1978; Schmutz et al., 2006). Increased storm frequency, precipitation, or prolonged wet conditions may reduce the frequency or duration of these recesses, thereby constraining energy intake during a critical life-history stage (Poussart et al., 2001).

If birds depart breeding areas in poorer condition after difficult summers, subsequent survival or performance during winter may be reduced, especially at sites with challenging winter conditions. Such carry-over effects between breeding and nonbreeding seasons are well

documented in migratory birds and can influence survival, timing of life history events (i.e. migration and breeding phenology), and future reproduction (Harrison et al., 2011; Norris & Marra, 2007; Sedinger et al., 2011). Emperor geese wintering at Shemya, which presents a more challenging winter environment than Kodiak, may be more sensitive to cumulative effects of both breeding-season and winter weather conditions. These findings suggest that the same regional climate signal can translate into different demographic outcomes depending on where birds winter. These findings should be interpreted with some caution, however, as survival estimates were limited to recent years with this study beginning in 2020. With relatively few years available for demographic comparisons, our ability to detect long-term relationships at each site between climate conditions and survival was limited, and additional years of monitoring would improve inference.

Given that Emperor geese wintering on Shemya experience lower apparent survival and lower juvenile representation, an obvious question remains: "why do emperor geese continue to winter there?". Many waterfowl species show strong fidelity and return repeatedly to historical wintering areas (G. Robertson & Cooke, 1999) with migratory routes persisting through learned behaviors or 'socially inherited' migratory strategies. Uher-Koch et al. (2021) found that most emperor geese equipped with geolocators used the same wintering sites across years, indicating high site fidelity to wintering locations. Although it does not seem advantageous to winter on Shemya in recent years, historically, the western Aleutians may have been a profitable wintering region for Emperor Geese. Shemya lies farther west but at a lower latitude than Kodiak, and under colder historical climate, likely offered milder winter conditions and more reliable ice-free foraging habitats than sites farther north and east. Kodiak, in contrast, was likely a less favorable

winter location historically, being more prone to increased snow cover and intertidal icing events that locked geese out of potentially rich intertidal foraging zones.

Alaska has warmed substantially in recent decades, with especially strong changes in winter climate across many coastal regions (Walsh & Brettschneider, 2019; Wendler et al., 2016). Under changing environmental conditions, winter site fidelity can potentially create an evolutionary trap, in which birds continue selecting historically suitable habitats even after those habitats no longer provide the demographic benefits they once did (Robertson & Hutto, 2006; Schlaepfer et al., 2002). If conditions in the western Aleutians have become less favorable because of changing storm regimes, altered food availability, or other environmental shifts linked to climate change (Overland & Wang, 2005, 2025; Smith et al., 2019), emperor geese may continue to winter there despite experiencing reduced survival or productivity.

These climatic shifts also raise the possibility that historical advantages of wintering in the western Aleutian Islands may be diminishing, while conditions at Kodiak have become increasingly favorable. Our findings provide a potential demographic mechanism underlying the redistribution of Emperor Geese documented by Uher-Koch et al. (2021). If wintering at Shemya is associated with consistently lower juvenile survival, poorer body condition, and reduced recruitment, individuals wintering closer to the breeding grounds may contribute disproportionately to emperor goose population dynamics. Indeed, these hypothetical changes appear to be reflected in number of Emperor Geese wintering at each site, with Shemya numbers remaining relatively steady or slight declining over the last several decades (Pohlen et al., 2023), while number of geese wintering in Chiniak Bay on Kodiak have increased ten fold from the mid-1990s to 2016 (Wilson, 2016). It is important to consider that this study focused on two specific wintering locations, Women's Bay on Kodiak and Shemya Island in the western

Aleutians, which may not fully represent broader regional conditions in between these extremes. It may therefore be inappropriate to assume that patterns observed at Shemya characterize all western Aleutian wintering areas, or that patterns at Women's Bay reflect the entirety of Kodiak. Additional work across multiple wintering sites would help determine whether the differences observed here reflect broad regional structure or site-specific local conditions

Management implications

Collectively, these findings have several implications for the conservation and management of emperor geese. Management decisions are largely based on a population-wide index measured consistently during summer surveys. Yet, our results suggest that productivity and survival rates may differ among birds wintering in different regions. If birds wintering in the western Aleutians experience lower survival or recruitment, they contribute differently to future population trajectories and may be more sensitive to additional stressors such as severe winters or harvest. Kodiak appears to have become an increasingly important wintering area in recent decades, as more emperor geese use the eastern portion of the winter range (Uher-Koch et al. 2021; *Supplementary Fig. 1.4*). Our results further suggest that Emperor geese seem to experience increased productivity and apparent survival there. As winter distribution changes, improved understanding of regional demographic variation may become increasingly valuable for future management decisions. Incorporating information on survival, recruitment, and winter distribution across regions could help managers better anticipate how localized environmental change may scale-up to affect the broader population (Mengak et al., 2022; Naves et al., 2025; Pacific Flyway Council, 2016).

Tables and Figures

Table 1.1: Model selection results for candidate age-ratio models evaluating variation in juvenile-to-adult emperor goose ratios among wintering sites and years. 'npar' stands for number of parameters.

Age ratio models	npar	AICc	ΔAICc	AICc weight
Site × Year	6	607.29	0.00	1.00
Site + Year	4	700.39	93.10	0.00
Site	2	854.44	247.16	0.00
Year	3	1,587.65	980.36	0.00
Null	1	1,820.35	1,213.07	0.00

Table 1.2: AICc model selection results for candidate Cormack–Jolly–Seber models evaluating detection probability (p) of emperor geese at Shemya.

Φ model	p model	npar	AICc	ΔAICc	Weight
Age	$Year_{Categorical}$	5	648.61	0.00	0.55
Age	$Sex + Year_{Categorical}$	6	649.60	0.99	0.34
Age	Null	3	652.92	4.31	0.06
Age	Sex	4	653.75	5.15	0.04
Null	$Year_{Categorical}$	4	658.56	9.95	0.00
Null	$Year_{Categorical} + Sex$	5	659.55	10.94	0.00

Table 1.3: AICc model selection results for candidate Cormack–Jolly–Seber models evaluating detection probability (p) of emperor geese at Kodiak.

Φ model	p model	npar	AICc	ΔAICc	Weight
Null	$Year_{Categorical}$	6	834.40	0.00	0.55
Age	$Year_{Categorical}$	7	835.60	1.20	0.30
Age	Sex + $Year_{Categorical}$	8	837.56	3.17	0.11
Null	Null	2	841.19	6.79	0.02
Age	Null	3	842.48	8.08	0.01
Age	Sex	4	844.47	10.07	0.00

Table 1.4: AICc model selection results for candidate Cormack–Jolly–Seber models evaluating apparent survival (Φ) of emperor geese at Shemya. In all cases, p was modeled with respect to year treated as a categorical predictor; $Year_{Categorical}$.

Φ model	npar	AICc	ΔAICc	Weight
$Age + Year_{Linear}$	6	647.65	0.00	0.41
Age	5	648.61	0.96	0.26
$Age + Year_{Categorical}$	8	650.25	2.60	0.11
Age + Sex	6	650.52	2.87	0.10
$Age + Sex + Year_{Linear}$	8	651.08	3.43	0.07
$Age + Sex + Year_{Categorical}$	9	652.19	4.54	0.04
Null	4	658.56	10.91	0.00
$Year_{Linear}$	5	658.65	11.01	0.00
Sex	5	660.55	12.90	0.00
$Sex + Year_{Linear}$	6	660.64	13.00	0.00
$Year_{Categorical}$	7	661.95	14.30	0.00
Null	2	664.24	16.59	0.00

Table 1.5: AICc model selection results for candidate Cormack–Jolly–Seber models evaluating apparent survival (Φ) of emperor geese at Kodiak. In all cases, p was modeled with respect to year treated as a categorical predictor; $Year_{Categorical}$.

Φ model	npar	AICc	ΔAICc	Weight
$Year_{Categorical}$	11	831.54	0.00	0.27
Sex + $Year_{Categorical}$	12	832.61	1.06	0.16
$Year_{Linear}$	7	833.29	1.74	0.11
Age + $Year_{Categorical}$	12	833.44	1.89	0.11
Age + $Year_{Linear}$	8	834.20	2.66	0.07
Null	6	834.40	2.85	0.07
Age + Sex + $Year_{Categorical}$	13	834.51	2.97	0.06
Sex	7	835.10	3.55	0.05
Age × Sex + $Year_{Linear}$	10	835.58	4.03	0.04
Age	7	835.60	4.05	0.04
Age + Sex	8	836.31	4.77	0.03
Null	2	841.19	9.64	0.00

Table 1.6: AICc model selection results for candidate Cormack–Jolly–Seber models evaluating effects of seasonal ALBSA climate indices on apparent survival (Φ) of emperor geese at Shemya. Seasonal covariates represent conditions in the season preceding each survival interval. In all cases, p was modeled with respect to year treated as a categorical predictor; $Year_{Categorical}$.

Φ model	npar	AICc	ΔAICc	Weight
Age + Sex + $ALBSA_{Prior\ Summer}$	7	649.46	0.00	0.24
Age + Sex + $ALBSA_{Prior\ Winter}$	7	649.75	0.29	0.21
Age + Sex + $ALBSA_{Prior\ Fall}$	7	650.09	0.63	0.17
Age + Sex + $ALBSA_{Prior\ Spring}$	7	650.23	0.77	0.16
Age + Sex	6	650.52	1.06	0.14
Age + Sex + $ALBSA_{Annual}$	7	651.62	2.16	0.08
Null	2	664.24	14.78	0.00
$ALBSA_{Prior\ Spring}$	4	789.28	139.81	0.00
$ALBSA_{Annual}$	4	789.75	140.29	0.00
$ALBSA_{Prior\ Fall}$	4	789.89	140.43	0.00
$ALBSA_{Prior\ Winter}$	4	789.92	140.46	0.00
$ALBSA_{Prior\ Summer}$	4	789.92	140.46	0.00

Table 1.7: AICc model selection results for candidate Cormack–Jolly–Seber models evaluating effects of seasonal ALBSA climate indices on apparent survival (Φ) of emperor geese at Kodiak. Seasonal covariates represent conditions in the season preceding each survival interval. In all cases, p was modeled with respect to year treated as a categorical predictor; $Year_{Categorical}$.

Φ model	npar	AICc	ΔAICc	Weight
Age + Sex + $ALBSA_{Prior\ Winter}$	9	832.60	0.00	0.6669
Age + Sex	8	836.31	3.71	0.1045
Age + Sex + $ALBSA_{Prior\ Spring}$	9	836.95	4.34	0.0760
Age + Sex + $ALBSA_{Prior\ Summer}$	9	837.29	4.68	0.0641
Age + Sex + $ALBSA_{Prior\ Fall}$	9	838.24	5.64	0.0398
Age + Sex + $ALBSA_{Annual}$	9	838.25	5.65	0.0396
Null	2	841.19	8.58	0.0091
$ALBSA_{(Prior\ Fall)}$	6	1099.08	266.47	0.0000
$ALBSA_{(Prior\ Summer)}$	6	1119.38	286.77	0.0000
$ALBSA_{(Prior\ Spring)}$	6	1132.02	299.42	0.0000
$ALBSA_{(Prior\ Winter)}$	6	1166.32	333.71	0.0000

Table 1.8: Summary of winter age-ratio surveys for Emperor Geese conducted at Kodiak and Shemya, Alaska, during 2024–2026. Values include the number of survey days, total adults and juveniles aged, by site and year. Model-estimated juvenile to adult ratios (J:A) and 95% confidence intervals were derived from a quasi-Poisson generalized linear model including Site × Year effects.

Site	Year	Surveyor days	Adults aged	Juveniles aged	Model-estimated J:A [95% CI]
Kodiak	2024	14	3,764	910	0.24 [0.21–0.28]
Kodiak	2025	11	4,429	734	0.17 [0.14–0.20]
Kodiak	2026	8	3,243	906	0.28 [0.24–0.33]
Shemya	2024	14	3,983	117	0.03 [0.02–0.05]
Shemya	2025	6	2,081	94	0.04 [0.03–0.07]
Shemya	2026	8	1,137	151	0.13 [0.09–0.19]

Table 1.9: Likelihood ratio tests evaluating potential transmitter effects on apparent survival (Φ) and detection probability (p) for emperor geese at Kodiak and Shemya, Alaska. Comparisons are between null models and models including transmitter status as a covariate.

Site	Reduced model	Full model	Likelihood ratio χ^2	df	p-value
Kodiak	Φ = Null, p = Null	Φ = Transmitter, p = Null	0.54	1	0.462
Kodiak	Φ = Null, p = Null	Φ = Null, p = Transmitter	0.37	1	0.542
Shemya	Φ = Null, p = Null	Φ = Transmitter, p = Null	1.02	1	0.312
Shemya	Φ = Null, p = Null	Φ = Null, p = Transmitter	1.94	1	0.163

Table 1.10: Parameter estimates (± SE and 95% CI) from the top-supported Cormack–Jolly–Seber model for emperor geese at Shemya where apparent survival (Φ) varied by Age + $Year_{Linear}$.

Age	Interval/Encounter Period	Parameter	Estimate	SE	LCL
Adult	2022–2023	Φ	0.843	0.032	0.771
Adult	2023–2024	Φ	0.813	0.023	0.763
Adult	2024–2025	Φ	0.778	0.023	0.728
Adult	2025–2026	Φ	0.738	0.040	0.653
Juvenile	2022–2023	Φ	0.492	0.112	0.287
Juvenile	2023–2024	Φ	0.439	0.106	0.252
Juvenile	2024–2025	Φ	0.386	0.106	0.208
Juvenile	2025–2026	Φ	0.337	0.109	0.163
—	2023	p	0.735	0.054	0.617
—	2024	p	0.858	0.043	0.752
—	2025–2026	p	0.949	0.029	0.854

Table 1.11: Parameter estimates (± SE and 95% CI) from the top-supported Cormack–Jolly–Seber model for emperor geese at Kodiak where apparent survival (Φ) varied by $Year_{Categorical}$.

Encounter Period	Parameter	Estimate	SE	LCL	UCL
2020–2021	Φ	0.827	0.060	0.679	0.916
2021–2022	Φ	0.980	0.040	0.471	1.000
2022–2023	Φ	0.827	0.043	0.725	0.897
2023–2024	Φ	0.862	0.029	0.795	0.909
2024–2025	Φ	0.892	0.028	0.825	0.935
2025–2026	Φ	0.769	0.031	0.702	0.825
2021	p	0.714	0.076	0.546	0.839
2022	p	0.897	0.056	0.727	0.966
2023	p	0.917	0.035	0.817	0.965
2024	p	0.934	0.023	0.873	0.966
2025–2026	p	0.970	0.017	0.910	0.990

Table 1.12: Estimates (± SE and 95% CI) from the top supported Cormack–Jolly–Seber seasonal climate model for emperor geese at Shemya. Apparent survival (Φ) varied by age, sex and prior summer ALBSA conditions.

Age	Sex	Survival Interval	$ALBSA_{Prior\ Summer}$	Estimate (Φ)	SE	LCL	UCL
Adult	Male	2022–2023	-1.381	0.853	0.044	0.744	0.920
Adult	Male	2023–2024	0.303	0.771	0.036	0.692	0.834
Adult	Male	2024–2025	0.080	0.783	0.034	0.708	0.843
Adult	Male	2025–2026	0.998	0.728	0.050	0.619	0.816
Juvenile	Male	2022–2023	-1.381	0.496	0.125	0.269	0.725
Juvenile	Male	2023–2024	0.303	0.364	0.112	0.181	0.597
Juvenile	Male	2024–2025	0.080	0.381	0.112	0.195	0.610
Juvenile	Male	2025–2026	0.998	0.313	0.115	0.138	0.566
Adult	Female	2022–2023	-1.381	0.864	0.039	0.770	0.924
Adult	Female	2023–2024	0.303	0.787	0.027	0.730	0.835
Adult	Female	2024–2025	0.080	0.799	0.026	0.744	0.844
Adult	Female	2025–2026	0.998	0.747	0.042	0.656	0.820
Juvenile	Female	2022–2023	-1.381	0.520	0.118	0.299	0.733
Juvenile	Female	2023–2024	0.303	0.386	0.109	0.204	0.607
Juvenile	Female	2024–2025	0.080	0.403	0.108	0.219	0.619
Juvenile	Female	2025–2026	0.998	0.334	0.114	0.156	0.578

Table 1.13: Estimates (± SE and 95% CI) from the second top supported Cormack–Jolly–Seber seasonal climate model for emperor geese at Shemya. Apparent survival (Φ) varied by age, sex and prior winter ALBSA conditions.

Age	Sex	Survival Interval	$ALBSA_{Prior\ Winter}$	Estimate (Φ)	SE	LCL	UCL
Adult	Male	2022–2023	0.66	0.811	0.035	0.732	0.871
Adult	Male	2023–2024	1.06	0.825	0.038	0.739	0.888
Adult	Male	2024–2025	-0.44	0.766	0.037	0.687	0.831
Adult	Male	2025–2026	-1.34	0.725	0.052	0.613	0.814
Juvenile	Male	2022–2023	0.66	0.444	0.115	0.242	0.666
Juvenile	Male	2023–2024	1.06	0.468	0.119	0.257	0.692
Juvenile	Male	2024–2025	-0.44	0.379	0.111	0.195	0.607
Juvenile	Male	2025–2026	-1.34	0.329	0.113	0.153	0.572
Adult	Female	2022–2023	0.66	0.825	0.028	0.764	0.873
Adult	Female	2023–2024	1.06	0.839	0.031	0.769	0.891
Adult	Female	2024–2025	-0.44	0.783	0.028	0.724	0.832
Adult	Female	2025–2026	-1.34	0.744	0.044	0.650	0.819
Juvenile	Female	2022–2023	0.66	0.468	0.109	0.272	0.675
Juvenile	Female	2023–2024	1.06	0.492	0.112	0.287	0.700
Juvenile	Female	2024–2025	-0.44	0.402	0.107	0.220	0.616
Juvenile	Female	2025–2026	-1.34	0.351	0.111	0.173	0.583

Table 1.14: Estimates (± SE and 95% CI) from the second top supported Cormack–Jolly–Seber seasonal climate model for emperor geese at Shemya. Apparent survival (Φ) varied by age, sex and prior fall ALBSA conditions.

Age	Sex	Survival Interval	$ALBSA_{Prior\ Fall}$	Estimate (Φ)	SE	LCL	UCL
Adult	Male	2022–2023	1.33	0.840	0.043	0.737	0.907
Adult	Male	2023–2024	0.13	0.792	0.034	0.717	0.851
Adult	Male	2024–2025	-0.46	0.764	0.038	0.682	0.830
Adult	Male	2025–2026	-1.00	0.737	0.049	0.631	0.821
Juvenile	Male	2022–2023	1.33	0.484	0.124	0.262	0.712
Juvenile	Male	2023–2024	0.13	0.405	0.113	0.214	0.630
Juvenile	Male	2024–2025	-0.46	0.367	0.113	0.183	0.600
Juvenile	Male	2025–2026	-1.00	0.334	0.115	0.154	0.581
Adult	Female	2022–2023	1.33	0.852	0.037	0.765	0.911
Adult	Female	2023–2024	0.13	0.807	0.026	0.752	0.853
Adult	Female	2024–2025	-0.46	0.781	0.029	0.719	0.832
Adult	Female	2025–2026	-1.00	0.755	0.040	0.668	0.826
Juvenile	Female	2022–2023	1.33	0.508	0.117	0.292	0.721
Juvenile	Female	2023–2024	0.13	0.429	0.107	0.241	0.639
Juvenile	Female	2024–2025	-0.46	0.390	0.109	0.207	0.610
Juvenile	Female	2025–2026	-1.00	0.356	0.113	0.174	0.592

Table 1.15: Estimates (± SE and 95% CI) from the second top supported Cormack–Jolly–Seber seasonal climate model for emperor geese at Shemya. Apparent survival (Φ) varied by age, sex and prior spring ALBSA conditions.

Age	Sex	Survival Interval	$ALBSA_{Prior\ Spring}$	Estimate (Φ)	SE	LCL	UCL
Adult	Male	2022–2023	-0.52	0.762	0.039	0.677	0.831
Adult	Male	2023–2024	0.56	0.805	0.035	0.726	0.866
Adult	Male	2024–2025	1.08	0.824	0.039	0.734	0.888
Adult	Male	2025–2026	-1.12	0.736	0.050	0.627	0.822
Juvenile	Male	2022–2023	-0.52	0.377	0.112	0.193	0.606
Juvenile	Male	2023–2024	0.56	0.438	0.115	0.239	0.660
Juvenile	Male	2024–2025	1.08	0.469	0.120	0.256	0.694
Juvenile	Male	2025–2026	-1.12	0.345	0.114	0.164	0.586
Adult	Female	2022–2023	-0.52	0.779	0.030	0.714	0.833
Adult	Female	2023–2024	0.56	0.819	0.027	0.759	0.867
Adult	Female	2024–2025	1.08	0.837	0.032	0.764	0.890
Adult	Female	2025–2026	-1.12	0.754	0.042	0.663	0.827
Juvenile	Female	2022–2023	-0.52	0.399	0.107	0.217	0.615
Juvenile	Female	2023–2024	0.56	0.462	0.108	0.267	0.668
Juvenile	Female	2024–2025	1.08	0.492	0.113	0.286	0.701
Juvenile	Female	2025–2026	-1.12	0.367	0.111	0.185	0.596

Table 1.16: Estimates (± SE and 95% CI) from the top supported Cormack–Jolly–Seber seasonal climate model for emperor geese at Kodiak. Apparent survival (Φ) varied by age, sex and prior winter ALBSA conditions.

Age	Sex	Survival Interval	$ALBSA_{Prior\ Winter}$	Estimate (Φ)	SE	LCL	UCL
Adult	Male	2020–2021	1.173	0.885	0.027	0.820	0.929
Adult	Male	2021–2022	0.367	0.857	0.025	0.799	0.900
Adult	Male	2022–2023	-0.561	0.818	0.027	0.758	0.865
Adult	Male	2023–2024	0.820	0.873	0.026	0.812	0.917
Adult	Male	2024–2025	-0.234	0.832	0.026	0.776	0.877
Adult	Male	2025–2026	-1.565	0.766	0.040	0.678	0.836
Juvenile	Male	2020–2021	1.173	0.856	0.052	0.723	0.931
Juvenile	Male	2021–2022	0.367	0.822	0.055	0.689	0.906
Juvenile	Male	2022–2023	-0.561	0.776	0.061	0.635	0.873
Juvenile	Male	2023–2024	0.820	0.842	0.053	0.709	0.921
Juvenile	Male	2024–2025	-0.234	0.793	0.058	0.656	0.885
Juvenile	Male	2025–2026	-1.565	0.717	0.074	0.554	0.838
Adult	Female	2020–2021	1.173	0.905	0.020	0.858	0.938
Adult	Female	2021–2022	0.367	0.881	0.018	0.842	0.912
Adult	Female	2022–2023	-0.561	0.848	0.019	0.807	0.881
Adult	Female	2023–2024	0.820	0.895	0.019	0.852	0.927
Adult	Female	2024–2025	-0.234	0.860	0.017	0.823	0.891
Adult	Female	2025–2026	-1.565	0.803	0.032	0.732	0.859
Juvenile	Female	2020–2021	1.173	0.881	0.042	0.771	0.942
Juvenile	Female	2021–2022	0.367	0.852	0.045	0.741	0.920
Juvenile	Female	2022–2023	-0.561	0.812	0.051	0.691	0.893
Juvenile	Female	2023–2024	0.820	0.869	0.043	0.759	0.933
Juvenile	Female	2024–2025	-0.234	0.827	0.049	0.710	0.903
Juvenile	Female	2025–2026	-1.565	0.759	0.065	0.612	0.863

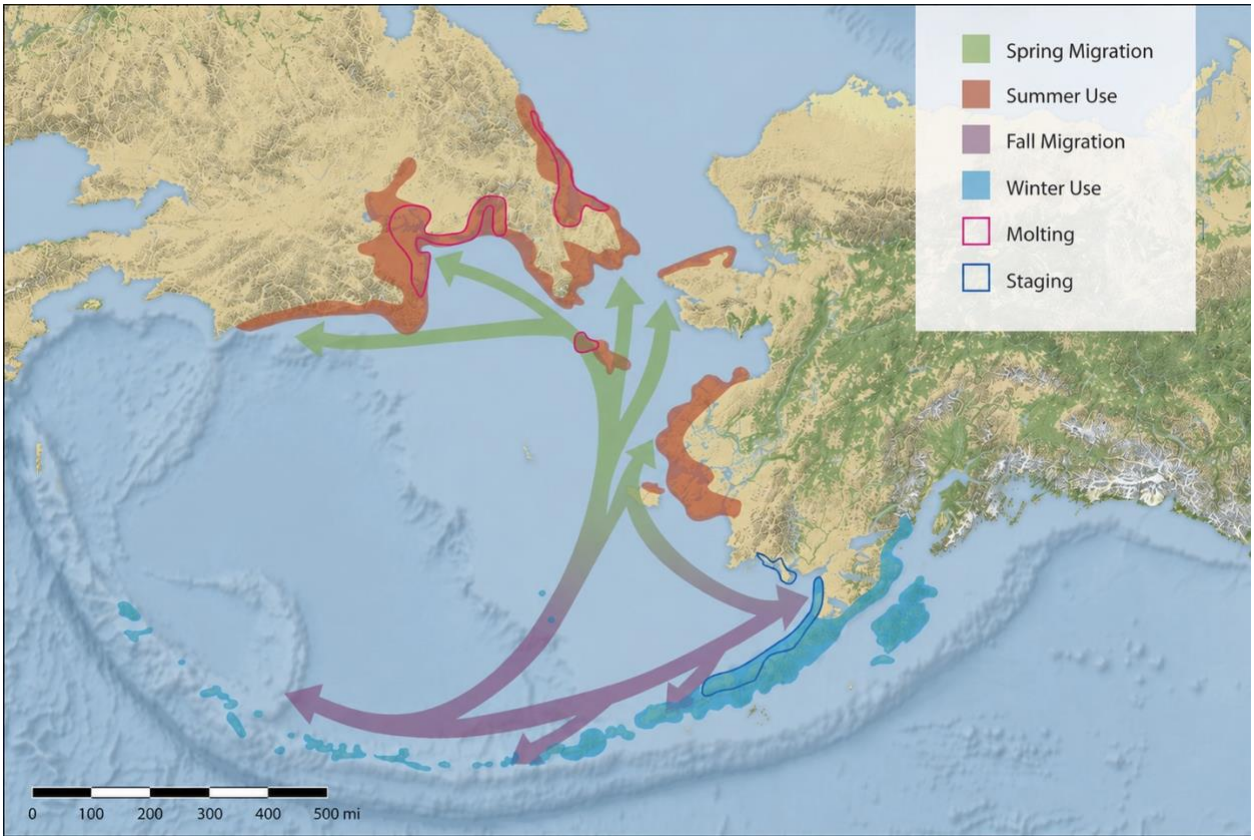

Figure 1.1: Generalized annual distribution and migration patterns of Emperor Geese across the Bering Sea region. Image adapted from the U.S. Fish and Wildlife Service Migratory Bird Program, 2022

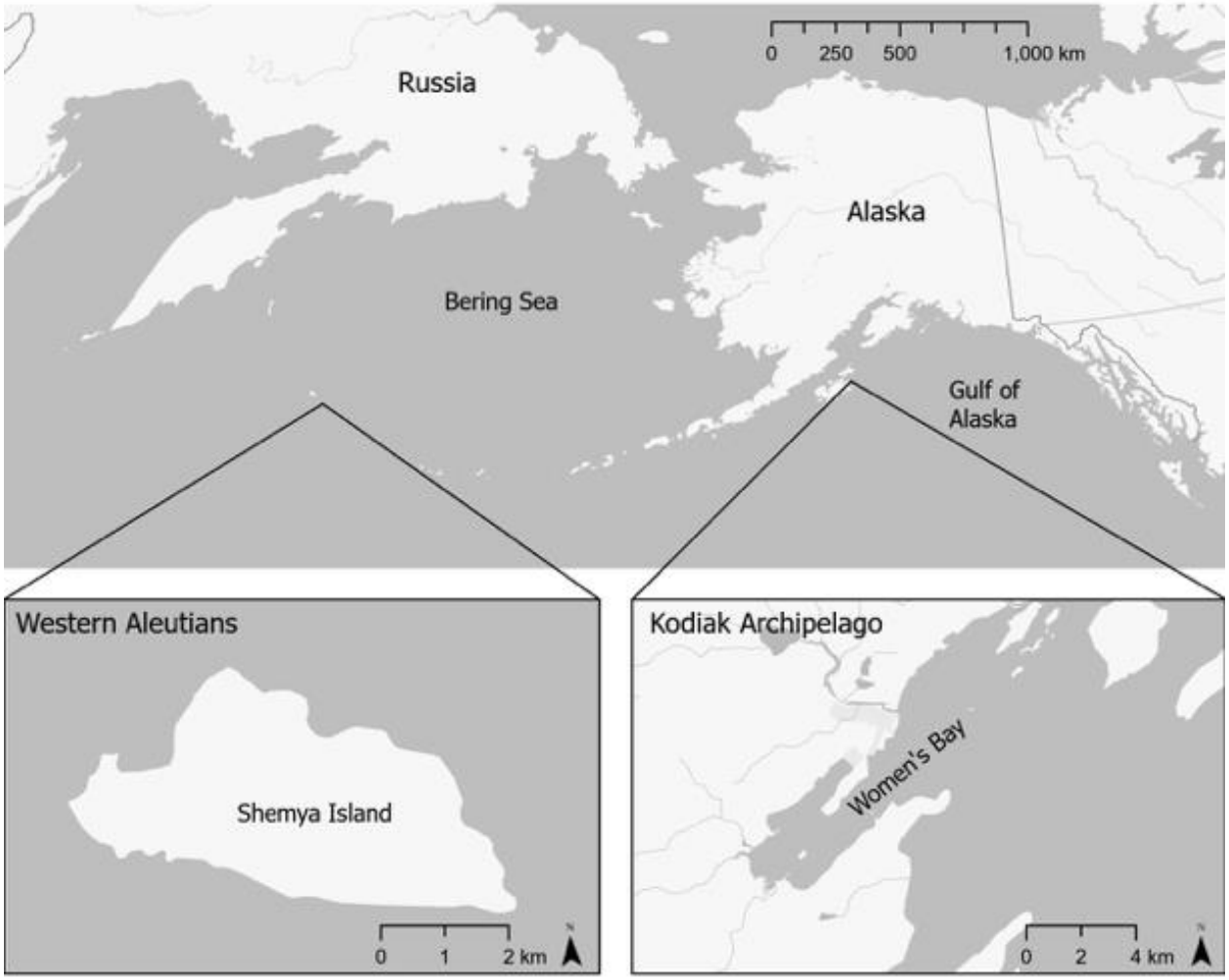

Figure 1.2: Location of Western Aleutian study site (Shemya) and Kodiak Archipelago study site (Women's Bay), Alaska, USA.

Figure 1.3: General Emperor Goose survey routes marked in red for Eareckson Air Station on Shemya Island (a) and Women's Bay on Kodiak Island (b).

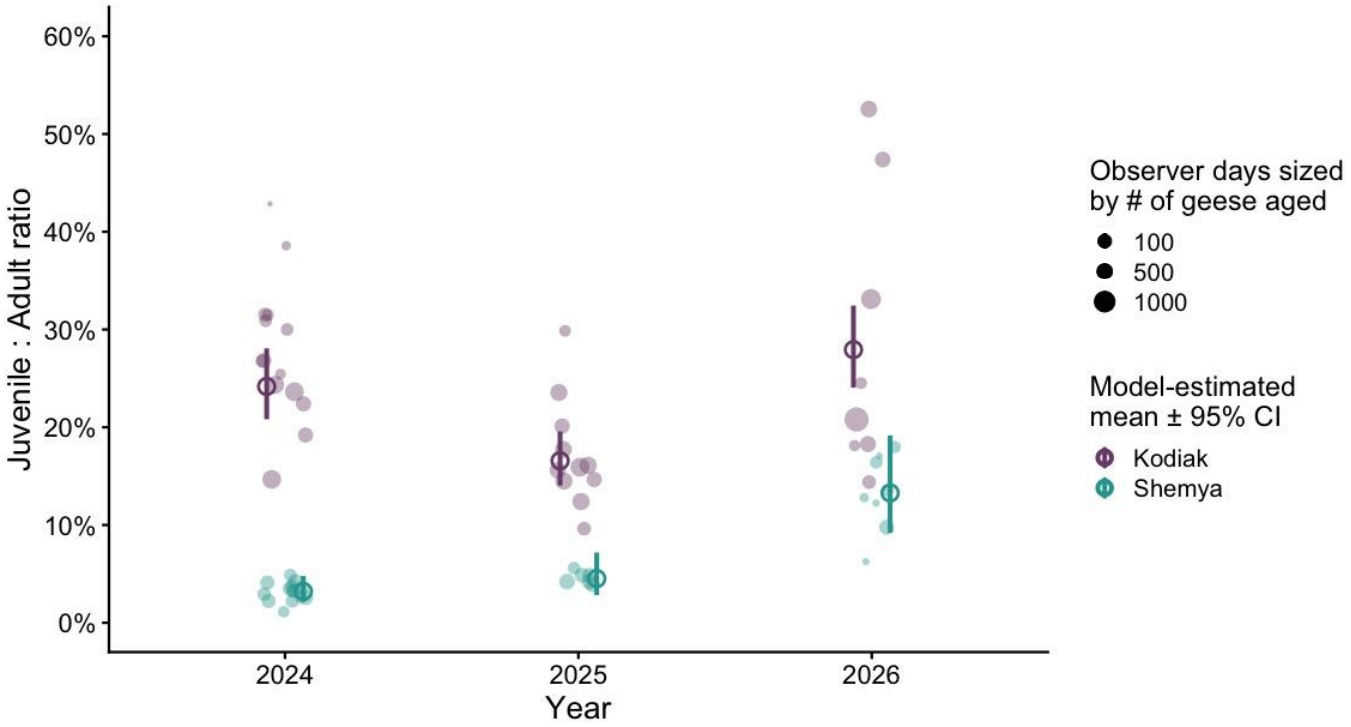

Figure 1.4. Winter juvenile-to-adult ratios of emperor geese observed at Kodiak and Shemya from. Filled circles represent observer days, with point size proportional to the number of geese aged that day. Symbols and error bars indicate model-estimated mean juvenile-to-adult ratios ± 95% confidence intervals for each site and year.

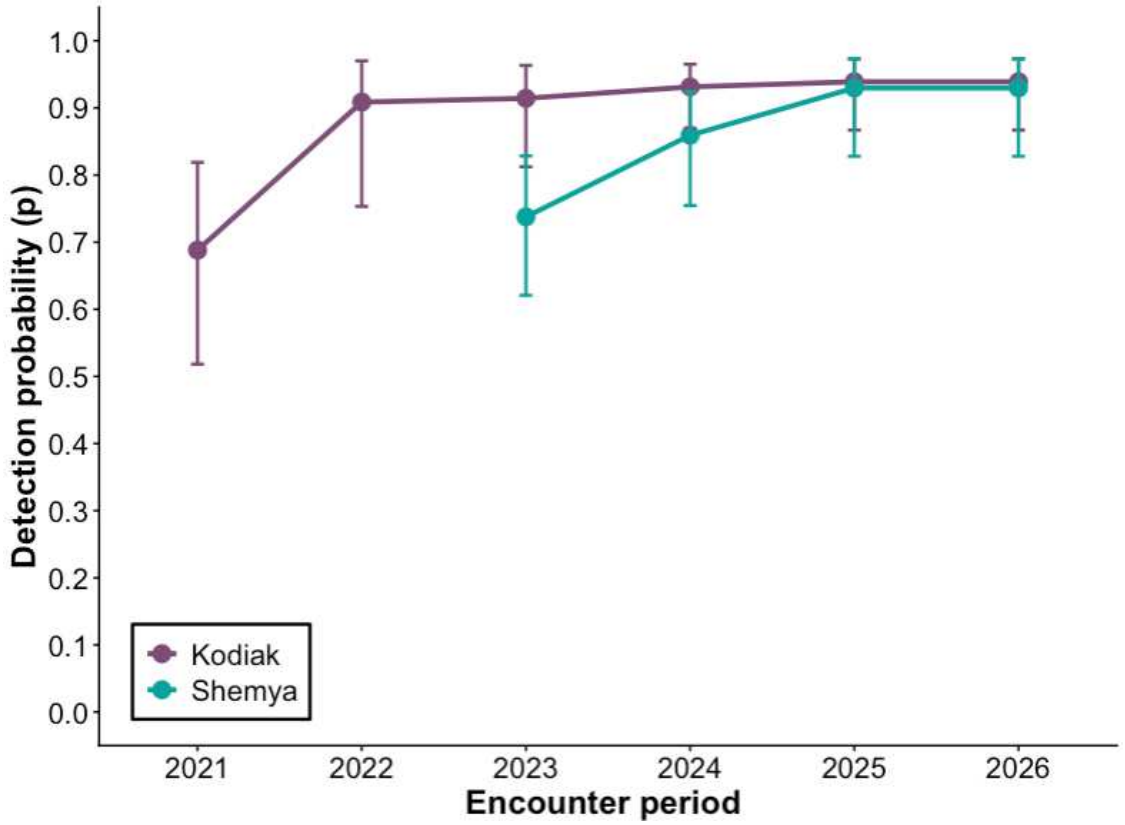

Figure 1.5: Detection probability estimates (Φ ± 95% CI) intervals from top-supported Cormack–Jolly–Seber models considering $Year_{Categorical}$

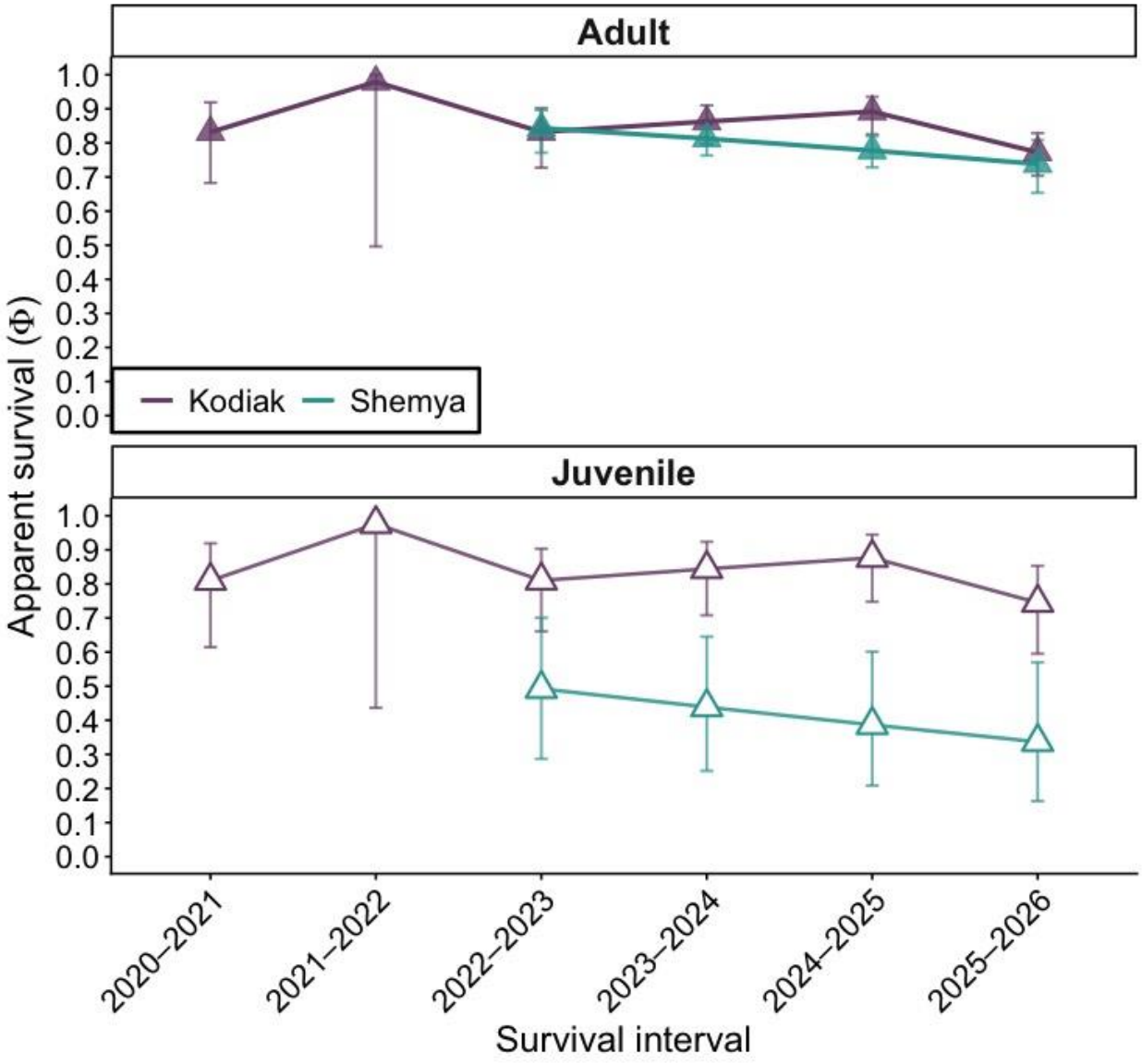

Figure 1.6: Apparent survival estimates ($\Phi \pm 95\%$ CI) for adult and juvenile emperor geese on Kodiak and Shemya, across winter-to-winter annual survival intervals.

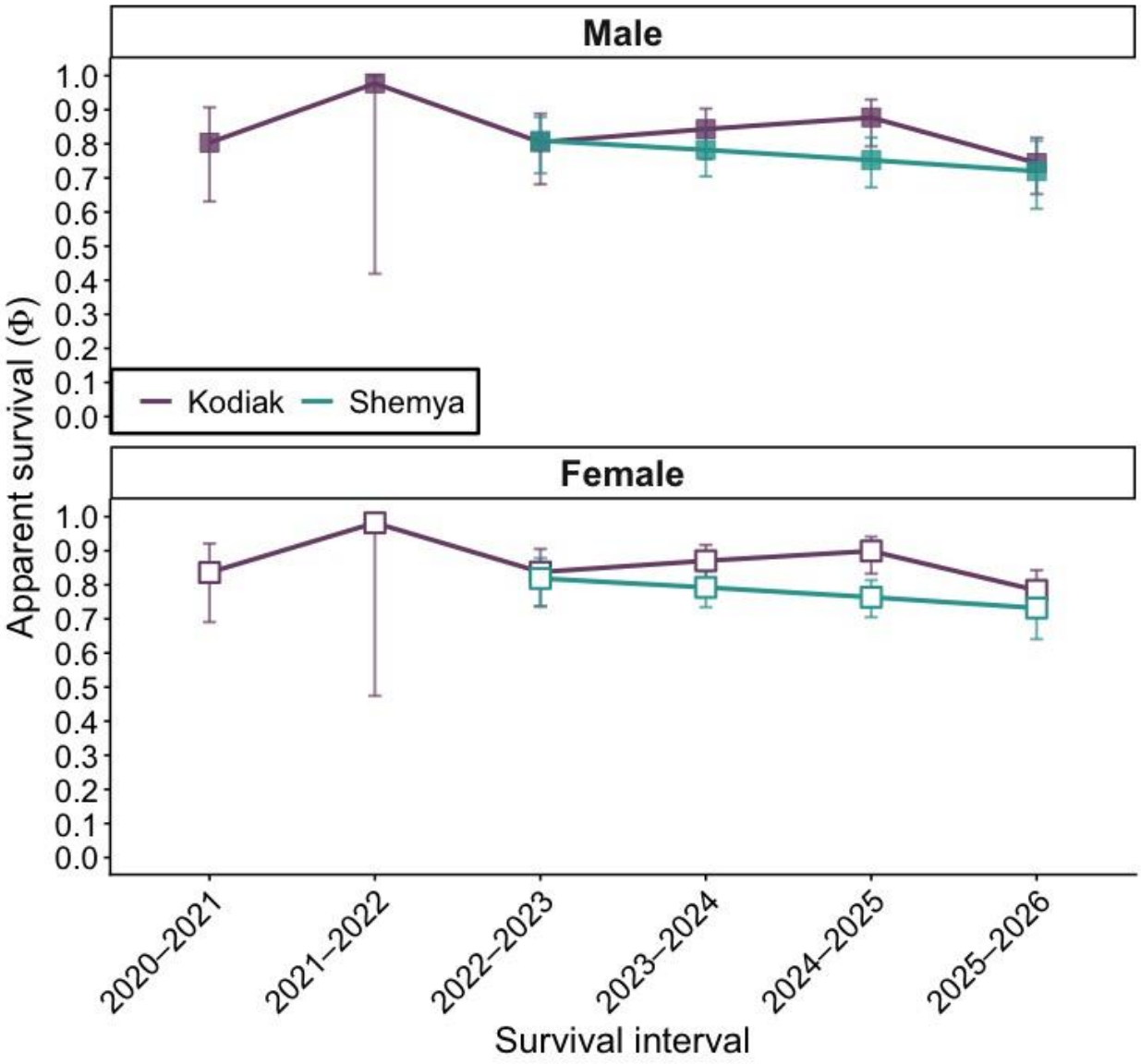

Figure 1.7: Apparent survival estimates ($\Phi \pm 95\%$ CI) for male and female emperor geese on Kodiak and Shemya, across winter-to-winter annual survival intervals.

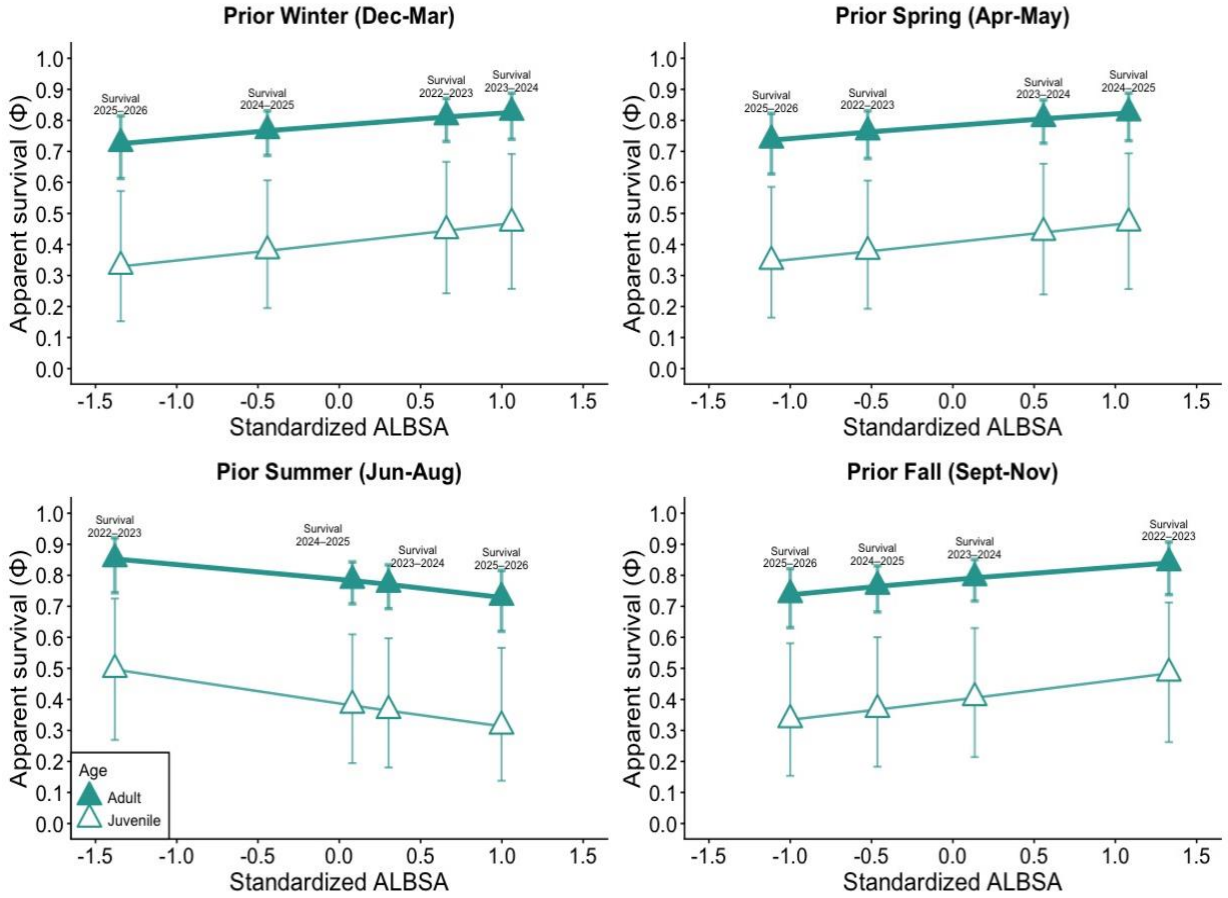

Figure 1.8: Predicted apparent annual survival (Φ) of adult and juvenile emperor geese wintering at Shemya as a function of standardized ALBSA from prior winter (Dec–Mar), spring (Apr–May), summer (Jun–Aug), and fall (Sep–Nov) periods. Survival increased under more positive prior winter, spring, and fall ALBSA conditions, but decreased under more positive prior summer ALBSA conditions. Juveniles were consistently lower than adults across all seasonal relationships. Error bars indicate 95% confidence intervals.

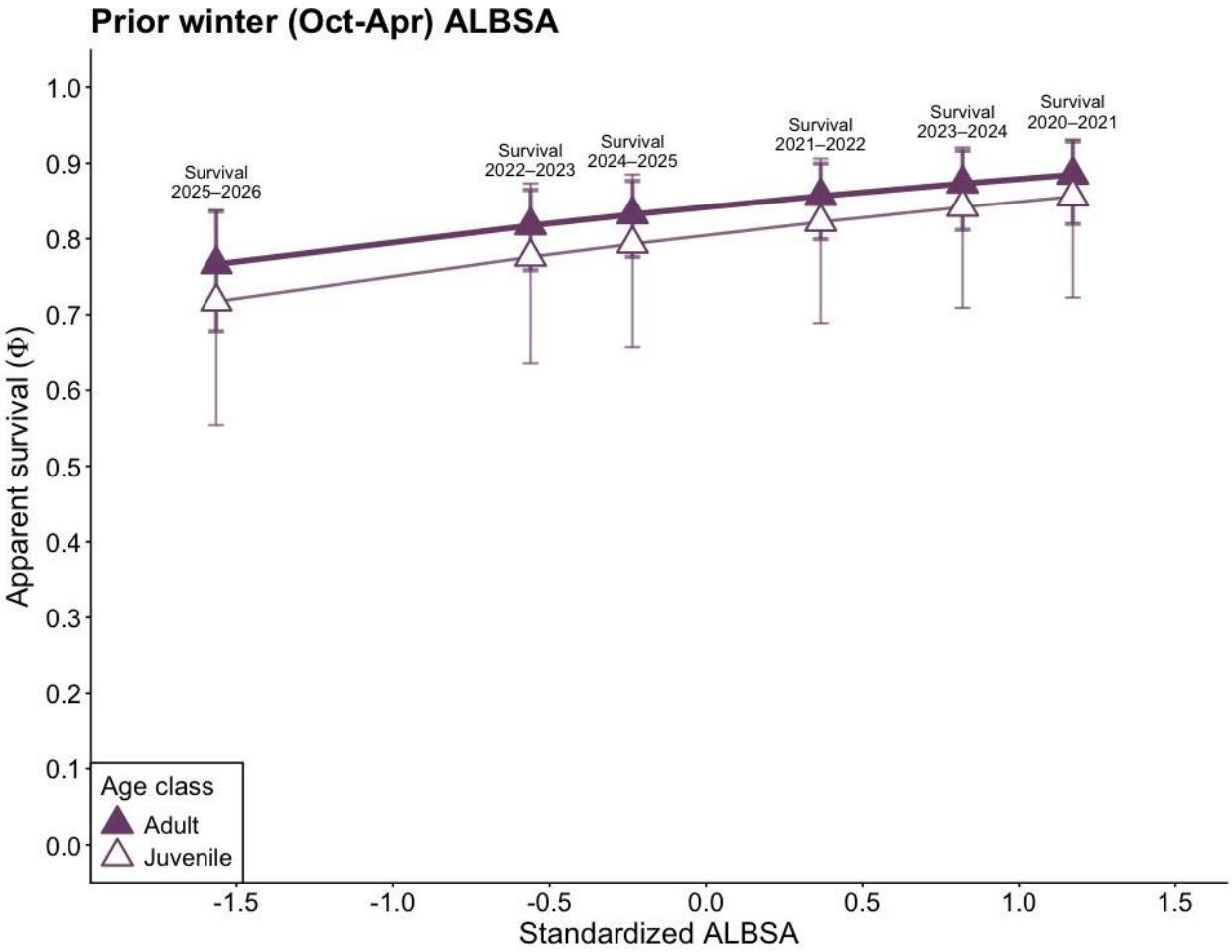

Figure 1.9: Predicted apparent annual survival (Φ) of adult and juvenile emperor geese wintering at Kodiak as a function of standardized ALBSA from the prior winter (Oct-Apr). Survival increased under more positive prior winter ALBSA conditions for both age classes, while juveniles were slightly lower. Error bars indicate 95% confidence intervals.

References

Afton, A., & Paulus, S. (1992). Incubation and Brood Care. In *Ecology and Management of Breeding Waterfowl* (1st ed., pp. 62–108). U of Minnesota Press.

Akaike, H. (1998). Information Theory and an Extension of the Maximum Likelihood Principle. In *Parzen, E., Tanabe, K. and Kitagawa, G., Eds., Selected Papers of Hirotugu Akaike* (pp. 199–213). Springer Series in Statistics (Perspectives in Statistics).

Alaska Department of Fish and Game. (2017). Customary and traditional use worksheet: Migratory game birds, featuring emperor goose. *Alaska Department of Fish and Game, Division of Subsistence*, *January 17 Board of Game Meeting*(01).

Alaska Migratory Bird Co-Management Council. (2016). *Management Plan for the Emperor Goose* (p. 12pp.).

Ankney, C., & Macinnes, C. (1978). Nutrient Reserves and Reproductive Performance of Female Lesser Snow Geese. *The Auk*, *95*(3). https://digitalcommons.usf.edu/auk/vol95/iss3/2

Aubry, L. M., Rockwell, R. F., Cooch, E. G., Brook, R. W., Mulder, C. P. H., & Koons, D. N. (2013). Climate change, phenology, and habitat degradation: Drivers of gosling body condition and juvenile survival in lesser snow geese. *Global Change Biology*, *19*(1), 149–160. https://doi.org/10.1111/gcb.12013

Bearhop, S., Fiedler, W., Furness, R. W., Votier, S. C., Waldron, S., Newton, J., Bowen, G. J., Berthold, P., & Farnsworth, K. (2005). Assortative mating as a mechanism for rapid evolution of a migratory divide. *Science*, *310*(5747), 502–504. https://doi.org/10.1126/science.1115661

Black, J. M., Carbone, C., Wells, R. L., & Owen, M. (1992). Foraging dynamics in goose flocks: The cost of living on the edge. *Animal Behaviour*, *44*(1), 41–50. https://doi.org/10.1016/S0003-3472(05)80752-3

Brêthes, J.-C., Ferreyra, G., & de la Vega, S. (1994). Distribution, growth and reproduction of the limpet Nacella (Patinigera) concinna (Strebel 1908) in relation to potential food availability, in Esperanza Bay (Antarctic Peninsula). *Polar Biology*, *14*(3), 161–170. https://doi.org/10.1007/BF00240521

Burnham, K. P., & Anderson, D. R. (1998). *Model Selection and Inference*. Springer New York. https://doi.org/10.1007/978-1-4757-2917-7

Burnham, K. P., Anderson, D. R., White, G. C., Brownie, C., & Pollock, K. H. (1987). *Design analysis methods for fish survival experiments based on release–recapture.*

Carrington, E. (2002). Seasonal variation in the attachment strength of blue mussels: Causes and consequences. *Limnology and Oceanography*, *47*(6), 1723–1733. https://doi.org/10.4319/lo.2002.47.6.1723

Clausen, K. K., Madsen, J., & Tombre, I. M. (2015). Carry-Over or Compensation? The Impact of Winter Harshness and Post-Winter Body Condition on Spring-Fattening in a Migratory Goose Species. *PLOS ONE*, *10*(7), e0132312. https://doi.org/10.1371/journal.pone.0132312

Cleasby, I. R., Bodey, T. W., Vigfusdottir, F., McDonald, J. L., McElwaine, G., Mackie, K., Colhoun, K., & Bearhop, S. (2017). Climatic conditions produce contrasting influences on demographic traits in a long-distance Arctic migrant. *Journal of Animal Ecology*, *86*(2), 285–295. https://doi.org/10.1111/1365-2656.12623

Cox, C. J., Stone, R. S., Douglas, D. C., Stanitski, D. M., & Gallagher, M. R. (2019). The Aleutian Low-Beaufort Sea Anticyclone: A Climate Index Correlated With the Timing of

Springtime Melt in the Pacific Arctic Cryosphere. *Geophysical Research Letters*, *46*(13), 7464–7473. https://doi.org/10.1029/2019GL083306

Eisenhauer, D. I., & Kirkpatrick, C. M. (1977). Ecology of the Emperor Goose in Alaska. *Wildlife Monographs*, (57,), 3–62.

Ely, C. R., Bollinger, K. S., Densmore, R. V., Rothe, T. C., Petrula, M. J., Takekawa, J. Y., & Orthmeyer, D. L. (2007). Reproductive Strategies of Northern Geese: Why Wait? *The Auk*, *124*(2), 594–605. https://doi.org/10.1093/auk/124.2.594

Ewanchuk, P. J., & Bertness, M. D. (2003). Recovery of a northern New England salt marsh plant community from winter icing. *Oecologia*, *136*(4), 616–626. https://doi.org/10.1007/s00442-003-1303-7

Fischer, J. B., Stehn, R. A., Bowman, T. D., Platte, R. M., Eldridge, W. D., Hodges, J. I., & Butler, W. I. (2018). Coordinated aerial and ground surveys document long-term recovery of geese and eiders on the Yukon–Kuskokwim Delta, Alaska, 1985–2014. In W. D. Shuford, R. E. Gill, & C. M. Handel, *Trends and Traditions: Avifaunal Change in Western North America* (pp. 148–160). Western Field Ornithologists. https://doi.org/10.21199/SWB3.7

Frederiksen, M., Daunt, F., Harris, M. P., & Wanless, S. (2008). The demographic impact of extreme events: Stochastic weather drives survival and population dynamics in a long-lived seabird. *Journal of Animal Ecology*, *77*(5), 1020–1029. https://doi.org/10.1111/j.1365-2656.2008.01422.x

Frost, C. J., Safine, D. E., Fischer, J. B., & Osnas, E. E. (2024). *Emperor Goose Population Index Update* [Application/pdf]. U.S. Fish and Wildlife Service, Migratory Bird Management, Alaska Region. https://doi.org/10.7944/P5AE-3E22

Gill, R. E., & Petersen, M. R. (1982). Population and status of Emperor Geese along the north side of the Alaska Peninsula. *Wildfowl*, *33*, 31–38.

Guéry, L., Descamps, S., Pradel, R., Hanssen, S. A., Erikstad, K. E., Gabrielsen, G. W., Gilchrist, H. G., & Bêty, J. (2017). Hidden survival heterogeneity of three Common eider populations in response to climate fluctuations. *Journal of Animal Ecology*, *86*(3), 683–693. https://doi.org/10.1111/1365-2656.12643

Gupte, P. R., Koffijberg, K., Müskens, G. J. D. M., Wikelski, M., & Kölzsch, A. (2019). Family size dynamics in wintering geese. *Journal of Ornithology*, *160*(2), 363–375. https://doi.org/10.1007/s10336-018-1613-5

Hanson, W. R. (1963). *Calculation of Productivity, Survival, and Abundance of Selected Vertebrates from Sex and Age Ratios*. Wildlife Society. https://www.jstor.org/stable/3830506

Harrison, X. A., Blount, J. D., Inger, R., Norris, D. R., & Bearhop, S. (2011). Carry-over effects as drivers of fitness differences in animals: Carry-over effects in animal populations. *Journal of Animal Ecology*, *80*(1), 4–18. https://doi.org/10.1111/j.1365-2656.2010.01740.x

Heppell, S. S., Caswell, H., & Crowder, L. B. (2000). Life histories and elasticity patterns: Perturbation analysis for species with minimal demographic data. *Ecology*, *81*(3), 654–665. https://doi.org/10.1890/0012-9658(2000)081[0654:LHAEPP]2.0.CO;2

Hupp, J. W., Schmutz, J. A., & Ely, C. R. (2008a). Seasonal Survival of Radiomarked Emperor Geese in Western Alaska. *The Journal of Wildlife Management*, *72*(7), 1584–1595. https://doi.org/10.2193/2007-358

Hupp, J. W., Schmutz, J. A., & Ely, C. R. (2008b). The Annual Migration Cycle of Emperor Geese in Western Alaska. *Arctic*, *61*(1), 23–34.

Koons, D. N., Gunnarsson, G., Schmutz, J. A., & Rotella, J. J. (2014). Drivers of waterfowl population dynamics: From teal to swans. *Wildfowl*, (Special Issue 4), 169–191.

Laake, J. L. (2013). *RMark: An R Interface for analysis of capture-recapture data with MARK* (AFSC Processed Rep. 2013-01; p. 25).

Laurenson, K., Wood, M. J., Birkhead, T. R., Priestley, M. D. K., Sherley, R. B., Fayet, A. L., Guilford, T., Hatchwell, B. J., & Votier, S. C. (2025). Long-term multi-species demographic studies reveal divergent negative impacts of winter storms on seabird survival. *Journal of Animal Ecology*, *94*(1), 139–153. https://doi.org/10.1111/1365-2656.14227

Lebreton, J.-D., Burnham, K. P., Clobert, J., & Anderson, D. R. (1992). Modeling Survival and Testing Biological Hypotheses Using Marked Animals: A Unified Approach with Case Studies. *Ecological Monographs*, *62*(1), 67–118. https://doi.org/10.2307/2937171

Lewis, T. L., Dimarzio, T. J., & Schamber, J. L. (2021). Distribution and Population Size of Emperor Geese during the Breeding Season on the Seward Peninsula, Alaska. *ARCTIC*, *74*(1), 12–21. https://doi.org/10.14430/arctic72055

Marra, P. P., Cohen, E. B., Loss, S. R., Rutter, J. E., & Tonra, C. M. (2015). A call for full annual cycle research in animal ecology. *Biology Letters*, *11*(8), 20150552. https://doi.org/10.1098/rsbl.2015.0552

Mason, D. D., Barboza, P. S., & Ward, D. H. (2006). Nutritional Condition of Pacific Black Brant Wintering at the Extremes of Their Range. *The Condor*, *108*(3), 678–690. https://doi.org/10.1093/condor/108.3.678

McCullagh, P., & Nelder, J. A. (2019). *Generalized Linear Models* (2nd ed.). Routledge. https://doi.org/10.1201/9780203753736

Mengak, L. F., Naves, L. C., & Schamber, J. L. (2022). Survival estimates and hunter outreach are priorities for the collaborative harvest management of Emperor Goose in Alaska. *Ornithological Applications*, *124*(4), duac036. https://doi.org/10.1093/ornithapp/duac036

Mesquita, M. S., Atkinson, D. E., & Hodges, K. I. (2010). Characteristics and Variability of Storm Tracks in the North Pacific, Bering Sea, and Alaska*. *Journal of Climate*, *23*(2), 294–311. https://doi.org/10.1175/2009JCLI3019.1

Naves, L., Mengak, L., & Fall, J. (2025). Integrating Indigenous knowledge across homelands and scientific knowledge to support collaborative harvest management for Emperor Goose in Alaska. *Ecology and Society*, *30*(4), art10. https://doi.org/10.5751/ES-16409-300410

Newton, I. (2004). Population limitation in migrants. *Ibis*, *146*(2), 197–226. https://doi.org/10.1111/j.1474-919X.2004.00293.x

Newton, I. (2007). Chapter 26—Population limitation – breeding and wintering areas. In *The Migration Ecology of Birds* (First, pp. 751–775). Acedmic Press. https://doi.org/10.1016/B978-012517367-4.50026-7

Norris, D. R., & Marra, P. P. (2007). Seasonal Interactions, Habitat Quality, and Population Dynamics in Migratory Birds. *The Condor*, *109*(3), 535–547. https://doi.org/10.1093/condor/109.3.535

Norris, D. R., & Taylor, C. M. (2006). Predicting the consequences of carry-over effects for migratory populations. *Biology Letters*, *2*(1), 148–151. https://doi.org/10.1098/rsbl.2005.0397

O'Hara, R. B., & Kotze, D. J. (2010). Do not log-transform count data. *Methods in Ecology and Evolution*, *1*(2), 118–122. https://doi.org/10.1111/j.2041-210X.2010.00021.x

Overland, J. E., & Wang, M. (2005). The Arctic climate paradox: The recent decrease of the Arctic Oscillation. *Geophysical Research Letters*, *32*(6). https://doi.org/10.1029/2004GL021752

Overland, J. E., & Wang, M. (2025). Future Climate Change in the Northern Bering Sea. *International Journal of Climatology*, *45*(1), e8697. https://doi.org/10.1002/joc.8697

Pacific Flyway Council. (2016). *Management plan for the emperor goose*. Pacific Flyway Council, Care of U.S. Fish and Wildlife Service, Division of Migratory Bird Management, Vancouver, WA, USA.

Pearce, J. M., Dooley, J., Patil, V., Sformo, T. L., Daniels, B. L., Greene, A., & Leafloor, J. (2022). *Arctic Geese of North America*. https://doi.org/10.25923/txnp-hb02

Petersen, M. R. (1992). Reproductive Ecology of Emperor Geese: Survival of Adult Females. *The Condor*, *94*(2), 398–406. https://doi.org/10.2307/1369212

Pohlen, Z. M., Johnson, J. A., DiMarzio, T. J., & Lewis, T. (2023). *Emperor Goose Surveys at Eareckson Air Station, Alaska* (Unpublished Report VNMHOS220777; p. 17). USFWS Division of Migratory Birds.

Poussart, C., Gauthier, G., & Larochelle, J. (2001). Incubation behaviour of greater snow geese in relation to weather conditions. *Canadian Journal of Zoology*, *79*(4), 671–678. https://doi.org/10.1139/z01-023

Prevett, J. P., & MacInnes, C. D. (1980). Family and Other Social Groups in Snow Geese. *Wildlife Monographs*, (71), 3–46.

R Core Team. (2024). *R: A language and environment for statistical computing.* [Computer software]. https://www.R-project.org/

Robertson, B. A., & Hutto, R. L. (2006). A Framework for Understanding Ecological Traps and an Evaluation of Existing Evidence. *Ecology*, *87*(5), 1075–1085. https://doi.org/10.1890/0012-9658(2006)87[1075:AFFUET]2.0.CO;2

Robertson, G., & Cooke, F. (1999). Winter Philopatry in Migratory Waterfowl. *The Auk*, *116*(1). https://digitalcommons.usf.edu/auk/vol116/iss1/3

Rodionov, S. N., Bond, N. A., & Overland, J. E. (2007). The Aleutian Low, storm tracks, and winter climate variability in the Bering Sea. *Deep Sea Research Part II: Topical Studies in Oceanography*, *54*(23–26), 2560–2577. https://doi.org/10.1016/j.dsr2.2007.08.002

Rönkä, M., Saari, L., Hario, M., Hänninen, J., & Lehikoinen, E. (2011). Breeding success and breeding population trends of waterfowl: Implications for monitoring. *Wildlife Biology*, *17*(3), 225–239. https://doi.org/10.2981/09-064

Root, T. (1988). Energy Constraints on Avian Distributions and Abundances. *Ecology*, *69*(2), 330–339. https://doi.org/10.2307/1940431

Rushing, C. S., Hostetler, J. A., Sillett, T. S., Marra, P. P., Rotenberg, J. A., & Ryder, T. B. (2017). Spatial and temporal drivers of avian population dynamics across the annual cycle. *Ecology*, *98*(11), 2837–2850. https://doi.org/10.1002/ecy.1967

Sæther, B.-E., & Bakke, Ø. (2000). Avian life history variation and contribution of demographic traits to the population growth rate. *Ecology*, *81*(3), 642–653. https://doi.org/10.1890/0012-9658(2000)081[0642:ALHVAC]2.0.CO;2

Scheiber, I. B. R., Weiß, B. M., Frigerio, D., & Kotrschal, K. (2005). Active and passive social support in families of greylag geese (Anser anser). *Behaviour*, *142*(11–12), 1535–1557. https://doi.org/10.1163/156853905774831873

Schlaepfer, M. A., Runge, M. C., & Sherman, P. W. (2002). Ecological and evolutionary traps. *Trends in Ecology & Evolution*, *17*(10), 474–480. https://doi.org/10.1016/S0169-5347(02)02580-6

Schmutz, J. A. (1995). Evidence of Emperor Geese Breeding in Russia and Staging in Alaska. *The Auk*, *112*(4), 1037–1038. https://doi.org/10.2307/4089035

Schmutz, J. A., Cantor, S. E., & Petersen, M. R. (1994). Seasonal and Annual Survival of Emperor Geese. *The Journal of Wildlife Management*, *58*(3), 525. https://doi.org/10.2307/3809325

Schmutz, J. A., Hobson, K. A., & Morse, J. A. (2006). An isotopic assessment of protein from diet and endogenous stores: Effects on egg production and incubation behaviour of geese. *Ardea*, *94*(3), 385–397.

Schmutz, J. A., Petersen, M. R., & Rockwell, R. F. (2020). Emperor Goose (Anser canagicus). In S. M. Billerman, B. K. Keeney, P. G. Rodewald, & T. S. Schulenberg (Eds.), *Birds of the World Online*. Cornell Lab of Ornithology. https://doi.org/10.2173/bow.empgoo.01

Schmutz, J. A., Rockwell, R. F., & Petersen, M. R. (1997). Relative Effects of Survival and Reproduction on the Population Dynamics of Emperor Geese. *The Journal of Wildlife Management*, *61*(1), 191. https://doi.org/10.2307/3802428

Sedinger, J. S., Chelgren, N. D., Ward, D. H., & Lindberg, M. S. (2008). Fidelity and breeding probability related to population density and individual quality in black brent geese Branta bernicla nigricans. *Journal of Animal Ecology*, *77*(4), 702–712. https://doi.org/10.1111/j.1365-2656.2008.01403.x

Sedinger, J. S., Lindberg, M. S., & Chelgren, N. D. (2001). Age-specific breeding probability in black brant: Effects of population density. *Journal of Animal Ecology*, *70*(5), 798–807. https://doi.org/10.1046/j.0021-8790.2001.00535.x

Sedinger, J. S., Schamber, J. L., Ward, D. H., Nicolai, C. A., & Conant, B. (2011). Carryover Effects Associated with Winter Location Affect Fitness, Social Status, and Population Dynamics in a Long-Distance Migrant. *The American Naturalist*, *178*(5), E110–E123. https://doi.org/10.1086/662165

Sherry, T. W., & Holmes, R. T. (1995). Summer versus winter limitation of populations: What are the issues and what is the evidence? In *Ecology and management of neotropical migraotory birds: A synthesis and review of critical issues* (pp. 85–121). Oxford University Press.

Smith, M. A., Sullender, B. K., Koeppen, W. C., Kuletz, K. J., Renner, H. M., & Poe, A. J. (2019). An assessment of climate change vulnerability for Important Bird Areas in the Bering Sea and Aleutian Arc. *PLOS ONE*, *14*(4), e0214573. https://doi.org/10.1371/journal.pone.0214573

Stearns, S. C. (1992). *The Evolution of Life Histories*. Oxford University Press.

Uher-Koch, B. D., Buchheit, R. M., Eldermire, C. R., Wilson, H. M., & Schmutz, J. A. (2021). Shifts in the wintering distribution and abundance of emperor geese in Alaska. *Global Ecology and Conservation*, *25*, e01397. https://doi.org/10.1016/j.gecco.2020.e01397

USFWS. (1989). *Comprehensive management plans for arctic nesting geese in Alaska.* (p. 99pp.).

USFWS. (2025). *Waterfowl Population Status, 2025*. U.S. Department of the Interior.

Vermaire, J. C., Pisaric, M. F. J., Thienpont, J. R., Courtney Mustaphi, C. J., Kokelj, S. V., & Smol, J. P. (2013). Arctic climate warming and sea ice declines lead to increased storm

surge activity. *Geophysical Research Letters*, *40*(7), 1386–1390. https://doi.org/10.1002/grl.50191

Walsh, J. E., & Brettschneider, B. (2019). Attribution of recent warming in Alaska. *Polar Science, ISAR-5/ Fifth International Symposium on Arctic Research*, *21*, 101–109. https://doi.org/10.1016/j.polar.2018.09.002

Wendler, G., Galloway, K., & Stuefer, M. (2016). On the climate and climate change of Sitka, Southeast Alaska. *Theoretical and Applied Climatology*, *126*(1), 27–34. https://doi.org/10.1007/s00704-015-1542-7

White, G. C., & Burnham, K. P. (1999). Program MARK: Survival estimation from populations of marked animals. *Bird Study*, *46*(sup1), S120–S139. https://doi.org/10.1080/00063659909477239

Wilson, H. M. (2016). *Distribution and abundance of waterbirds in the Kodiak Archipelago, Alaska winter 2015* [Interim Report for Kodiak Subsistence Regional Advisory Council Meeting]. U.S. Fish and Wildlife Service, Waterfowl Management.

CHAPTER 2:

DIET, RESOURCE USE AND BODY CONDITION OF EMPEROR GEESE AT THE GEOGRAPHIC EXTREMES OF THEIR WINTER RANGE

Introduction

When populations occupy environmentally distinct regions within a species' range, differences in resource availability, composition or accessibility can lead to spatial variation in diet and resource use (Leibold et al., 2004; Wiens, 1989). As a result, consumers adjust their foraging behavior in ways that maximize energy intake under constraint, as formalized by optimal foraging theory (Fretwell & Lucas, 1969). Such adjustments can manifest as shifts in diet composition, changes in dietary niche breadth, or increased individual specialization, especially when preferred resources are limited or patchily distributed. These differences can, in turn, influence energetic stores, body condition, and ultimately individual fitness (Harrison et al., 2011).

Migratory birds provide a useful context for examining links between resource availability, diet, niche structure, and individual fitness – many species occupy geographically diverse ranges that frequently shift throughout the year as individuals migrate to access new resources. Moreover, conditions experienced during different parts of the annual cycle, such as breeding or winter, can influence fitness through carry-over effects in subsequent seasons (Norris & Taylor, 2006; Sedinger et al., 2011). For many migratory birds, winter is often the most energetically constraining period of the annual cycle, when individuals must maintain body condition and build energy reserves necessary for subsequent migration and breeding (Salewski & Bruderer, 2007). During winter, individuals must meet energetic demands while operating

within the constraints of local environmental conditions. For avian species with broad winter ranges, individuals may encounter strong gradients in environmental conditions, resulting in spatial variation in resource availability and divergent foraging strategies across the winter range (Newton, 2004). Successful overwintering often depends on the ability to maintain energy balance through consistent access to resources, despite variability in weather and habitat conditions (Araújo et al., 2019). Under optimal foraging theory, individuals are expected to maximize energetic efficiency by minimizing foraging costs while maximizing nutrient intake (Pyke et al., 1977). Consequently, more constrained environments—where resources are less diverse, less abundant, or more difficult to access—may increase competition for profitable resources, leading some individuals to rely heavily on energetically efficient prey while others are forced to exploit lower-quality resources. This may result in greater variation in resource use among individuals and altered patterns of dietary diversity. In contrast, less constrained environments should provide access to a broader range of profitable resources, allowing broader niche use and greater dietary diversity.

The Emperor Goose (*Anser canagicus*) provides an ideal species to test these predictions under challenging winter conditions. Emperor Geese are endemic and year-round occupants of the Bering Sea, breeding primarily on the Yukon–Kuskokwim Delta in western Alaska and wintering across a broad range spanning thousands of kilometers that includes the Alaska Peninsula, Kodiak Archipelago, Aleutian Islands, and eastern Russia (Hupp et al., 2008*; Fig. 1.1*). Unlike many North American geese that winter at more southerly latitudes and rely heavily on terrestrial vegetation and agricultural subsidies, Emperor Geese occupy coastal habitats at remote northern latitudes (Eisenhauer & Kirkpatrick, 1977) where they forage almost exclusively in marine intertidal ecosystems during winter (Cottam, 1939; Schmutz et al., 2020). Resource

availability of emperor geese during winter is strongly influenced by tidal cycles, intertidal icing, substrate type, and oceanographic conditions (i.e. wind and waves action driven by storm frequency and intensity), and these factors often differ widely across their winter range. Thus, uch differences likely shape the potential to shape both the composition of prey communities and how individuals access them, creating strong potential for spatial variation in diet composition and resource across the winter range.

We leveraged this range-wide heterogeneity by comparing resource use and body condition of Emperor Geese wintering at two geographic extremes of their wintering range: the Kodiak Archipelago at the eastern end of their range and Shemya Island at the western end (*Fig. 1.2*). Kodiak is characterized by large, sheltered bays and extensive estuarine systems that support diverse and accessible food resources, including abundant mariner invertebrates (Clark, 1998). In contrast, Shemya is a small, exposed island in the western Aleutian Island chain with predominantly rocky shorelines and persistent wind and wave disturbances, limiting food availability and access (Rodionov et al., 2007). Because Emperor Geese rely almost exclusively on intertidal resources during winter, these two wintering sites provide a natural contrast to evaluate how environmental conditions shape diet composition and niche dynamics.

We used stable isotope analysis to quantify resource use, which captures assimilated diets over relevant temporal scales. Stable isotope analysis is a powerful tool for examining spatial variation in resource use because $\delta^{13}C$ and $\delta^{15}N$ values allow inference on resource origin and trophic position (Peterson & Fry, 1987; Post, 2002), while variation among individuals provides insight into population-level dietary isotopic niche breadth and individual specialization (Bearhop et al., 2004). Because isotope values integrate diet over ecologically relevant time

scales, they can reveal spatial patterns in resource use not detectable through direct observation alone (Bearhop et al., 1999; Votier et al., 2003).

Variation in resource use across wintering environments may also be reflected in differences in body condition, which represents the balance between energy intake and expenditure (Brown, 1996). In migratory birds, body condition provides an integrated measure of energetic state and can reflect both the quality and availability of resources within a given environment (Harrison et al., 2011). If environmental conditions and constraints differ across wintering regions, then theory predicts corresponding differences in both resource use and body condition. Drawing from this foundation, we tested three hypotheses: first, diet composition will differ between Kodiak and Shemya, reflecting shifts in resource use consistent with local resource availability and accessibility. Second, isotopic niche breadth will be narrower in the more constrained environment (Shemya), consistent with reduced resource diversity, availability and foraging constraints. Third, body condition will be lower and/or more variable in the constrained environment (Shemya), reflecting limited resource availability, diversity and potential for energy acquisition.

By quantifying spatial variation in winter resource use, isotopic niche structure, and body condition, this study provides mechanistic insights into how environmental heterogeneity in winter resources shapes foraging ecology of emperor geese, with implications for individual fitness, whilst highlighting the potential costs and benefits of winter site selection.

Methods

Study area

Shemya Island (52°N, 174°W) is a small (15 km²), low-lying island characterized by exposed rocky coastlines and frequent storm activity (Gibson, 1981; Rodionov et al., 2005).

Over the winter study period (2022-2025), winter conditions (November—April) on Shemya were characterized by relatively mild mean temperatures, averaging 35.3 °F (± SD 0.9 °F), and consistently high wind speeds (average windspeed: 17.2 ± SD 1.2 kts; average maximum sustained windspeed 29.0 ± SD 0.6 kts). Precipitation was relatively low (average winter precipitation during the study period ≈ 12.4 ± 4.68cm; Shemya Airforce Station; NOAA, 1999; *Supplementary Table 2.1)*. Suitable foraging habitat is of limited availability and primarily consists of intertidal macroalgae and sparse coastal plants (Uher-Koch et al., 2021). Emperor geese occur at relatively low densities and are distributed along the island's perimeter.

The Kodiak Archipelago (57°N and 152°W) is a collection of 14 islands located in the Gulf of Alaska. Kodiak is influenced by the Alaska Current, a northward-flowing coastal current that transports relatively warm water along the Gulf of Alaska. Interaction of this current with the continental shelf promotes mixing and retention of nutrients in nearshore environments, supporting productive coastal food webs (Stabeno et al., 2016). Kodiak is characterized by mountain ranges, rainforests, and deep bays with estuaries at their heads (Clark, 1998; USGS, 1995). Winter conditions on Kodiak were more variableover the winter study period (2020-2025), included more variable temperatures(34.4 ± SD 1.5 °F, and substantially lower wind speeds (9.7 ± 0.3 kts; maximum 18.8 ± 0.6 kts), and higher precipitation (average winter precipitation during study period 41.0 ± 9.72 at Kodiak Airport; NOAA 1999) compared to Shemya. Kodiak supports large aggregations of wintering emperor geese that occupy estuarine and intertidal habitats (Wilson, 2016). Our study occurred primarily in Women's Bay, a protected inlet with multiple freshwater inputs and extensive intertidal flats located within greater Chiniak Bay on the northeastern side of Kodiak Island (*Fig. 1.3b*). These habitats provide access to a broad and diverse resource base, including intertidal invertebrates (e.g. bivalves and

crustaceans) and vegetative resources (e.g. macroalgae and intertidal grasses; Arsan et al., 2025; Konar et al., 2009).

Sampling

Live captures. Emperor geese were captured on Shemya from 2022–2026 in January and on Kodiak from 2020—2026 in February–March using rocket nets deployed in intertidal habitats. Nets measured approximately 10 m × 15 m and were configured with 4.5-cm mesh, multiple tie-down points, and three to four rocket bridles. Depending on substrate and tidal conditions, rockets were either buried or mounted on tripod stanchions to accommodate substrate and tidal variation. In some cases, emperor goose decoys were used to attract birds into capture areas. Nets were triggered remotely (50–200 m distance) using a handheld blaster that was hardwired to the rockets.

Upon capture, we measured body mass (g) using an electronic scale and recorded structural size as total tarsus length (mm) using calipers. We collected a blood sample from each bird in 2024 and 2025. For each individual, we also determined age class (juvenile or adult) via plumage and foot coloration (*Supplemental Fig. 1.2*), and sex was determined via a cloacal examination for all individuals at time of capture. All capture and handling procedures were approved by the Alaska Department of Fish and Game Institutional Animal Care and Use Committee (IACUC protocol 0080-2024-0001) and followed established guidelines for ethical handling of wildlife.

Stable Isotope Analysis. We collected approximately 0.5 mL of whole blood was collected from the tarsal or jugular vein using 21-gauge syringes for analysis of stable isotope composition. Samples were stored on ice in the field and centrifuged (7000 rpm, 10 min) within 24 hours to separate plasma and red blood cells. Components were stored frozen at −20°C until

analysis. Prior to isotopic analysis, samples were dried at 60°C for 48 hours and homogenized. Samples (1.0–1.2 mg) were weighed into tin capsules and analyzed at EcoCore Analytical Services (Fort Collins, Colorado, USA) using a Costech ECS 4010 elemental analyzer coupled to a Thermo-Fisher Delta V Advantage isotope ratio mass spectrometer. Stable isotope ratios ($\delta^{13}C$ and $\delta^{15}N$) are reported in standard delta (δ) notation:

$$\delta X = [(R_{sample} / R_{standard}) - 1] \times 1000$$

where X represents ^{13}C or ^{15}N, and R is the corresponding isotope ratio ($^{13}C/^{12}C$ or $^{15}N/^{14}N$). Carbon and Nitrogen values are referenced to Vienna Pee Dee Belemnite (VPDB) for $\delta^{13}C$ and atmospheric nitrogen for $\delta^{15}N$. Internal glycine standards (n = 83) were used for quality control yielding standard deviations of ± 0.186 ‰ for $\delta^{13}C$ and ± 0.178 ‰ for $\delta^{15}N$.

Prey item sampling, baseline correction and lipid normalization. Potential dietary sources at each study site were collected from intertidal habitats where emperor geese frequently foraged during the winter sampling period. Sessile invertebrates, including barnacles (*Balanus* spp.; acorn barnacle) and mussels (*Mytilus* spp.; blue mussel), were collected by hand opportunistically from rocky substrates within the intertidal zone. Vegetation, including seaweeds (*Pyropia* spp.; nori and *Fucus* spp.; rockweed) and coastal grasses (*Leymus* spp.; beach rye), were collected from the intertidal zone and adjacent shoreline habitats. All samples were rinsed with deionized water to remove debris and stored frozen at −20°C until processing. Prior to analysis, samples were dried at 60°C for 48 hours and homogenized. For invertebrate samples, soft tissues were removed from shells prior to drying. Homogenized subsamples (1.0 – 1.2 mg for invertebrate and 3.0 – 3.2 mg for vegetation) were weighed into tin capsules and analyzed for $\delta^{13}C$ and $\delta^{15}N$ as described for blood samples.

Because isotopic baselines vary among ecosystems (France, 1994; Vizzini et al., 2005), raw $\delta^{13}C$ and $\delta^{15}N$ emperor goose blood values were corrected using site-specific primary consumer baselines. We used barnacles (*Balanomorpha spp.)* as baseline organisms because they are long-lived sessile filter feeders that integrate local isotopic conditions and represent a stable reference for trophic comparisons (Fukumori et al., 2008; Kristensen et al., 2016; Post, 2002). Emperor goose isotope values were baseline-corrected as:

$$\delta^{15}N_{\text{Baseline corrected}} = \delta^{15}N_{\text{goose}} - \delta^{15}N_{\text{baseline}}$$

$$\delta^{13}C_{\text{Baseline corrected}} = \delta^{13}C_{\text{goose}} - \delta^{13}C_{\text{baseline}}$$

Because lipids are depleted in ^{13}C relative to proteins and carbohydrates, variation in lipid content can bias $\delta^{13}C$ values. Barnacle tissues were therefore lipid-corrected using a normalization approach (Post et al., 2007):

$$\delta\,^{13}C_{\text{normalized}} = \delta + {}^{13}C_{\text{ untreated}} + \Delta^{13}C$$

Where: $\Delta^{13}C = -3.32 + 0.99$ C:N

This method uses the measured carbon-to-nitrogen (C:N) ratio as a proxy for lipid content and produces values comparable to chemical lipid extraction while preserving sample integrity for $\delta^{15}N$ analysis (Post et al., 2007). We did not apply lipid correction to blood samples because avian blood contains low lipid concentrations making lipid effects on $\delta^{13}C$ minimal (Bearhop et al., 2000, 2002) and C:N ratios for blood components did not exceed 3 for any samples.

Statistical Analyses

All analysis were carried out in program R, version 4.4.3. (R Core Team., 2024).

Tissue comparison. Plasma and red blood cell isotope values were compared using paired samples from individual birds, with baseline-corrected $\delta^{13}C$ and $\delta^{15}N$ values to account for spatial variation in isotopic baselines at each site. Linear mixed-effects models ('lme4' and

'lmerTest' packages; 'lmer' function; Bates et al., 2015; Kuznetsova et al., 2017) were used to test for differences between tissue types (red blood cell vs. plasma), with tissue type included as a fixed effect and individual bird included as a random effect. To evaluate whether tissue-specific differences varied between wintering regions, an additional model included site and a tissue × site interaction as fixed effects. Pearson correlations were used to assess concordance between tissues ('stats' package; 'cor.test' function; R Core Team 2024). In large-bodied seabirds, plasma typically reflects diet integrated over approximately two weeks, whereas red blood cells integrate diet over longer periods of one to two months (Barquete et al., 2013; Hobson & Clark, 1992a). Thus, because sampling on Shemya occurred roughly 3-6 weeks after arrival at this wintering site, red blood cell values may reflect assimilated diet from both Shemya and prior staging areas , whereas plasma values likely reflect only those resources as assimilated on Shemya

Isotopic niche analysis. We quantified isotopic niche width of emperor geese, as well as overlap between wintering sites, using the Stable Isotope Bayesian Ellipses in R (SIBER package; 'createSiberObject', 'siberEllipses', 'siberMVN', 'groupMetricsML' functions; Jackson et al., 2011). SIBER characterizes niche width in bivariate $\delta^{13}C$–$\delta^{15}N$ space by fitting standard ellipses to isotope data, providing a multivariate estimate of core isotopic niche area. We conducted analyses separately by site (Kodiak, Shemya) and year (2024, 2025). For each group, we calculated the small sample size–corrected standard ellipse area (SEA_C) as a maximum-likelihood estimate of core niche width, which encompasses approximately 40% of the data.

To account for uncertainty and enable statistical comparisons among groups, we estimated Bayesian standard ellipse areas (SEA_B) using Markov chain Monte Carlo simulations

(10,000 iterations). Posterior distributions of SEA_B were used to derive median niche width estimates, 95% credible intervals, and the probability that niche width differed among site–year groups.

We quantified pairwise niche overlap by calculating the proportional area of intersection between posterior standard ellipses. For each comparison, ellipses were reconstructed from posterior draws of group mean vectors and covariance matrices, and overlap was calculated for each draw. Directional overlap was summarized as posterior means, medians, and 95% credible intervals, representing the proportion of one group's niche contained within the other and vice versa.

Stable isotope mixing model. To estimate the proportional contribution of major dietary sources to emperor goose diets, we used Bayesian stable isotope mixing models implemented in the R package '*SIMMR'* ('simmr_load' and 'simmr_mcmc' functions; Parnell & Inger, 2016). We fit separate models for each site (Kodiak and Shemya) using isotope values from our plasma samples.

Dietary sources were grouped into ecologically relevant categories based on taxonomic identity and isotopic similarity (*Table 2.1*). Potential dietary sources were collected from intertidal habitats at each study site during the 2024 winter sampling period. Mussels were not observed on Shemya and therefore were not included as a source at that site, but barnacles were retained as a distinct source. Additional sources included marine vegetation (seaweed; genera *Pyropia* or "nori" and *Fucus* or "rockweed") and coastal grass (genus *Leymus* or "beach rye"). Source isotope values ($\delta^{13}C$ and $\delta^{15}N$) were summarized by site to generate mean and standard deviation estimates for each source group.

Trophic discrimination factors of 1.0 ± 0.3 ‰ for $\delta^{13}C$ and 3.0 ± 0.5 ‰ for $\delta^{15}N$ were incorporated into the mixing models to account for isotopic enrichment between diet and consumer tissues (Hobson & Clark, 1992b; Post, 2002). Mixing models were fit using Markov chain Monte Carlo (MCMC) sampling, and convergence was assessed using Gelman–Rubin diagnostics ($\hat{R}$), with values near 1 indicating adequate convergence. Posterior distributions were used to estimate the proportional contribution of each dietary source, and results are reported as medians with 95% credible intervals (2.5–97.5%).

Because source availability differed between sites, models were parameterized using site-specific source pools (see 'Results' section). Thus, the sessile invertebrate category on Kodiak (i.e. mussels and barnacles) is not strictly equivalent to the barnacle-only source on Shemya; therefore, comparisons between sites focus on broader differences in invertebrate versus vegetation contributions rather than direct comparisons of individual prey types.

Body condition index. We estimated body condition of Emperor Geese as the residuals from a linear regression of body mass (g) on tarsus length (mm), providing a size-corrected index of body condition where tarsus length serves as the index of structural size. Positive residuals indicated individuals were heavier than expected for their structural size, whereas negative residuals indicated individuals were lighter than expected. To evaluate variation in body condition, we fit linear models that included the following predictors: study site (Kodiak, Shemya), capture year (2024, 2025, 2026), age class (adult, juvenile), and sex ('stats' package, 'lm' function). We considered additive models as well as models including a site × year interaction to test for spatially varying annual differences in body condition. Candidate models were compared using Akaike's Information Criterion corrected for small sample size (Akaike, 1998; Burnham & Anderson, 1998; Mazerolle, 2023) using the 'AICc modavg' package, and the

'aictab' function. We used the most parsimonious model to interpret patterns of variation in body condition across sites and years (*Table 2.2*).

To assess whether variation in isotopic values was associated with body condition, we examined relationships between plasma $\delta^{13}C$ and $\delta^{15}N$ values and body condition. We standardized body condition (z-scored) prior to analysis and used linear models to evaluate relationships between isotopic values and body condition within each site while accounting for capture year ('stats' package, 'lm' function). Additional models including site × isotope interaction terms were used to test whether relationships differed between wintering sites.

Results

Tissue differences and baseline correction

$\delta^{13}C$ and $\delta^{15}N$ values were strongly correlated between plasma and red blood cells ($\delta^{13}C$: $r = 0.80$; $\delta^{15}N$: $r = 0.77$; $p < 0.001$ for both signatures) within an individual, indicating consistent individual-level patterns across tissues. However, isotope values differed between tissues (*Fig. 2.1*); red blood cells (RBC) were enriched in $\delta^{13}C$ relative to plasma ($\beta = 0.91 \pm 0.06$ SE, $t = 14.85$, $p < 0.001$), whereas $\delta^{15}N$ values were lower in red blood cells compared to plasma ($\beta = -0.36 \pm 0.04$ SE, $t = -8.09$, $p < 0.001$). The magnitude of the plasma–RBC difference in $\delta^{13}C$ varied by site, with greater enrichment on Shemya than Kodiak (tissue × site interaction: $\beta = 0.67 \pm 0.11$ SE, $p < 0.001$), in contrast to $\delta^{15}N$ tissue offsets where there was very little difference across sites ($p = 0.06$). Given these patterns, and the timing of Emperor Goose arrival to wintering grounds relative to tissue-specific integration periods, all subsequent isotopic analyses were conducted using solely plasma isotope values.

Barnacle isotopic values were consistent within sites across years but differed between sites (*Table 2.3*, *Fig. 2.2*). $\delta^{15}N$ was consistently higher on Kodiak (2024: 10.10 ± 0.17 ‰; 2025: 10.04 ± 0.08 ‰) than on Shemya (2024: 8.26 ± 0.07 ‰; 2025: 8.07 ± 0.04 ‰), indicating clear spatial variation in baseline nitrogen signatures. In contrast, $\delta^{13}C$ values were similar across both sites and years (Kodiak: -16.07 ± 0.25 ‰ in 2024, -16.30 ± 0.17 ‰ in 2025; Shemya: -16.40 ± 0.21 ‰ in 2024, -16.37 ± 0.18 ‰ in 2025). Overall, these results indicated stable baseline conditions within sites across years, with pronounced spatial differences in $\delta^{15}N$ between Kodiak and Shemya.

Isotopic Niche Width and Overlap

Mean $\delta^{13}C_{Plasma}$ and $\delta^{15}N_{Plasma}$ values differed among site–year groups (*Table 2.4*), with higher $\delta^{15}N_{Plasma}$ on Kodiak (2024: 3.79 ± 95% CI: 3.43,4.14 and 2025: 2.79 ± 95% CI: 2.66, 2.92) than Shemya (2024: 1.35 ± 95% CI: 1.16,1.55 and 2025: 2.07 ± 95% CI: 1.91, 2.23) in both years. Kodiak samples (2024: -1.16 ± 95% CI: -1.86, -0.45 and 2025: -1.50 ± 95% CI: -1.76, -1.25) also had higher $\delta^{13}C_{Plasma}$ than Shemya samples (2024: 3.15 ± 95% CI: -3.53, -2.76 and 2025: -2.53 ± 95% CI: -2.85, -2.22) in both years. These differences were reflected in isotopic niche width (SEA_C) – in n 2024, niche width on Shemya (SEA_C = 4.68) was substantially greater than on Kodiak (SEA_C = 0.44), while in 202, niche widths were similar between sites (Kodiak: SEA_C = 1.81; Shemya: SEA_C = 1.97). Across the two years of our study, niche width increased on Kodiak while decreasing on Shemya (*Fig. 2.4 and Fig. 2.4*).

Bayesian estimates (SEA_B) supported these same patterns. Credible intervals for niche width did not overlap between sites in 2024 but overlapped in 2025 (*Table 2.4*). Posterior probabilities (*P*) indicated strong support for a larger niche on Shemya than on Kodiak in 2024 ($P = 0$) for Kodiak > Shemya, but weaker support for such differences in 2025 ($P = 0.324$).

There was also strong support for an increase in niche width on Kodiak ($P = 1$) and a decrease on Shemya ($P = 0$) between years, and Bayesian niche overlap estimates further reflected these patterns (*Table 2.5*). There was no overlap in isotopic niche space between sites in 2024 (median = 0% in either direction), but moderate overlap in isotopic niche space in 2025 (median = 19.8% of the Kodiak isotopic niche within Shemya and 18.4% of the Shemya isotopic niche within Kodiak). Overlap between years was minimal on Kodiak (median = 0% in both directions), but greater and asymmetric on Shemya, with 23.2% of Shemya's 2024 isotopic niche overlapping the 2025 isotopic niche and 55.1% of Shemya's 2025 isotopic niche overlapping its 2024 isotopic niche. Nearly all posterior overlap distributions contained many values near zero with a small number of much larger overlap estimates, resulting in strongly skewed distributions where means were sensitive to extreme values and differed from medians. Therefore, overlap was summarized using posterior medians and 95% credible intervals, which better represent the typical posterior estimate and associated uncertainty.

Stable isotope mixing model

Stable isotope mixing models indicated differences in diet composition between sites. It should be noted that mussels (genus *Mytilus* or "blue mussel") and barnacles (genus *Balanus* or "acorn barnacle") collected on Kodiak exhibited similar $\delta^{13}C$ (-16.1 ± 0.56 ‰ vs. -15.7 ± 0.96 ‰) and $\delta^{15}N$ (10.1 ± 0.38 ‰ vs. 9.59 ± 0.55 ‰) values, with substantial overlap in isotopic space. Given this overlap, these sources could not be reliably distinguished in mixing models and were pooled into a single "sessile invertebrate" category. Mussels were not present on Shemya, therefore, only barnacles were included in the "invertebrate" category. On Shemya, barnacles (median = 0.57, 95% CI: 0.52–0.62) and seaweed comprised a substantial proportion of the diet (median = 0.32, 95% CI: 0.22–0.40), while coastal grasss comprised a smaller proportion of the

diet (median = 0.11, 95% CI: 0.04–0.20; *Fig. 2.5*). In contrast, diets on Kodiak were more dominated by sessile invertebrates, which comprised a median of 0.78 (95% credible interval: 0.72–0.85) of the diet (*Fig. 2.6*; *Table 2.6*), while seaweed (median = 0.12, 95% CI: 0.02–0.23) and coastal grasses (median = 0.10, 95% CI: 0.02–0.19) comprised less of the diet and were and more annually variable. Posterior distributions indicated greater reliance on invertebrate prey on Kodiak relative to Shemya, whereas birds on Shemya exhibited greater use of marine vegetation.

Body Condition

Model selection supported an interaction between site and year, whilst controlling for age and sex-specific differences (AICc = 1.00), indicating that differences in body condition between sites varied across years (*Table 2.2*). In 2024, individuals on Shemya were in poorer body condition than birds on Kodiak ($\beta = -312.54 \pm 59.03$, $p < 0.001$). In 2025, body condition on Kodiak was lower than the prior year ($\beta = -289.96 \pm 54.36$, $p < 0.001$), resulting in similar body condition across wintering sites for that year. In 2026, body condition on Kodiak was again higher than on Shemya, although the difference was less pronounced than in 2024 (*Fig. 2.7a; Table 2.7*).

Across all years, juveniles had markedly lower body condition than adults ($\beta = -295.83 \pm 21.26$, $p < 0.001$; Fig. 2.7b.), and males had slightly higher body condition than females ($\beta = 95.81 \pm 16.68$, $p < 0.001$; Fig. 2.7c). Uncorrected adult body mass uncorrected for structural metrics differed significantly between sites as well, with emperor geese on Kodiak (n = 344) weighing 219g more than on Shemya on average (n = 146; 95% CI: 170–269 g; $t = 8.67$, $p < 0.001$; *Fig. 2.8; Table 2.7*). Total tarsus length did not differ between Kodiak and Shemya ($p = 0.21$), indicating similar structural body size across sites despite site-specific differences in mass (*Fig. 2.9; Table 2.7*).

The relationship between $\delta^{15}N$ and body condition differed between sites. On Kodiak, $\delta^{15}N$ was negatively associated with body condition ($\beta = -0.42 \pm 0.20$ SE, $p = 0.039$), indicating that individuals with higher $\delta^{15}N$ values tended to have lower body condition, although the effect size was modest. In contrast, there was no relationship between $\delta^{15}N$ and body condition on Shemya ($\beta = 0.16 \pm 0.12$ SE, $p = 0.20$).The interaction between $\delta^{15}N$ and site was not significant ($p = 0.17$), indicating that slopes did not differ strongly between sites (*Fig. 2.10*).

Discussion

Resource use, isotopic niche structure, and body condition of emperor geese varied between wintering sites and among years. Notably, isotopic niche patterns, as measured by niche ellipses, strongly differed between Kodiak and Shemya, with complete ellipsoid dissociation between sites in 2024 (zero overlap of niche ellipses) and moderate to strong dissociation in 2025 (19% overlap). Similarly, diet composition as estimated from isotope values, suggested that emperor geese relied on different resources between wintering sites, with birds on Shemya relying on lower quality grasses and algae versus birds on Kodiak relying more heavily on sessile invertebrates. Body condition of geese largely reflected these dietary differences, with birds on Shemya generally in poorer condition than those on Kodiak, likely due to their reliance on lower quality grasses and algae versus the higher quality and more digestible diet of geese on Kodiak. . Overall, these results suggest that wintering habitats vary widely across the range of emperor geese, driving significant differences in s both resource use and body condition of emperor geese.

We inferred diets of wintering emperor geese using isotope values from plasma as opposed to red blood cells. Plasma is a more metabolically active tissue and integrates diet over shorter timeframes, while red blood cells reflect longer-term assimilated diet (Barquete et al.,

2013; Hobson & Clark, 1992a). Because emperor geese on Shemya were sampled roughly 3-6 weeks after their arrival on the wintering grounds, isotopic values of their red blood cells likely reflected, at least in part, diet acquired during fall staging or migration, whereas plasma more closely reflects local winter foraging. The larger $\delta^{13}C$ offset between tissues (i.e., plasma versus red blood cells) on Shemya may therefore reflect a shift between staging and wintering habitats, potentially driven by differences in baseline carbon sources or resource use across these periods. In contrast, birds on Kodiak are known to largely bypass fall staging grounds (Thomas, unpublished data) while arriving earlier on the wintering grounds (Naves et al., 2025; Uher-Koch et al., 2021), likely reducing the contrast between pre-arrival and winter diet and thus resulting in the small isotopic difference between tissues. Alternatively, the lack of important differences in $\delta^{15}N$ offsets between the tissue and winter sites suggests that trophic position was relatively consistent across time and space, whereas $\delta^{13}C$ better captured shifts in habitat or primary carbon sources. Overall, these patterns highlight how timing of arrival can influence interpretation of isotope values across wintering regions, especially depending on the tissue type considered (Hobson & Clark, 1992a; Phillips & Eldridge, 2006). Future baseline sampling at staging areas along the Alaska Peninsula would help distinguish whether the larger $\delta^{13}C$ offset on Shemya reflects shifts in habitat use, resource composition, or baseline isotope values.

Differences in baseline isotope values between sites provides additional context for understanding site-specific patterns. Baseline $\delta^{15}N$, as measured primarily from barnacles, was consistently higher on Kodiak than on Shemya (~1.8–2 ‰ difference), suggesting differences in local nutrient inputs and food web structure. Kodiak has more freshwater inputs and substantial salmon runs, both of which influence nitrogen cycling and contribute to higher $\delta^{15}N$ at the base of the food web (Naiman et al., 2002; Post et al., 2007; Schindler et al., 2003). In contrast, $\delta^{13}C$

baseline values were relatively similar between sites (~0.2–0.3‰ difference), suggesting that primary carbon sources were broadly comparable between Kodiak and Shemya.

Isotopic niche patterns also differed between sites and among years (*Fig. 2.3*), indicating that resource use was variable across wintering regions and years of study. In 2024, birds on Shemya occupied a much broader isotopic niche than those on Kodiak (SEAc = 4.68 vs. 0.44), suggesting greater variability in resource use at that site. In contrast, the relatively narrow niche on Kodiak in 2024 suggests more consistent resource use among individuals, which may be supported by greater availability or accessibility of preferred prey. In 2025, niche width was more similar between sites (Kodiak SEAc = 1.81; Shemya SEAc = 1.97), although overlap remained quite limited (~18–20% overlap). Overall, isotopic niche patterns were somewhat unexpected, as we predicted that the more constrained environment on Shemya would result in a narrower niche, consistent with expectations from optimal foraging and niche theory, where limited resource availability is often associated with reduced niche breadth (Pielou, 1972; Roughgarden, 1972). Instead, the broader niche on Shemya in 2024 likely reflects greater variability in resource use, potentially driven by differences in individual foraging strategies or limited access to preferred resources. Limited access could be due to storm events on Shemya, where individuals can go days without having access to good intertidal forage due to storm surges and intense wave action. Thus, during periods of limited access, Shemya birds' may shift to low quality grasses, sedges, wrack which may increase their isotopic niche breadth. Under these more variable conditions, individuals rely on a wider range of available resources, resulting in greater spread in isotopic values at the population level, even if individual diets remain relatively specialized. This pattern is consistent with the niche variation hypothesis, where

increases in population niche width can arise from greater differences among individuals rather than broader diets within individuals (Bolnick et al., 2010).

The shift from zero to partial overlap in niche width between Kodiak and Shemya across years suggests that these patterns are not fixed and may vary annually with environmental conditions or resource availability. sThese patterns, however, were only evaluated across two years, making it difficult to determine whether annual differences in niche width reflect consistent site-level patterns, or broader regional variation across the winter range between years. Interestingly, a small number of adults on Shemya (n = 4) in 2025 had notably elevated $\delta^{15}N$ values (>1 ‰). One possible explanation is nutritional stress, as fasting or protein catabolism can enrich tissue $\delta^{15}N$ when individuals begin relying on endogenous protein reserves (Hertz et al., 2015). This pattern was not clearly associated with body condition, however, as elevated $\delta^{15}N$ occurred in birds both below and above expected body condition. It is possible that nutritional stress may have contributed to elevated $\delta^{15}N$ values for some individuals, although elevated $\delta^{15}N$ values could also reflect short-term differences in diet, localized baseline variation, or use of more enriched foraging areas. Because this pattern was limited to only a few individuals in one year, it should be interpreted cautiously, but it may help explain some of the broader isotopic variation observed on Shemya in 2025. Differences in diet composition between sites, estimated via isotopic mixing models, also provides additional context for our observed isotopic niche patterns. On Kodiak, estimated diet proportions were primarily sessile invertebrates (median = 0.78), with relatively small contributions from seaweed (median= 0.12) and coastal grasses (0.10). In contrast, estimated diet proportions on Shemya indicated a greater contribution of multiple resource types, with barnacles comprising a smaller proportion of the

diet (median = 0.57) and marine vegetation like seaweed contributing more substantially (median = 0.32).

The difference we observed in estimated diet composition across sites may reflect site-specific differences in intertidal habitat diversity, habitat structure, and relative prey availability. Kodiak is characterized by more sheltered bays and estuarine environments, which tend to support higher biomass and diversity of benthic invertebrates, including mussel beds (Paine, 1966). In contrast, Shemya is a small island with limited and high coastline exposure, leading to increased wave action that likely affects the distribution, diversity, and accessibility of benthic invertebrates. In particular, mussels were nearly absent from intertidal zones in Shemya, presumably due to the inability of larval mussels to latch and grow in the consistently high energy, wave exposed coastlines (Blanchette & Gaines, 2007; Denny, 1995). Under these conditions, emperor geese may utilize a wider range of available resources, which is consistent with the broader isotopic niche observed on Shemya. On Kodiak, the strong reliance on sessile invertebrates is consistent with more uniform resource use among individuals, which may contribute to the narrower niche observed at that site. Anecdotal field observations were consistent with these patterns, as barnacles were difficult to locate on Shemya and mussels were not observed at all, whereas both were locally abundant on Kodiak.

Body mass corrected for structural size differed between sites, years, age classes, and sex, broadly reflecting patterns in resource use as measured by isotopes. Birds on Shemya were consistently in poorer body condition than those on Kodiaks, suggesting poorer resource availability, accessibility, or quality at this site. Similar spatial differences in body condition have been documented in other migratory waterfowl during winter, where variation in habitat quality among wintering areas leads to consistent differences in energetic reserves. For example,

Pacific greater white-fronted geese *(Anser albifrons*) exhibited strong regional variation in winter body condition, with birds in better habitats having higher body condition than those in more constrained areas, especially when drought conditions reduced food and habitat availability (Skalos et al., 2021). Similar patterns were observed for northern pintails (*Anas acuta*), in which the magnitude of lipid losses differed among wintering areas, likely due to better foraging conditions in certain areas that allowed birds to offset energetic costs more effectively (Moon & Haukos, 2009).

Body mass corrected for structural size on Kodiak was lower in 2025 when compared to 2024 and 2026, resulting in similar values to Shemya in that year. Comparable interannual fluctuations in body condition for other waterfowl species have been linked to variation in winter weather severity forage accessibility, and resource availability in other waterfowl species (Fleskes et al., 2016; Miller, 1986). At both sites, however, juveniles had consistently and substantially lower body condition than adults. This pattern is expected because young birds are less efficient foragers than experienced adults and continue to allocate energy toward structural growth during their first winter (Cooch et al., 1991; Loonen et al., 1997). Among adults, individuals on Shemya were in poorer body condition than those on Kodiak, and this pattern was most pronounced for females, which may be especially important given that females bear the energetic costs of reproduction (Alisauskas & Ankney, 1992; Ankney & Macinnes, 1978). Importantly, reduced body condition during winter may carry over to the breeding season, potentially affecting timing of reproduction, breeding propensity, clutch size, or reproductive success (Guillemain et al., 2008). Such carryover effects are widely documented in migratory waterfowl, where winter conditions influence subsequent reproductive investment and success (Drent et al., 2006; Harrison et al., 2011).

Similar to our observations for stable isotopes, site-specific patterns in body condition suggest that resources differ substantially between our study sites. On Shemya, consistently lower body condition across years likely reflects a more constrained wintering environment, as also indicated by stable isotope differences between sites. Resources may be of lower quality (e.g., algae and grasses) or less accessible because of frequent wave action and storm exposure. In contrast, the higher and more variable body condition on Kodiak suggests that resource availability fluctuates among years, potentially due to interannual variation in the abundance or accessibility of intertidal prey. Greater reliance on sessile invertebrates on Kodiak may support improved body condition when those resources are available, whereas birds on Shemya may rely on a smaller suite of resources that are available more consistently. Together, these results demonstrate that differences in wintering environments influence body condition in ways that may carry over to later stages of the annual cycle (Fox et al., 2005; Harrison et al., 2011; Sedinger & Alisauskas, 2014). Such carryover effects are consistent with life-history theory, which predicts that variation in resource acquisition influences survival and reproductive investment (Stearns, 1992) with potential consequences for reproductive success, survival, and ultimately population dynamics (Marra et al., 2015).

Given the limited temporal scope of our results, it is difficult to know whether the patterns observed here reflect consistent differences between Kodiak and Shemya specifically, or broader differences between eastern and western portions of the emperor goose wintering range. Much of the western portion of the winter range is similar to Shemya, being composed of exposed and isolated islands in the Bering Sea, while the eastern portion of the range includes the Alaska Peninsula and largely mirrors Kodiak with its large embayments and estuarine waters. Additional years of diet, isotope, and body condition data, especially from more wintering sites

across the Aleutians, Alaska Peninsula, and Kodiak Archipelago, would help determine whether these patterns are site-specific or represent broader regional differences in winter resource use and body condition of emperor geese.

This research highlights the value of using stable isotope analysis alongside measures of body condition to understand how variation in wintering environments influences individual performance. Stable isotopes provide insight into assimilated diet and habitat use over ecologically relevant timeframes (Hobson & Clark, 1992a; Post, 2002); while body condition reflects the net energetic outcomes of those foraging environments and serves as a widely used proxy for individual performance (Jakob et al., 1996; Stephens et al., 2014). Together, these metrics provide complementary perspectives on how contrasted environments translate into different fitness costs and benefits for individuals.

In the context of ongoing environmental change, these fitness differences may become increasingly relvant, as warming temperatures and shifting marine conditions have the potential to alter the distribution, accessibility, and quality of intertidal resources across the winter range of Emperor Geese (Harley et al., 2006; Weitzman et al., 2021). In winter locations such as Kodiak, where birds appear to rely on higher-quality but potentially more variable resources, these changes could either enhance foraging conditions or amplify year-to-year variability in resource availability. While such wintering locations may provide substantial energetic benefits when conditions are favorable, they may also introduce greater risk if key resources become unavailable or access is limited (Osgood, 2008; Lohmann et al., 2023). Alternatively, at wintering areas similar to Shemya, increased winter storm activity in the Bering Sea, as predicted by climate models (Mesquita et al., 2010; Overland & Wang, 2025; Rodionov et al., 2007), could push already resource and body condition limited geese closer to the edge.

Tables and Figures

Table 2.1. Stable isotope values (mean ± SD) for potential dietary sources collected at Kodiak and Shemya in 2024.

Body condition model	npar	AICc	ΔAICc	Weight
Site × Year + Age + Sex	9	6341.87	0.00	1.00
Site + Year + Age + Sex	7	6357.15	15.28	0.00
Site × Year + Age	8	6372.21	30.34	0.00
Site + Year + Age	6	6388.34	46.47	0.00
Age	3	6522.13	180.26	0.00
Site + Year + Sex	6	6525.10	183.23	0.00
Year	4	6554.15	212.27	0.00
Site	3	6595.21	253.33	0.00
Sex	3	6604.77	262.90	0.00
Null	2	6625.64	283.76	0.00

[1] Kodiak, mussels (*Mytilus* spp.; $\delta^{13}C = -16.1 \pm 0.56‰$, $\delta^{15}N = 10.1 \pm 0.38‰$) and barnacles (*Balanus* spp.; $\delta^{13}C = -15.7 \pm 0.96‰$, $\delta^{15}N = 9.59 \pm 0.55‰$) showed substantial isotopic overlap and were pooled into a single sessile invertebrate category.

Table 2.2: Model selection results for linear models evaluating variation in emperor goose body condition, corrected for structural body size, as a function of site, year, age, and sex.

Site	Prey category	n	$\delta^{15}N \pm SD$	$\delta^{13}C \pm SD$
Kodiak	Sessile invertebrates[1]	13	9.78 ± 0.54	-15.87 ± 0.82
Kodiak	Seaweed	4	4.97 ± 0.49	-24.97 ± 0.42
Kodiak	Grass (beach rye)	6	3.50 ± 0.83	-27.01 ± 0.73
Shemya	Barnacle	5	8.26 ± 0.17	-16.40 ± 0.48
Shemya	Seaweed	6	3.95 ± 0.59	-25.34 ± 0.83
Shemya	Grass (beach rye)	5	6.69 ± 0.71	-28.89 ± 2.46

Table 2.3: Mean (± SD) $\delta^{13}C$ (lipid-normalized) and $\delta^{15}N$ values of barnacles used as baseline organisms at Kodiak and Shemya in 2024 and 2025. $\delta^{15}N$ values were consistently higher at Kodiak than Shemya, indicating site-specific baseline differences.

Site	Year	n	Barnacle $\delta^{13}C_{\text{lipid normalized}}$ (‰) ± SE	Barnacle $\delta^{15}N$ (‰) ± SE
Kodiak	2024	5	-16.07 ± 0.25	10.10 ± 0.17
Kodiak	2025	12	-16.30 ± 0.17	10.04 ± 0.08
Shemya	2024	5	-16.40 ± 0.21	8.26 ± 0.07
Shemya	2025	12	-16.37 ± 0.18	8.07 ± 0.04

Table 2.4: Baseline-corrected $\delta^{13}C_{Plasma}$ and $\delta^{15}N_{Plasma}$ values and isotopic niche metrics for emperor geese by site and year. Isotope values are estimated marginal means (±95% confidence intervals) from linear models. Standard ellipse area (SEA_C) represents maximum likelihood estimates of core isotopic niche width (~40% of the data), and Bayesian standard ellipse area (SEA_B) is reported as the posterior median with 95% credible intervals (CrI).

Site	Year	$\delta^{13}C$ (‰) [95% CI]	$\delta^{15}N$ (‰) [95% CrI]	SEA_C	SEA_B [95% Crl]
Kodiak	2024	-1.16 [-1.86, -0.45]	3.79 [3.43, 4.14]	0.44	0.42 [0.25, 0.79]
Kodiak	2025	-1.50 [-1.76, -1.25]	2.79 [2.66, 2.92]	1.81	1.83 [1.50, 2.29]
Shemya	2024	-3.15 [-3.53, -2.76]	1.35 [1.16, 1.55]	4.68	4.68 [3.51, 6.51]
Shemya	2025	-2.53 [-2.85, -2.22]	2.07 [1.91, 2.23]	1.97	2.00 [1.54, 2.60]

Table 2.5: Bayesian posterior estimates of directional isotopic niche overlap (%) among emperor goose site–year groups based on standard ellipse areas representing 40% core niche space. Values are posterior medians with 95% credible intervals (CrI). Directional overlap represents the proportion of the focal group's niche contained within the comparison group.

Comparison	Direction of overlap	Median (%) [95% CrI]
Sites (2024)	Kodiak within Shemya	0.0 [0.0–0.0]
Sites (2024)	Shemya within Kodiak	0.0 [0.0–0.0]
Sites (2025)	Kodiak within Shemya	19.8 [1.4–45.3]
Sites (2025)	Shemya within Kodiak	18.4 [1.2–40.9]
Kodiak (2024 vs 2025)	2024 within 2025	0.0 [0.0–76.4]
Kodiak (2024 vs 2025)	2025 within 2024	0.0 [0.0–19.5]
Shemya (2024 vs 2025)	2024 within 2025	23.2 [7.9–41.7]
Shemya (2024 vs 2025)	2025 within 2024	55.1 [19.2–93.0]

Table 2.6. Median posterior estimates and 95% credible intervals (CrI) for proportional dietary contributions of major food sources to emperor goose diets at Kodiak and Shemya, Alaska, based on Bayesian stable isotope mixing models (SIMMR) using plasma samples.

Site	Source	Median proportion [95% CrI]
Kodiak	Sessile invertebrates	0.78 [0.72–0.85]
Kodiak	Seaweed	0.12 [0.02–0.23]
Kodiak	Grass	0.10 [0.02–0.19]
Shemya	Barnacle	0.57 [0.52–0.62]
Shemya	Seaweed	0.32 [0.22–0.40]
Shemya	Grass	0.11 [0.04–0.20]

Table 2.7. Body mass and body condition of emperor geese by site and year. Values are presented as mean ± SD. Body condition was calculated as residuals from a regression of body mass on tarsus length and represents deviation from expected mass for structural size. Tarsus measurements began in 2024; therefore body condition residuals are only available from 2024 onward.

Site	Year	n	Mass (g) mean ± SD	Total Tarsus Lenth (mm) ± SD	Body condition residual mean ± SD
Shemya	2022	14	1925.7 ± 236.0	—	—
Shemya	2023	23	2106.4 ± 276.7	—	—
Shemya	2024	41	2021.4 ± 260.8	78.2 ± 3.8	-125.9 ± 173.0
Shemya	2025	70	2062.8 ± 276.5	78.3 ± 4.0	-88.9 ± 204.8
Shemya	2026	30	2123.8 ± 273.2	79.1 ± 4.1	-66.5 ± 228.8
Kodiak	2020	9	1980.8 ± 141.0	—	—
Kodiak	2022	13	2158.5 ± 176.8	—	—
Kodiak	2023	86	2376.0 ± 252.1	—	—
Kodiak	2024	12	2367.8 ± 316.4	78.9 ± 2.6	189.8 ± 252.3
Kodiak	2025	120	2069.4 ± 282.8	78.8 ± 4.0	-104.8 ± 223.0
Kodiak	2026	206	2300.9 ± 274.9	79.0 ± 4.2	114.9 ± 218.2

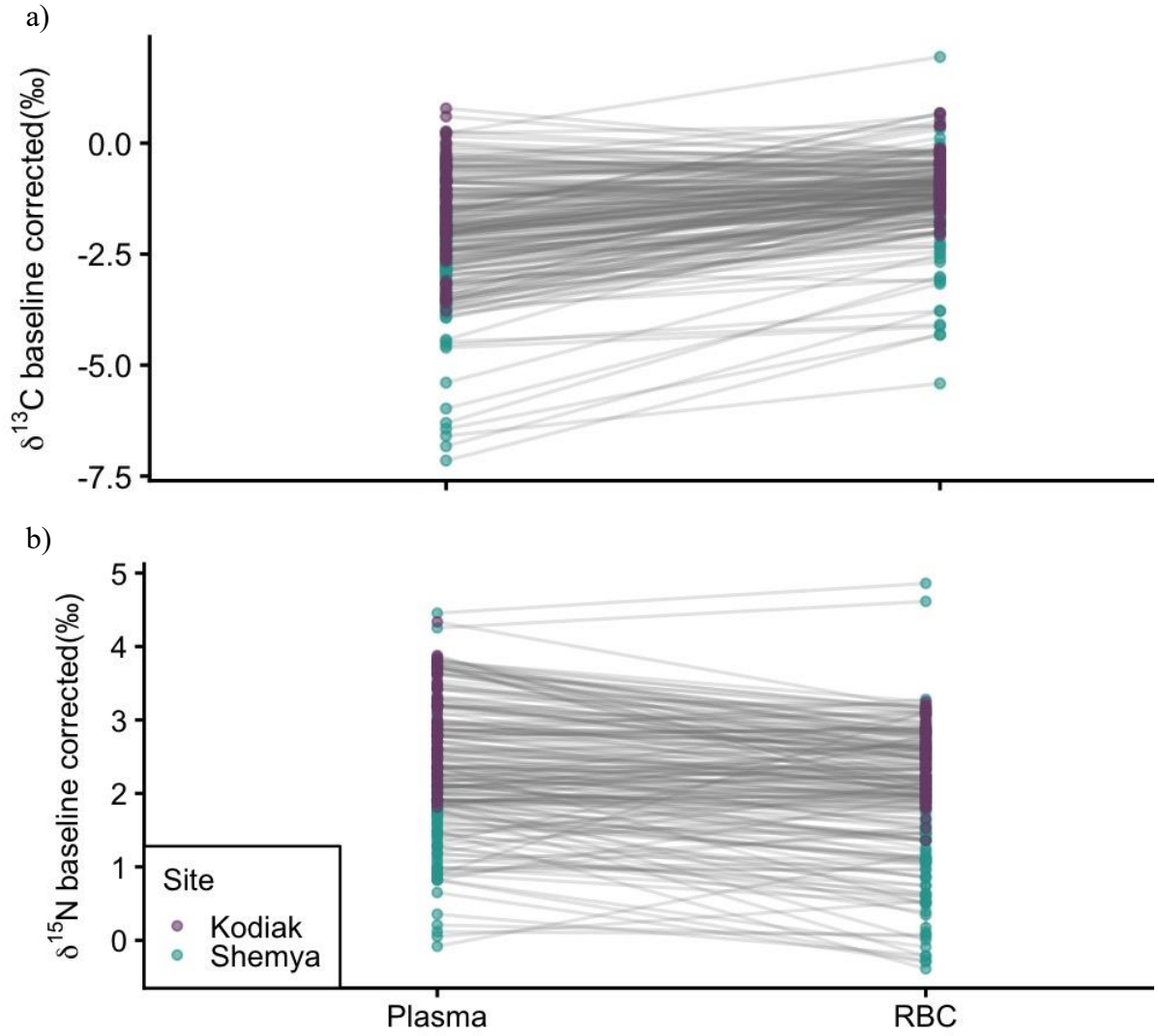

Figure 2.1: Paired comparison of baseline-corrected (a) $\delta^{13}C$ and (b) $\delta^{15}N$ values between plasma and red blood cells (RBC) in emperor geese from Kodiak (n = 101) and Shemya (n = 92). Points represent individual birds, with lines connecting paired samples from the same individual. Colors indicate site (Kodiak = purple; Shemya = teal). Red blood cells were enriched in $\delta^{13}C$ and depleted in $\delta^{15}N$ relative to plasma, consistent with tissue-specific differences in dietary integration.

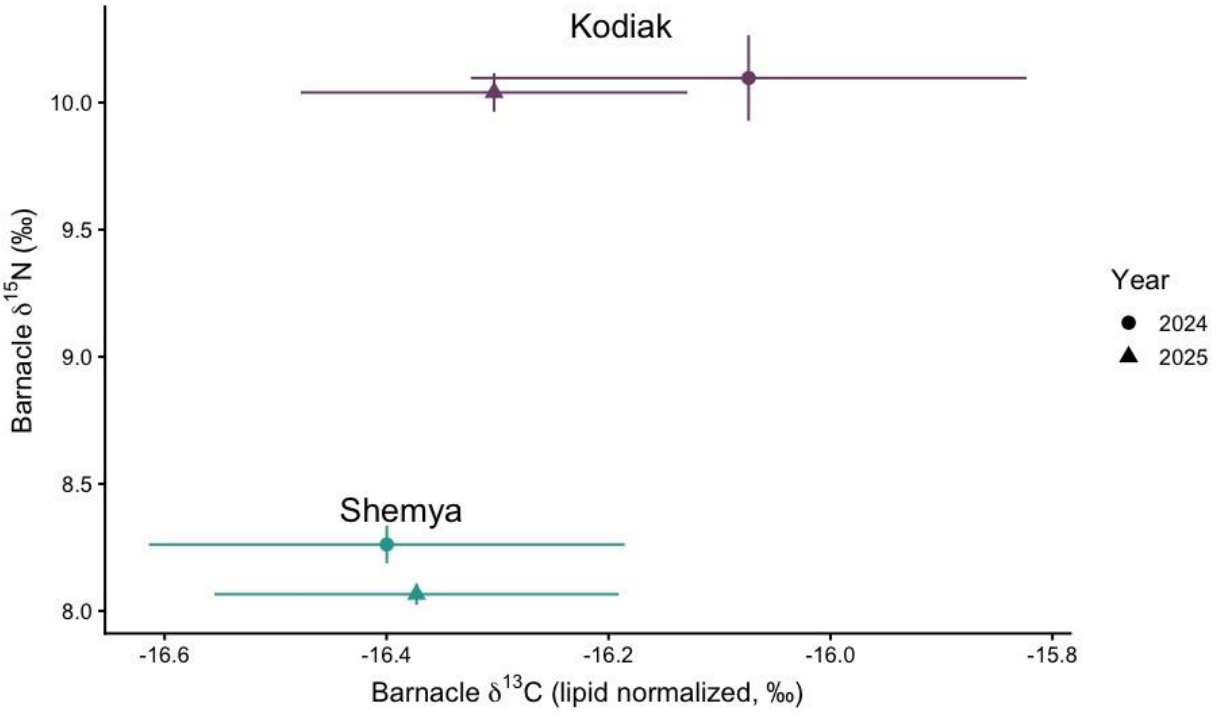

Figure 2.2: Mean (± 95% CI) $\delta^{13}C$ (lipid-normalized) and $\delta^{15}N$ values of barnacles used as baseline organisms at Kodiak and Shemya in 2024 and 2025. Baseline isotopic values were similar between years within sites but differed between sites, with Kodiak enriched in $\delta^{15}N$ relative to Shemya.

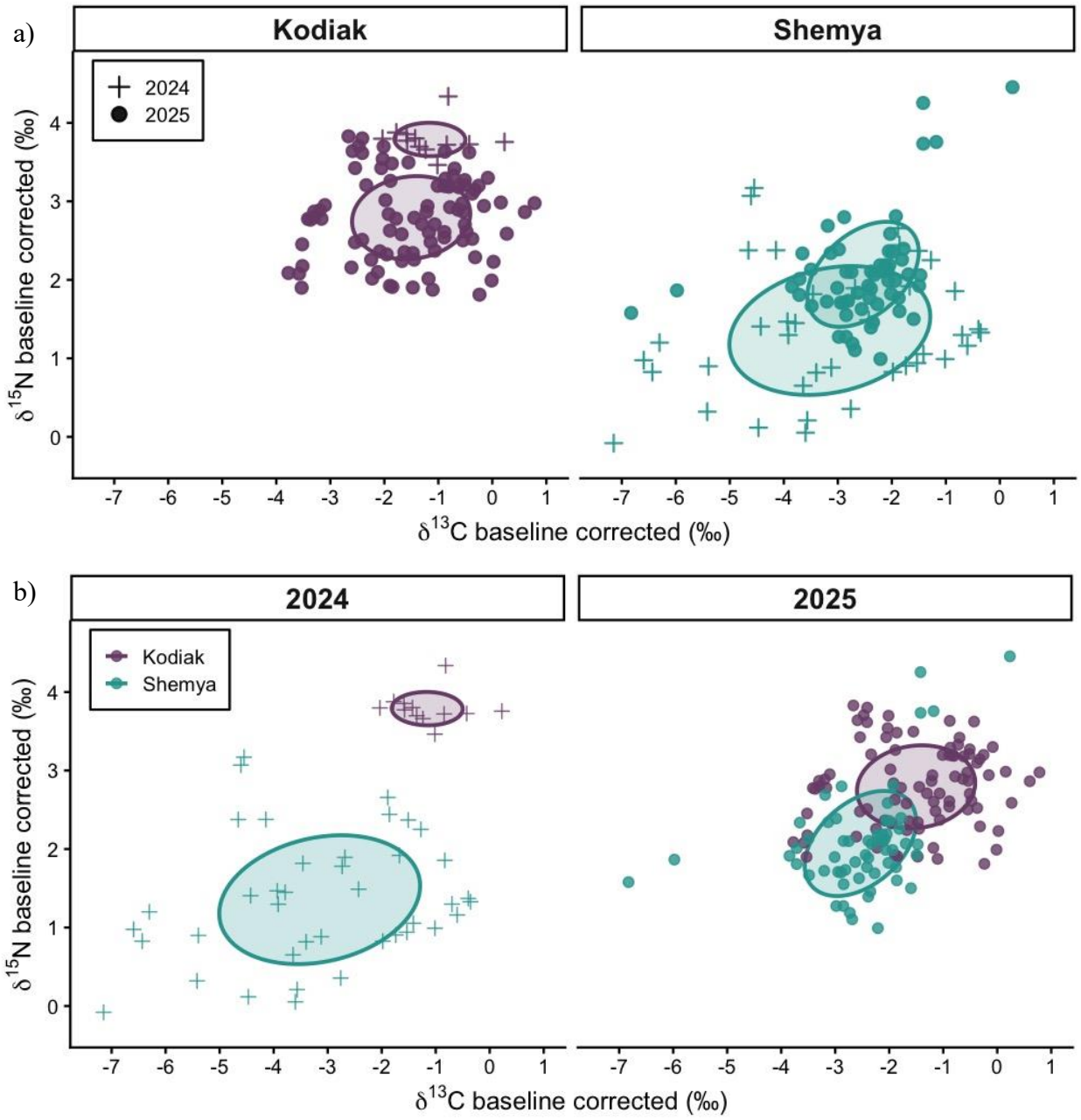

Figure 2.3: Isotopic niche space of emperor geese based on $\delta^{13}C_{Plasma}$ and $\delta^{15}N_{Plasma}$ values. (a) Comparison of years within sites, with panels showing Kodiak and Shemya separately. (b) Comparison of sites within years, with panels showing 2024 and 2025 separately. Points represent individual bird's values. Standard ellipses (SEA_C) represent core isotopic niche space (~40% of the data) for each group.

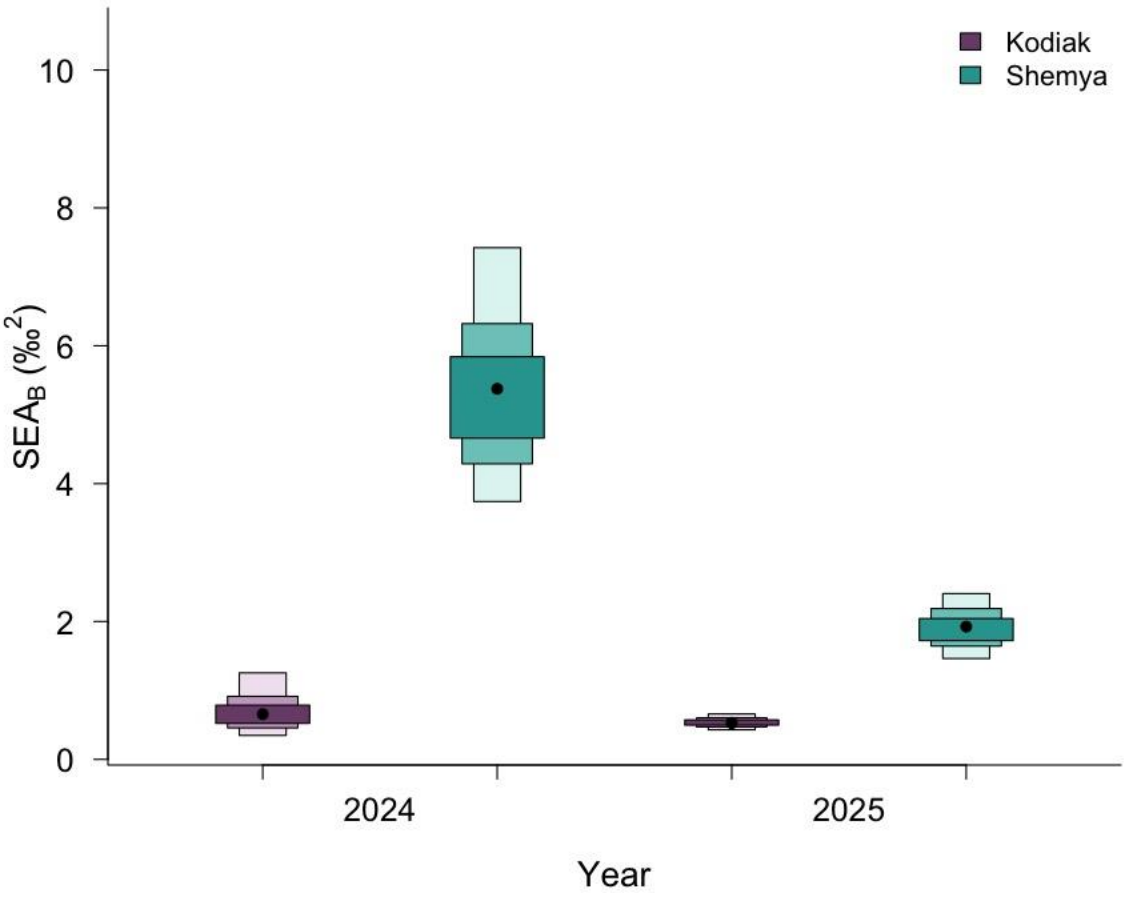

Figure 2.4: Bayesian standard ellipse area (SEA_B) for emperor geese for Kodiak in 2024 (n = 12) and 2025 (n = 90) and Shemya in 2024 (n = 32) and 2025 (n = 60). Density plots represent posterior distributions of SEA_B with the central point indicating the median and shaded regions representing the 50%, 75%, and 95% credible intervals. Larger ellipse areas indicate broader isotopic niche width.

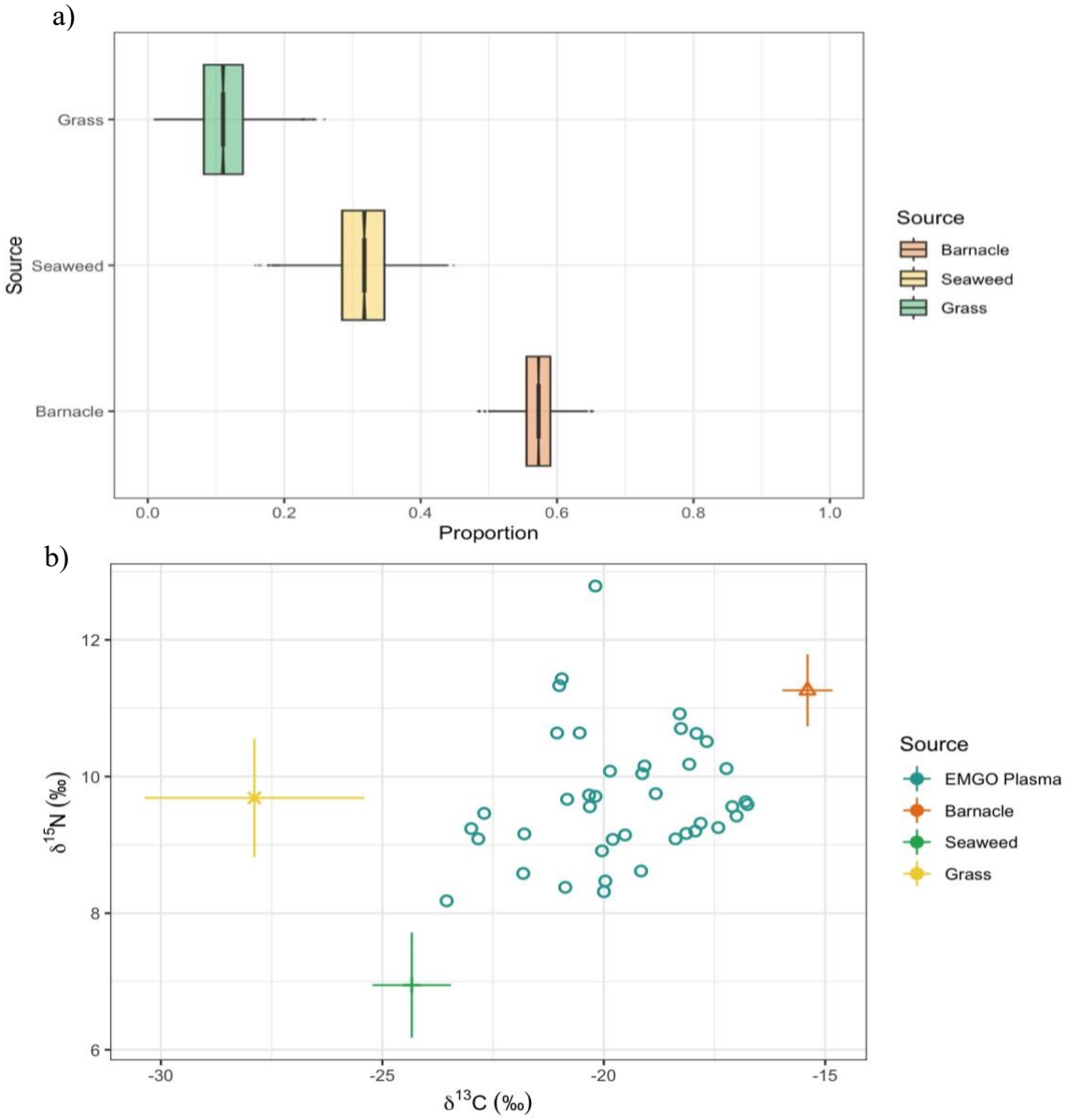

Figure 2.5. Diet items of emperor geese wintering at Shemya in 2024, estimated from isotopic mixing models utilizing plasma samples.
(a) Posterior distributions of estimated diet proportions for each source (barnacle, seaweed, and grass), shown as boxplots with medians and interquartile ranges. (b) panel: Biplot of $\delta^{13}C$ and $\delta^{15}N$ values for consumer samples (points) and source means (centroids) with ±1 SD error bars. Together, these panels illustrate both the isotopic separation among sources and the estimated contribution of each source to the diet.

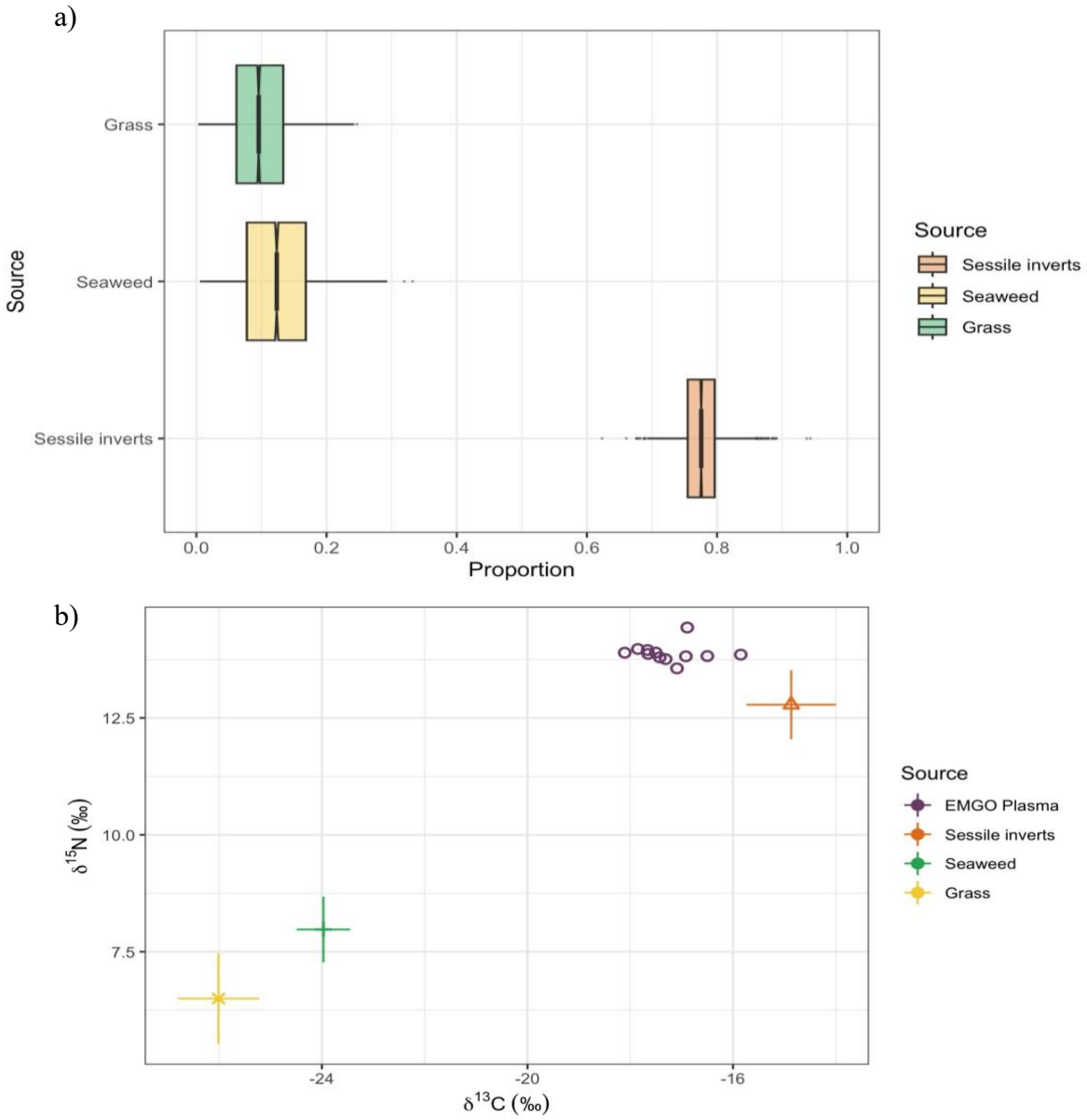

Figure 2.6: Diet items of emperor geese wintering at Kodiak in 2024, estimated from isotopic mixing models utilizing plasma samples.
(a) Posterior distributions of estimated diet proportions for each source (barnacle, seaweed, and grass), shown as boxplots with medians and interquartile ranges. (b) panel: Biplot of $\delta^{13}C$ and $\delta^{15}N$ values for consumer samples (points) and source means (centroids) with ±1 95% CI. Together, these panels illustrate both the isotopic separation among sources and the estimated contribution of each source to the diet.

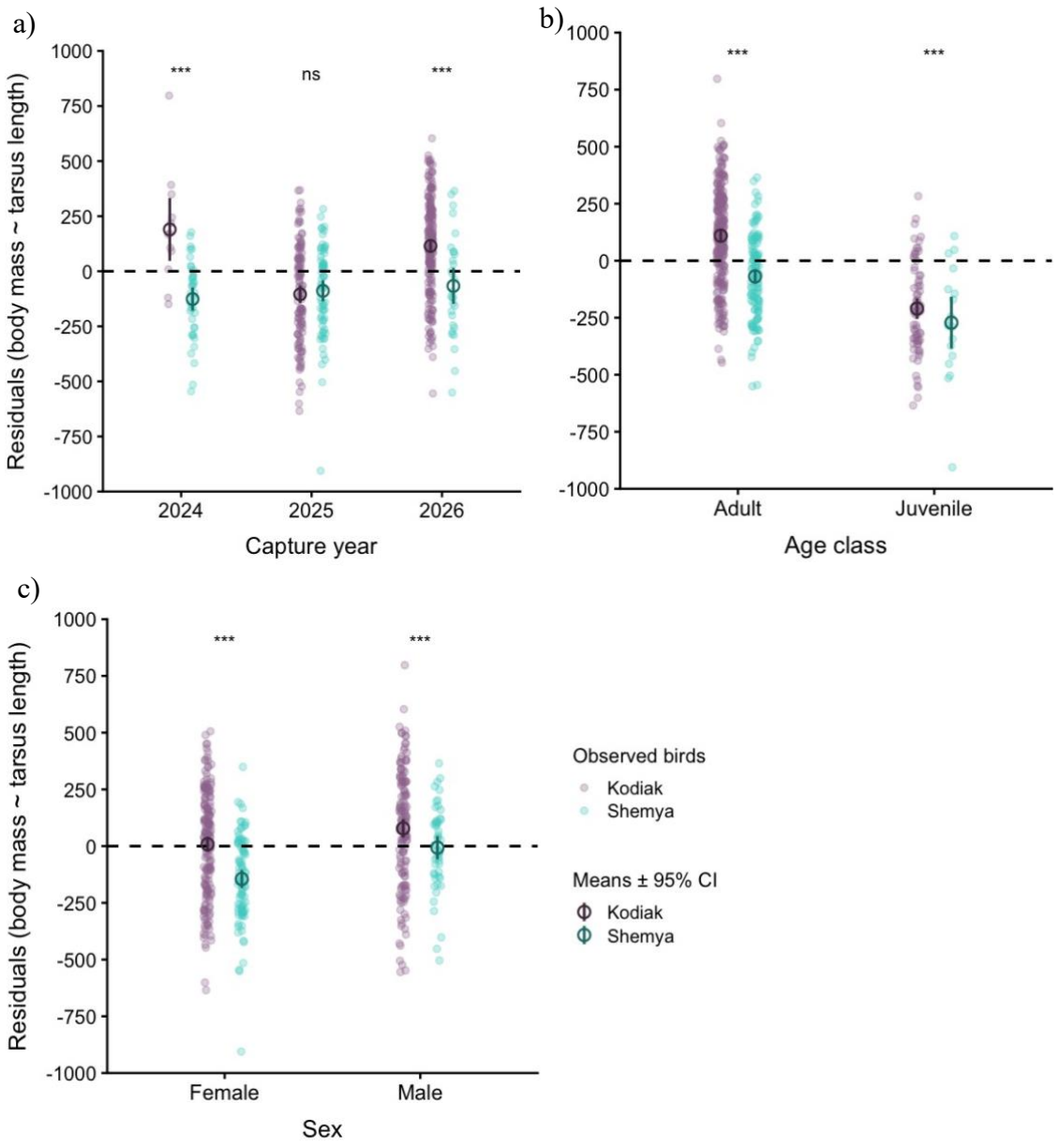

Figure 2.7: Body condition index of emperor geese at Kodiak and Shemya by (a) capture year, (b) age, and (c) sex. Body condition index was calculated as the residual from the regression of body mass on total tarsus length, with positive residuals indicating birds that were heavier than expected for their structural size and negative residuals indicating birds that were lighter than expected. Points represent individual birds, and darker circles indicate mean body condition ± 95% confidence intervals for each group. The dashed line at zero represents the expected body condition for a bird of a given structural size. Asterisks denote model-based differences in body condition between sites within each group (*** $p < 0.001$; ** $p < 0.01$; * $p < 0.05$; ns = not significant).

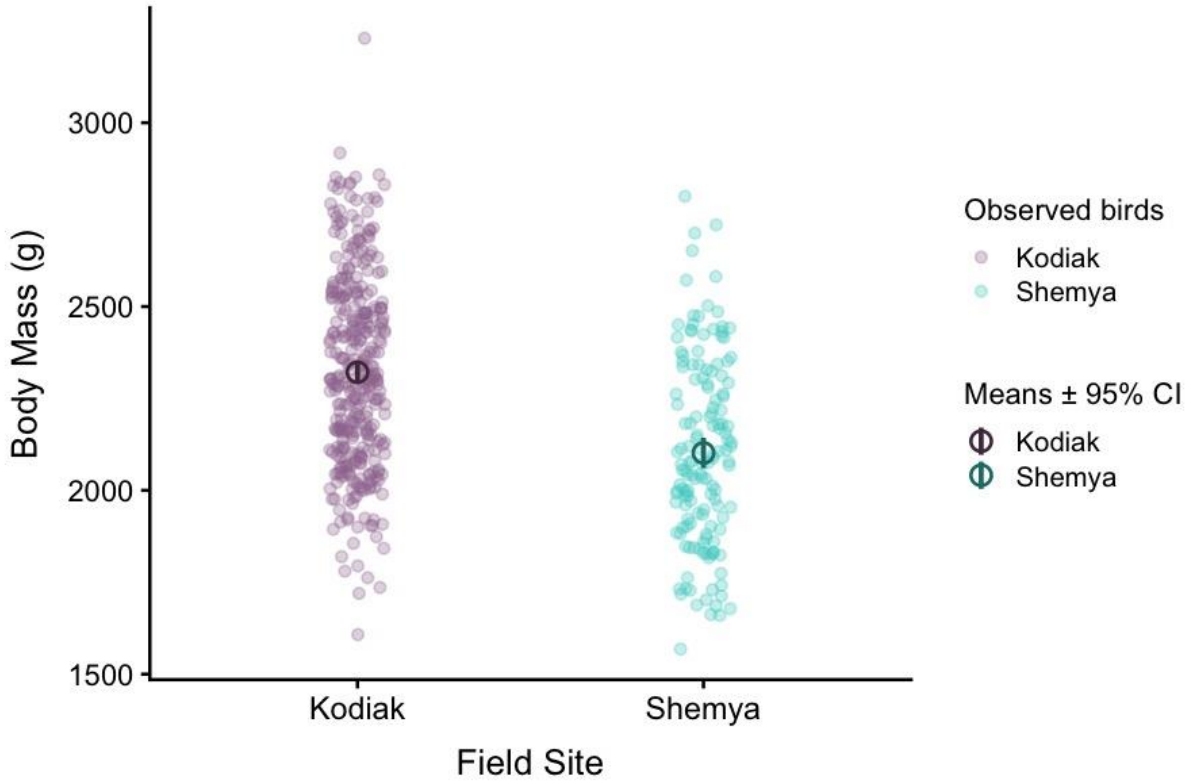

Figure 2.8. Body mass (g) of adult emperor geese captured at Kodiak (2023–2026, n = 344) and Shemya (2022–2026, n = 146). Points represent individual birds, and larger open circles indicate mean body mass ± 95% confidence intervals for each site.

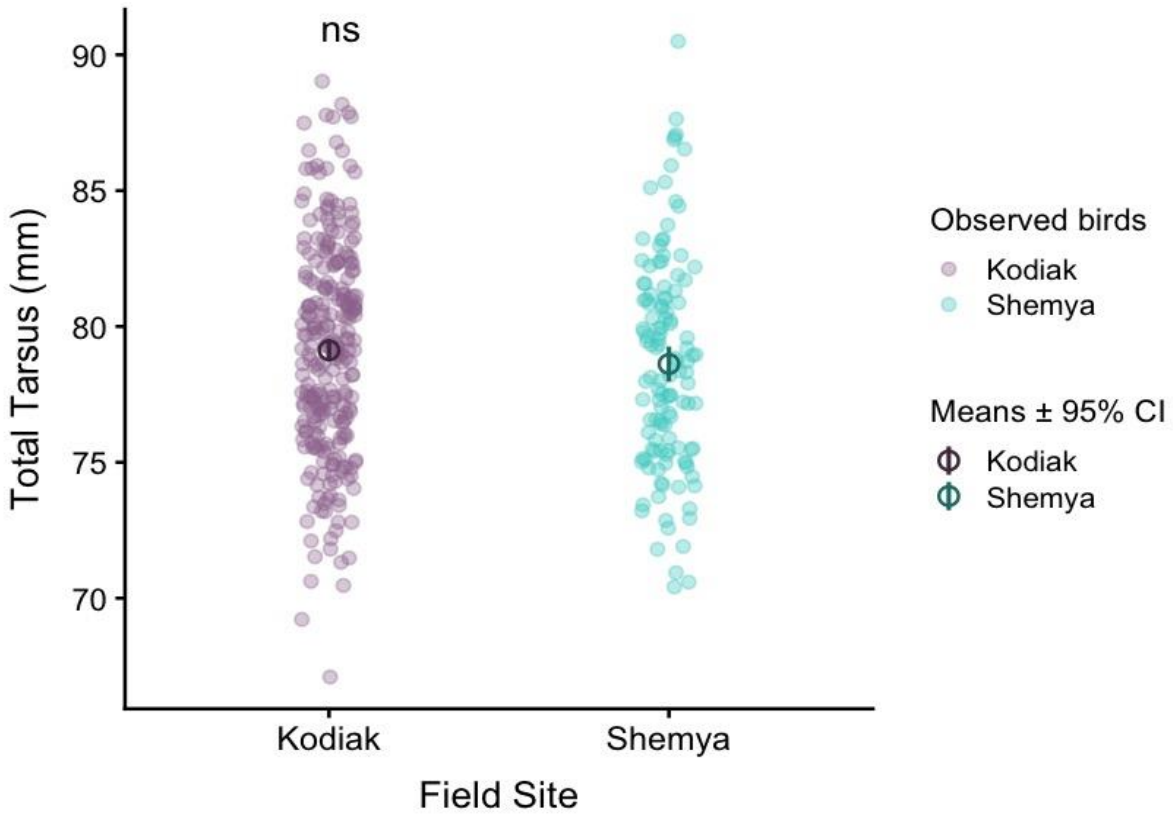

Figure 2.9: Total tarsus length (mm) of emperor geese at Kodiak and Shemya. Points represent individual birds, and larger open circles indicate mean values ± 95% confidence intervals for each site. No significant difference in tarsus length was detected between sites (ns).

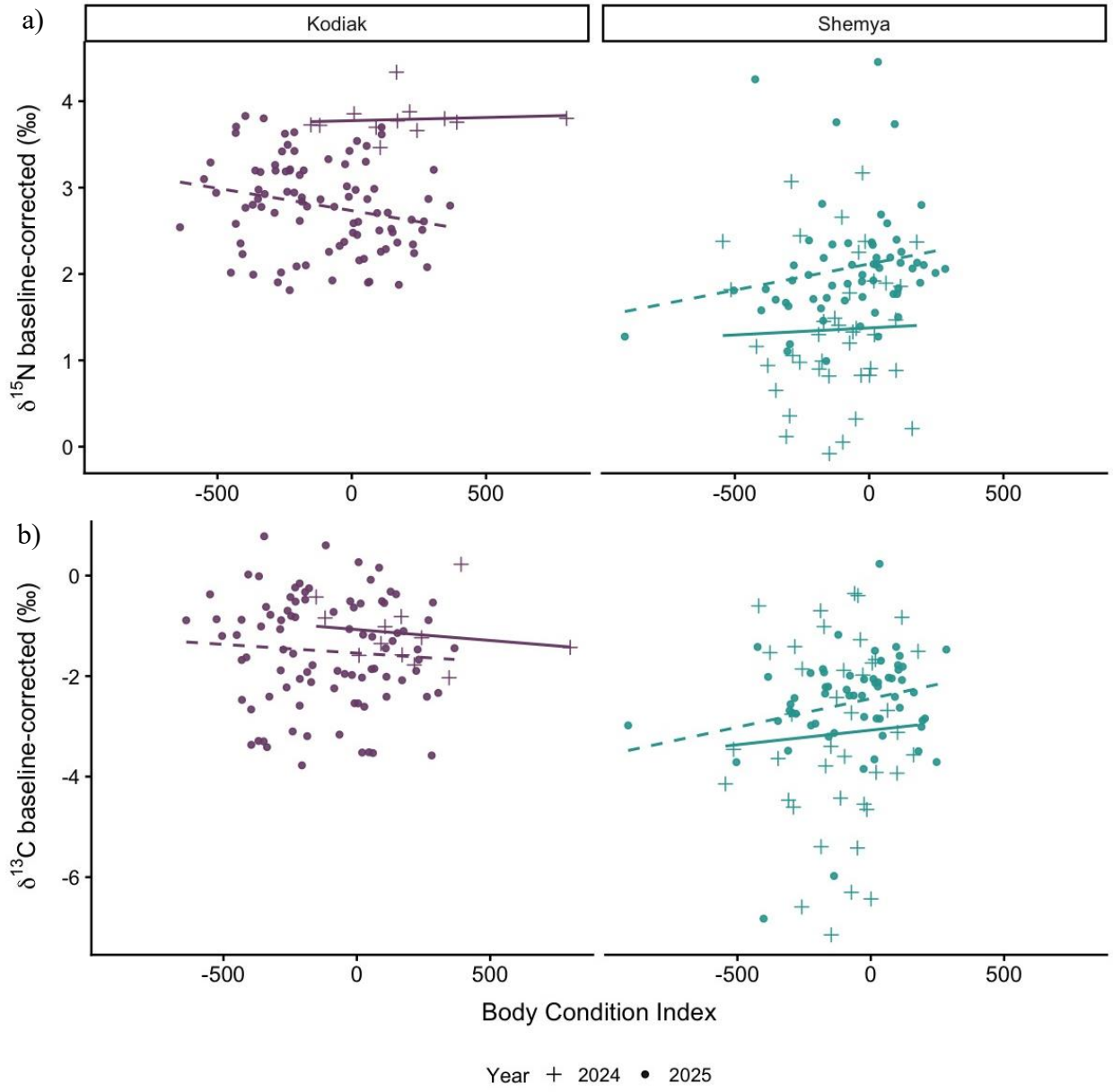

Figure 2.10: Relationships between plasma isotope values and body condition index (BCI) at Kodiak and Shemya. Panels show (a) plasma $\delta^{15}N$ and (b) plasma $\delta^{13}C$ in relation to BCI. Points represent individual birds and lines show linear models fit by site while accounting for year.

References

Akaike, H. (1998). Information Theory and an Extension of the Maximum Likelihood Principle. In *Parzen, E., Tanabe, K. and Kitagawa, G., Eds., Selected Papers of Hirotugu Akaike* (pp. 199–213). Springer Series in Statistics (Perspectives in Statistics).

Alisauskas, R. T., & Ankney, C. D. (1992). The cost of egg laying and its relationship to nutrient reserves in waterfowl. In *The Ecology and Management of Breeding Waterfowl* (pp. 30–61). U of Minnesota Press.

Ankney, C., & Macinnes, C. (1978). Nutrient Reserves and Reproductive Performance of Female Lesser Snow Geese. *The Auk*, *95*(3). https://digitalcommons.usf.edu/auk/vol95/iss3/2

Araújo, P. M., Viegas, I., Rocha, A. D., Villegas, A., Jones, J. G., Mendonça, L., Ramos, J. A., Masero, J. A., & Alves, J. A. (2019). Understanding how birds rebuild fat stores during migration: Insights from an experimental study. *Scientific Reports*, *9*(1), 10065. https://doi.org/10.1038/s41598-019-46487-z

Arsan, E. L., Lance, T., Krueger, K., & Shaftel, R. (2025). Marine Succession Rates on Intertidal and Subtidal New Armor Rock in Chiniak Bay, Kodiak, Alaska. *Northwest Science*, *98*(2), 86–98. https://doi.org/10.3955/046.098.0201

Barquete, V., Strauss, V., & Ryan, P. G. (2013). Stable isotope turnover in blood and claws: A case study in captive African Penguins. *Journal of Experimental Marine Biology and Ecology*, *448*, 121–127. https://doi.org/10.1016/j.jembe.2013.06.021

Bates, D., Mächler, M., Bolker, B., & Walker, S. (2015). Fitting Linear Mixed-Effects Models Using lme4. *Journal of Statistical Software*, *67*, 1–48. https://doi.org/10.18637/jss.v067.i01

Bearhop, S., Hilton, G. M., Votier, S. C., & Waldron, S. (2004). Stable isotope ratios indicate that body condition in migrating passerines is influenced by winter habitat. *Proceedings of the Royal Society of London. Series B: Biological Sciences*, *271*(suppl_4). https://doi.org/10.1098/rsbl.2003.0129

Bearhop, S., Teece, M. A., Waldron, S., & Furness, R. W. (2000). Influence of Lipid and Uric Acid on δ13C and δ15N Values of Avian Blood: Implications for Trophic Studies. *The Auk*, *117*(2), 504–507. https://doi.org/10.1093/auk/117.2.504

Bearhop, S., Thompson, D. R., Waldron, S., Russell, Ian. C., Alexander, G., & Furness, R. W. (1999). Stable isotopes indicate the extent of freshwater feeding by cormorants *Phalacrocorax carbo* shot at inland fisheries in England. *Journal of Applied Ecology*, *36*(1), 75–84. https://doi.org/10.1046/j.1365-2664.1999.00378.x

Bearhop, S., Waldron, S., Votier, S. C., & Furness, R. W. (2002). Factors That Influence Assimilation Rates and Fractionation of Nitrogen and Carbon Stable Isotopes in Avian Blood and Feathers. *Physiological and Biochemical Zoology*, *75*(5), 451–458. https://doi.org/10.1086/342800

Blanchette, C. A., & Gaines, S. D. (2007). Distribution, abundance, size and recruitment of the mussel, Mytilus californianus, across a major oceanographic and biogeographic boundary at Point Conception, California, USA. *Journal of Experimental Marine Biology and Ecology*, *340*(2), 268–279. https://doi.org/10.1016/j.jembe.2006.09.014

Bolnick, D. I., Ingram, T., Stutz, W. E., Snowberg, L. K., Lau, O. L., & Paull, J. S. (2010). Ecological release from interspecific competition leads to decoupled changes in population and individual niche width. *Proceedings. Biological Sciences*, *277*(1689), 1789–1797. https://doi.org/10.1098/rspb.2010.0018

Brown, M. E. (1996). Assessing Body Condition in Birds. In *Current Ornithology* (pp. 67–135). Plenum Press.

Burnham, K. P., & Anderson, D. R. (1998). *Model Selection and Inference*. Springer New York. https://doi.org/10.1007/978-1-4757-2917-7

Clark, D. W. (1998). Kodiak Island: The Later Cultures. *Arctic Anthropology*, *35*(1), 172–186.

Cooch, E. G., Lank, D. B., Dzubin, A., Rockwell, R. F., & Cooke, F. (1991). Body Size Variation in Lesser Snow Geese: Environmental Plasticity in Gosling Growth Rates. *Ecology*, *72*(2), 503–512. https://doi.org/10.2307/2937191

Cottam, C. (1939). Food of Some Uncommon North American Birds. *The Auk*, *56*(2), 138–169. https://doi.org/10.2307/4078038

Denny, M. (1995). Predicting Physical Disturbance: Mechanistic Approaches to the Study of Survivorship on Wave-Swept Shores. *Ecological Monographs*, *65*(4), 371–418. https://doi.org/10.2307/2963496

Drent, R. H., Fox, A. D., & Stahl, J. (2006). Traveling to breed. *Journal of Ornithology*. https://doi.org/10.1007/s10336-006-0066-4

Eisenhauer, D. I., & Kirkpatrick, C. M. (1977). Ecology of the Emperor Goose in Alaska. *Wildlife Monographs*, (57,), 3–62.

Fleskes, J. P., Yee, J. L., Yarris, G. S., & Loughman, D. L. (2016). Increased body mass of ducks wintering in California's Central Valley. *The Journal of Wildlife Management*, *80*(4), 679–690. https://doi.org/10.1002/jwmg.1053

Fox, A., Madsen, J., Boyd, H., Kuijken, E., Norriss, D., Tombre, I., & Stroud, D. (2005). Effects of agricultural change on abundance, fitness components and distribution of two Arctic-nesting goose populations. *Global Change Biology*, *11*, 881–893. https://doi.org/10.1111/j.1365-2486.2005.00941.x

France, R. (1994). Nitrogen isotopic composition of marine and freshwater invertebrates. *Marine Ecology Progress Series*, *115*, 205–207. https://doi.org/10.3354/meps115205

Fretwell, S. D., & Lucas, H. L. (1969). On territorial behavior and other factors influencing habitat distribution in birds: I. Theoretical development. *Acta Biotheoretica*, *19*(1), 16–36. https://doi.org/10.1007/BF01601953

Fukumori, K., Oi, M., Doi, H., Takahashi, D., Okuda, N., Miller, T. W., Kuwae, M., Miyasaka, H., Genkai-Kato, M., Koizumi, Y., Omori, K., & Takeoka, H. (2008). Bivalve tissue as a carbon and nitrogen isotope baseline indicator in coastal ecosystems. *Estuarine, Coastal and Shelf Science*, *79*(1), 45–50. https://doi.org/10.1016/j.ecss.2008.03.004

Gibson, D. D. (1981). Migrant Birds at Shemya Island, Aleutian Islands, Alaska. *The Condor: Ornithological Applications*, *83*(1), 65–77. https://doi.org/10.2307/1367606

Guillemain, M., Elmberg, J., Arzel, C., Johnson, A. R., & Simon, G. (2008). The income–capital breeding dichotomy revisited: Late winter body condition is related to breeding success in an income breeder. *Ibis*, *150*(1), 172–176. https://doi.org/10.1111/j.1474-919X.2007.00700.x

Harley, C. D. G., Randall Hughes, A., Hultgren, K. M., Miner, B. G., Sorte, C. J. B., Thornber, C. S., Rodriguez, L. F., Tomanek, L., & Williams, S. L. (2006). The impacts of climate change in coastal marine systems. *Ecology Letters*, *9*(2), 228–241. https://doi.org/10.1111/j.1461-0248.2005.00871.x

Harrison, X. A., Blount, J. D., Inger, R., Norris, D. R., & Bearhop, S. (2011). Carry-over effects as drivers of fitness differences in animals: Carry-over effects in animal populations. *Journal of Animal Ecology*, *80*(1), 4–18. https://doi.org/10.1111/j.1365-2656.2010.01740.x

Hertz, E., Trudel, M., Cox, M. K., & Mazumder, A. (2015). Effects of fasting and nutritional restriction on the isotopic ratios of nitrogen and carbon: A meta-analysis. *Ecology and Evolution*, *5*(21), 4829–4839. https://doi.org/10.1002/ece3.1738

Hobson, K. A., & Clark, R. G. (1992a). Assessing Avian Diets Using Stable Isotopes I: Turnover of $\delta^{13}C$ in Tissues. *The Condor*, *94*(1), 181–188. https://doi.org/10.2307/1368807

Hobson, K. A., & Clark, R. G. (1992b). Assessing Avian Diets Using Stable Isotopes II: Factors Influencing Diet-Tissue Fractionation. *The Condor*, *94*(1), 189–197. https://doi.org/10.2307/1368808

Hupp, J. W., Schmutz, J. A., & Ely, C. R. (2008). The Annual Migration Cycle of Emperor Geese in Western Alaska. *Arctic*, *61*(1), 23–34.

Jackson, A. L., Inger, R., Parnell, A. C., & Bearhop, S. (2011). Comparing isotopic niche widths among and within communities: SIBER - Stable Isotope Bayesian Ellipses in R: Bayesian isotopic niche metrics. *Journal of Animal Ecology*, *80*(3), 595–602. https://doi.org/10.1111/j.1365-2656.2011.01806.x

Jakob, E. M., Marshall, S. D., & Uetz, G. W. (1996). Estimating Fitness: A Comparison of Body Condition Indices. *Oikos*, *77*(1), 61–67. https://doi.org/10.2307/3545585

Konar, B., Iken, K., & Edwards, M. (2009). Depth-stratified community zonation patterns on Gulf of Alaska rocky shores. *Marine Ecology*, *30*(1), 63–73. https://doi.org/10.1111/j.1439-0485.2008.00259.x

Kristensen, P. B., Riis, T., Dylmer, H. E., Kristensen, E. A., Meerhoff, M., Olesen, B., Teixeira-de Mello, F., Baattrup-Pedersen, A., Cavalli, G., & Jeppesen, E. (2016). Baseline identification in stable-isotope studies of temperate lotic systems and implications for calculated trophic positions. *Freshwater Science*, *35*(3), 909–921. https://doi.org/10.1086/687284

Kuznetsova, A., Brockhoff, P. B., & Christensen, R. H. B. (2017). lmerTest Package: Tests in Linear Mixed Effects Models. *Journal of Statistical Software*, *82*(13). https://doi.org/10.18637/jss.v082.i13

Leibold, M. A., Holyoak, M., Mouquet, N., Amarasekare, P., Chase, J. M., Hoopes, M. F., Holt, R. D., Shurin, J. B., Law, R., Tilman, D., Loreau, M., & Gonzalez, A. (2004). The metacommunity concept: A framework for multi-scale community ecology. *Ecology Letters*, *7*(7), 601–613. https://doi.org/10.1111/j.1461-0248.2004.00608.x

Lohmann, A. C., Morton, J. P., Schofield, O. M., & Nowacek, D. P. (2023). Cyclical prey shortages for a marine polar predator driven by the interaction of climate change and natural climate variability. *Limnology and Oceanography*, *68*(12), 2668–2687. https://doi.org/10.1002/lno.12453

Loonen, M., OOSTERBEEK, K., & DRENT, R. (1997). Variation in growth of young and adult size in barnacle geese Branta leucopsis: Evidence for density dependence. *Ardea - Wageningen-*, *85*, 177–192.

Marra, P. P., Cohen, E. B., Loss, S. R., Rutter, J. E., & Tonra, C. M. (2015). A call for full annual cycle research in animal ecology. *Biology Letters*, *11*(8), 20150552. https://doi.org/10.1098/rsbl.2015.0552

Mazerolle, M. J. (2023). *AICcmodavg: Model Selection and Multimodel Inference Based on (Q)AIC(c)* (Version version 4.4.3) [R package]. https://cran.r-project.org/package=AICcmodavg.

Mesquita, M. S., Atkinson, D. E., & Hodges, K. I. (2010). Characteristics and Variability of Storm Tracks in the North Pacific, Bering Sea, and Alaska*. *Journal of Climate*, *23*(2), 294–311. https://doi.org/10.1175/2009JCLI3019.1

Miller, M. R. (1986). Northern Pintail Body Condition during Wet and Dry Winters in the Sacramento Valley, California. *The Journal of Wildlife Management*, *50*(2), 189–198. https://doi.org/10.2307/3801895

Moon, J. A., & Haukos, D. A. (2009). Factors Affecting Body Condition of Northern Pintails Wintering in the Playa Lakes Region. *Waterbirds: The International Journal of Waterbird Biology*, *32*(1), 87–95.

Naves, L., Mengak, L., & Fall, J. (2025). Integrating Indigenous knowledge across homelands and scientific knowledge to support collaborative harvest management for Emperor Goose in Alaska. *Ecology and Society*, *30*(4), art10. https://doi.org/10.5751/ES-16409-300410

Newton, I. (2004). Population limitation in migrants. *Ibis*, *146*(2), 197–226. https://doi.org/10.1111/j.1474-919X.2004.00293.x

NOAA. (1999). *Integrated Surface Data Set: Global Summary of the Day.* (January 2019-August 2025) [Dataset]. National Oceanic and Atmospheric Association: https://www.ncei.noaa.gov/access/search/data-search/global-summary-of-the-day

Norris, D. R., & Taylor, C. M. (2006). Predicting the consequences of carry-over effects for migratory populations. *Biology Letters*, *2*(1), 148–151. https://doi.org/10.1098/rsbl.2005.0397

Osgood, K. E. (2008). *Climate impacts on U.S. living marine resources: National Marine Fisheries Services concerns, activities and needs*. NOAA Fishereies-Office of Science and Technology. https://repository.library.noaa.gov

Overland, J. E., & Wang, M. (2025). Future Climate Change in the Northern Bering Sea. *International Journal of Climatology*, *45*(1), e8697. https://doi.org/10.1002/joc.8697

Paine, R. T. (1966). Food Web Complexity and Species Diversity. *The American Naturalist*, *100*(910), 65–75.

Parnell, A. C., & Inger, R. (2016). *SIMMR: A stable isotope mixing model* (Version 0.5.1.217) [R package].

Peterson, B. J., & Fry, B. (1987). Stable Isotopes in Ecosystem Studies. *Annual Review of Ecology, Evolution, and Systematics*, *18*(Volume 18, 1987), 293–320. https://doi.org/10.1146/annurev.es.18.110187.001453

Phillips, D. L., & Eldridge, P. M. (2006). Estimating the timing of diet shifts using stable isotopes. *Oecologia*, *147*(2), 195–203. https://doi.org/10.1007/s00442-005-0292-0

Pielou, E. C. (1972). Niche Width and Niche Overlap: A Method for Measuring Them. *Ecology*, *53*(4), 687–692. https://doi.org/10.2307/1934784

Post, D. M. (2002). Using Stable Isotopes to Estimate Trophic Position: Models, Methods, and Assumptions. *Ecology*, *83*(3), 703–718. https://doi.org/10.1890/0012-9658(2002)083[0703:USITET]2.0.CO;2

Post, D. M., Layman, C. A., Arrington, D. A., Takimoto, G., Quattrochi, J., & Montaña, C. G. (2007). Getting to the fat of the matter: Models, methods and assumptions for dealing with lipids in stable isotope analyses. *Oecologia*, *152*(1), 179–189. https://doi.org/10.1007/s00442-006-0630-x

Pyke, G. H., Pulliam, H. R., & Charnov, E. L. (1977). Optimal Foraging: A Selective Review of Theory and Tests. *The Quarterly Review of Biology*, *52*(2), 137–154.

R Core Team. (2024). *R: A language and environment for statistical computing.* [Computer software]. https://www.R-project.org/

Rodionov, S. N., Bond, N. A., & Overland, J. E. (2007). The Aleutian Low, storm tracks, and winter climate variability in the Bering Sea. *Deep Sea Research Part II: Topical Studies in Oceanography*, *54*(23–26), 2560–2577. https://doi.org/10.1016/j.dsr2.2007.08.002

Rodionov, S. N., Overland, J. E., & Bond, N. A. (2005). Spatial and temporal variability of the Aleutian climate. *Fisheries Oceanography*, *14*(s1), 3–21. https://doi.org/10.1111/j.1365-2419.2005.00363.x

Roughgarden, J. (1972). Evolution of Niche Width. *The American Naturalist*, *106*(952), 683–718. https://doi.org/10.1086/282807

Salewski, V., & Bruderer, B. (2007). The evolution of bird migration—A synthesis. *Naturwissenschaften*, *94*(4), 268–279. https://doi.org/10.1007/s00114-006-0186-y

Schmutz, J. A., Petersen, M. R., & Rockwell, R. F. (2020). Emperor Goose (Anser canagicus). In S. M. Billerman, B. K. Keeney, P. G. Rodewald, & T. S. Schulenberg (Eds.), *Birds of the World Online*. Cornell Lab of Ornithology. https://doi.org/10.2173/bow.empgoo.01

Sedinger, J. S., & Alisauskas, R. T. (2014). Cross-seasonal effects and the dynamics of waterfowl populations. *Wildfowl*, 277â€“304-277â€“304.

Skalos, D. A., Eadie, J. M., Yparraguirre, D. R., Weaver, M. l., Oldenburger, S. L., Ely, C. R., Yee, J. L., & Fleskes, J. P. (2021). Body Condition of Wintering Pacific Greater White-Fronted Geese. *The Journal of Wildlife Management*, *85*(3), 484–497. https://doi.org/10.1002/jwmg.21997

Stabeno, P. J., Bell, S., Cheng, W., Danielson, S., Kachel, N. B., & Mordy, C. W. (2016). Long-term observations of Alaska Coastal Current in the northern Gulf of Alaska. *Deep Sea Research Part II: Topical Studies in Oceanography, Understanding Ecosystem Processes in the Gulf of Alaska: Volume 1*, *132*, 24–40. https://doi.org/10.1016/j.dsr2.2015.12.016

Stearns, S. C. (1992). *The Evolution of Life Histories*. Oxford University Press.

Stephens, P. A., Houston, A. I., Harding, K. C., Boyd, I. L., & McNamara, J. M. (2014). Capital and income breeding: The role of food supply. *Ecology*, *95*(4), 882–896. https://doi.org/10.1890/13-1434.1

Uher-Koch, B. D., Buchheit, R. M., Eldermire, C. R., Wilson, H. M., & Schmutz, J. A. (2021). Shifts in the wintering distribution and abundance of emperor geese in Alaska. *Global Ecology and Conservation*, *25*, e01397. https://doi.org/10.1016/j.gecco.2020.e01397

USGS. (1995). *Overview of Environmental and Hydrogeologic Conditions near Kodiak, Alaska* (Open-File Report 95–406; Open-File Report).

Vizzini, S., Savona, B., Chi, T. D., & Mazzola, A. (2005). Spatial variability of stable carbon and nitrogen isotope ratios in a Mediterranean coastal lagoon. *Hydrobiologia*, *550*(1), 73–82. https://doi.org/10.1007/s10750-005-4364-2

Votier, S. C., Bearhop, S., MacCormick, A., Ratcliffe, N., & Furness, R. W. (2003). Assessing the diet of great skuas, Catharacta skua, using five different techniques. *Polar Biology*, *26*(1), 20–26. https://doi.org/10.1007/s00300-002-0446-z

Weitzman, B., Konar, B., Iken, K., Coletti, H., Monson, D., Suryan, R., Dean, T., Hondolero, D., & Lindeberg, M. (2021). Changes in Rocky Intertidal Community Structure During a Marine Heatwave in the Northern Gulf of Alaska. *Frontiers in Marine Science*, *8*. https://doi.org/10.3389/fmars.2021.556820

Wiens, J. A. (1989). Spatial Scaling in Ecology. *Functional Ecology*, *3*(4), 385. https://doi.org/10.2307/2389612

Wilson, H. M. (2016). *Distribution and abundance of waterbirds in the Kodiak Archipelago, Alaska winter 2015* [Interim Report for Kodiak Subsistence Regional Advisory Council Meeting]. U.S. Fish and Wildlife Service, Waterfowl Management.

CONCLUSION

The results from this thesis demonstrate that wintering location is an important source of demographic variation in emperor geese. Birds wintering on Shemya consistently had lower apparent survival and lower juvenile-to-adult ratios than those on Kodiak, indicating that not all portions of the winter range contribute equally to population dynamics. These differences were especially pronounced for juveniles, reinforcing the importance of recruitment processes in this long-lived species. Patterns in resource use and body condition were broadly consistent with these demographic differences with birds on Kodiak exhibiting a diet enriched in $\delta^{15}N$ and $\delta^{13}C$, indicating a higher protein and more marine based diet, as well as generally higher body condition. Birds on Shemya appeared to rely on a lower quality base and had lower body condition overall. These results suggest that environmental differences among wintering areas may influence both resource use and individual performance. Survival at both sites was also related to climatic conditions, although the seasonal drivers differed between regions, indicating that broad-scale climate forcing is filtered through local habitat conditions. Notably, conditions on Kodiak in 2025 deviated from other years, with lower $\delta^{15}N$ values, reduced body condition, lower juvenile-to-adult ratios, and the lowest winter ALBSA values observed during the study period. Although based on a single year, this pattern highlights that even more favorable wintering areas may experience periods of reduced habitat quality. These findings provide context for recent shifts in emperor goose winter distribution (*Supplemental Fig. 2.1*). Beyond distributional shifts, an increase in emperor geese in areas like Kodiak may also arise from differences in demographic performance, where birds wintering in more favorable environments contribute disproportionately to future abundance. This work highlights that winter ecology is

not uniform across the emperor goose's range, and that spatial variation in wintering conditions has important implications for survival, recruitment, population dynamics.

Chapter 1 Supplementary Materials

Supplementary Table 1.1. Number of banded emperor geese re-sighted in subsequent winter seasons at (a) Shemya and (b) Kodiak. Values within cells represent the number of bands re-sighted in each later season.

a) **Shemya**

Number of bands deployed	Dec 2022–Jan 2023	Dec 2023–Jan 2024	Dec 2024–Jan 2025	Dec 2025–Jan 2026
Winter 2022 (n = 99)	58	61	55	44
Winter 2023 (n = 24)		9	11	8
Winter 2024 (n = 33)			19	13
Winter 2025 (n = 55)				31
Winter 2026 (n = 27)				

Resight period

b) **Kodiak**

Number of bands deployed	Sep 2020–Apr 2021	Sep 2021–Apr 2022	Sep 2022–Apr 2023	Sep 2023–Apr 2024	Sep 2024–Apr 2025	Sep 2025–Apr 2026
Winter 2020 (n = 45)	25	32	28	26	23	12
Winter 2022 (n = 50)			39	32	28	23
Winter 2023 (n = 87)				71	69	57
Winter 2024 (n = 12)					8	5
Winter 2025 (n = 108)						82
Winter 2026 (n = 175)						

Resight period

Supplementary Table 1.2. Annual observer effort at Kodiak and Shemya wintering sites, summarized as the number of days emperor goose resights were reported and the number of observers contributing reports each winter season, which included the 3-week band re-sight survey period as well as auxiliary reports from each site.

Site	Resight Season	Days with Resights	Number of Observers
Kodiak	Aug 2020–Apr 2021	35	6
Kodiak	Aug 2021–Apr 2022	52	5
Kodiak	Aug 2022–Apr 2023	39	4
Kodiak	Aug 2023–Apr 2024	55	5
Kodiak	Aug 2024–Apr 2025	63	11
Kodiak	Aug 2025–Apr 2026	33	8
Shemya	Dec 2022–Jan 2023	11	3
Shemya	Dec 2023–Jan 2024	31	3
Shemya	Dec 2024–Jan 2025	20	2
Shemya	Dec 2025–Apr 2026	32	4

Supplementary Table 1.3. Standardized seasonal ALBSA climate index values (z-scores) used as environmental covariates in Cormack–Jolly–Seber survival models for emperor geese wintering at Shemya and Kodiak, Alaska. Values were standardized within site and season (mean = 0, SD = 1), with positive values indicating above-average conditions and negative values indicating below-average conditions relative to the site-specific seasonal mean.

Site	Year	Summer[1]	Fall[2]	Winter[3]	Spring[4]	Annual[5]
Shemya	2022	-1.38	1.33	0.66	-0.52	1.34
	2023	0.30	0.13	1.06	0.56	0.18
	2024	0.08	-0.46	-0.44	1.08	-0.85
	2025	1.00	-1.00	-1.34	-1.12	-0.67
Kodiak	2020	-1.87	-1.28	1.17	-0.49	-0.20
	2021	0.27	-1.10	0.37	-1.00	-0.71
	2022	-0.32	0.22	-0.56	0.74	1.82
	2023	0.56	0.80	0.82	1.59	0.45
	2024	0.44	1.20	-0.23	0.69	-0.79
	2025	0.92	0.16	-1.56	-0.64	-0.56

Seasonal bins were defined to reflect regional phenology and migration timing:

[1]Summer = June–August at both sites

[2]Fall = September–November at Shemya and September at Kodiak

[3]Spring = April–May at Shemya and May at Kodiak

[4]Winter = December–March at Shemya and October–April at Kodiak

[5]Annual values represent April–March conditions at both sites

Supplementary Table 1.4: Pearson correlation matrices among prior seasonal and annual Aleutian Low–Beaufort Sea Anticyclone (ALBSA) indices used as climate covariates in apparent survival models for emperor geese wintering at (a) Shemya and (b) Kodiak, Alaska. Values represent correlations among standardized site-specific ALBSA seasonal bins aligned to the subsequent annual survival interval.

a) Shemya Seasonal Bins	$ALBSA_{Prior\ Winter}$	$ALBSA_{Prior\ Fall}$	$ALBSA_{Prior\ Spring}$	$ALBSA_{Prior\ Summer}$	$ALBSA_{Annual}$
$ALBSA_{Prior\ Winter}$	1.00	-0.38	0.16	-0.60	-0.02
$ALBSA_{Prior\ Fall}$	-0.38	1.00	0.77	0.63	0.16
$ALBSA_{Prior\ Spring}$	0.16	0.77	1.00	0.20	0.54
$ALBSA_{Prior\ Summer}$	-0.60	0.63	0.20	1.00	-0.20
$ALBSA_{Annual}$	-0.02	0.16	0.54	-0.20	1.00

b) Kodiak Seasonal Bins	$ALBSA_{Prior\ Winter}$	$ALBSA_{Prior\ Fall}$	$ALBSA_{Prior\ Spring}$	$ALBSA_{Prior\ Summer}$	$ALBSA_{Annual}$
$ALBSA_{Prior\ Winter}$	1.00	0.80	0.37	-0.62	0.74
$ALBSA_{Prior\ Fall}$	0.80	1.00	0.00	-0.94	0.96
$ALBSA_{Prior\ Spring}$	0.37	0.00	1.00	-0.04	-0.26
$ALBSA_{Prior\ Summer}$	-0.62	-0.94	-0.04	1.00	-0.84
$ALBSA_{Annual}$	0.74	0.96	-0.26	-0.84	1.00

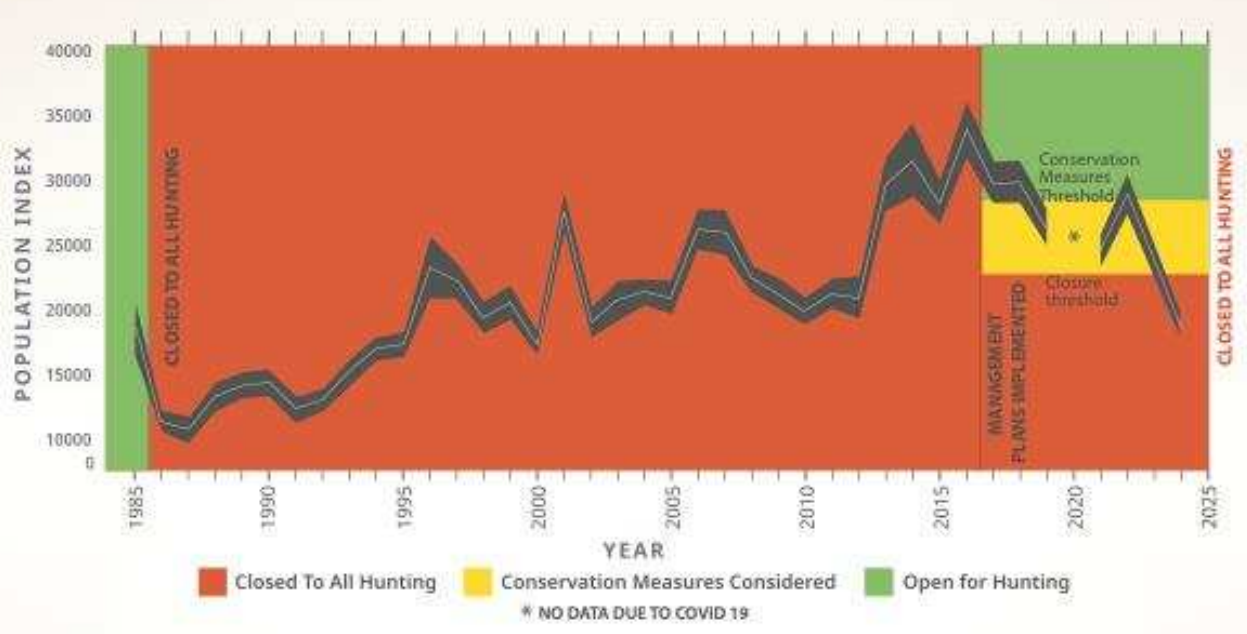

Supplementary Figure 1.1: Emperor Goose abundance index based on primary management spring surveys from 1984-2024, excluding 2019/2020. Adapted from Waterfowl population status, publication date July, 2024 (Frost et al., 2024b).

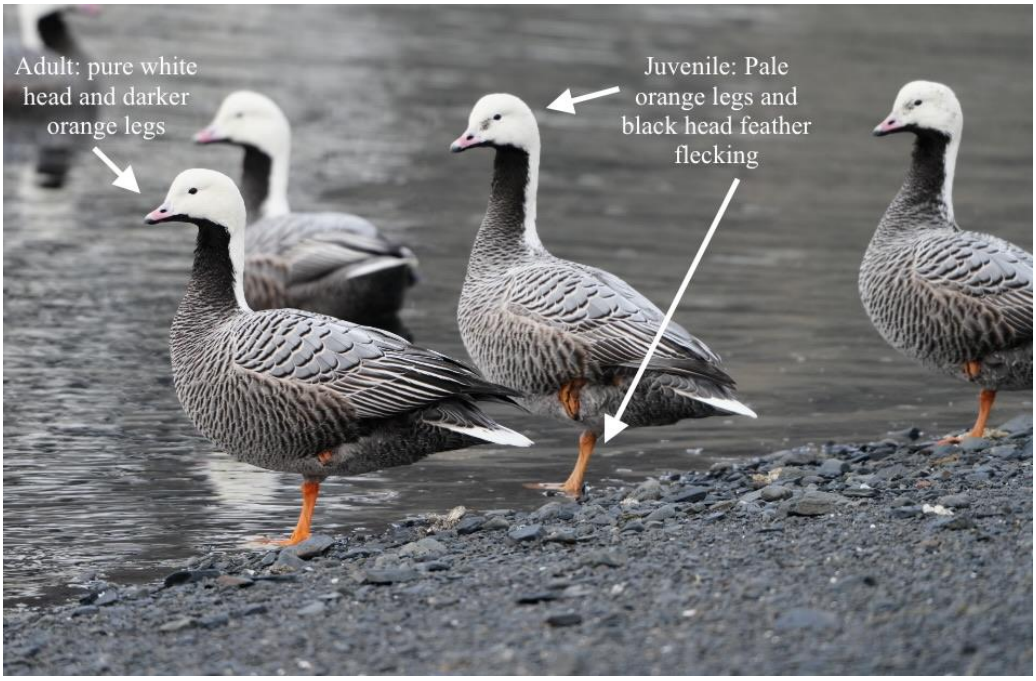

Supplementary Figure 1.2: Head plumage and leg color differences in emperor goose age classes.

Supplementary Figure 1.3: Emperor Goose adult with a metal USGS band on left leg and a uniquely coded plastic field-readable band on right leg.

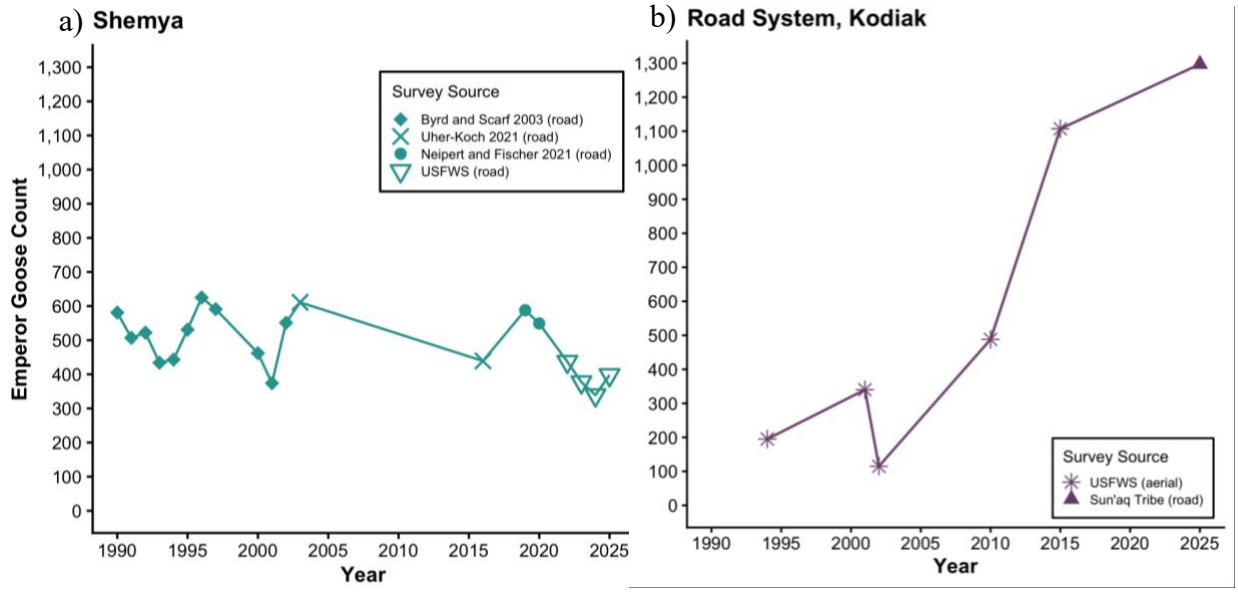

Supplementary Figure 1.4. Historical counts of Emperor Geese observed during winter surveys at (a) Shemya and (b) Kodiak. Counts are compiled from multiple survey efforts and methods, as indicated by symbol type. These data are presented descriptively to illustrate broad changes in winter distribution and are not standardized estimates of total abundance.

Chapter 2 Supplementary Materials

Supplementary Table 2.1: Winter weather at Kodiak and Shemya across study years (November–April). Values represent mean ± SD for minimum, maximum, and mean temperatures (°C), mean windspeed and maximum sustained windspeed (kts), and average daily precipitation (cm). Total precipitation is reported as the cumulative precipitation over each winter period. Weather data were derived from daily runway observations obtained through the NOAA Global Surface Summary of the Day.

Site	Winter	Minimum Temp. (°C)	Maximum Temp. (°C)	Mean Temp. (°C)	Mean Windspeed (kts)	Maximum Sustained Windspeed (kts)	Daily Precip. (cm)	Total Precip. (cm)
Shemya	2022-2023	-0.3 ± 2.8	3.7 ± 2.1	1.8 ± 2.1	17.9 ± 6.7	28.5 ± 9.4	0.25 ± 0.56	44.7
Shemya	2023-2024	-1.3 ± 3.0	3.3 ± 2.4	1.3 ± 2.4	17.9 ± 7.2	28.8 ± 9.3	0.13 ± 0.28	21.8
Shemya	2024-2025	0.0 ± 2.8	4.2 ± 1.7	2.3 ± 2.0	15.8 ± 7.2	29.6 ± 11.1	0.18 ± 0.33	27.9
Kodiak	2019-2020	-2.6 ± 3.8	5.0 ± 2.5	1.4 ± 2.9	9.7 ± 5.1	19.7 ± 7.6	0.66 ± 0.99	117.3
Kodiak	2020-2021	-3.1 ± 5.1	4.6 ± 4.3	0.9 ± 4.4	9.5 ± 5.0	18.3 ± 7.4	0.48 ± 0.94	86.4
Kodiak	2021-2022	-2.7 ± 3.4	4.9 ± 2.6	1.2 ± 2.9	9.8 ± 5.3	18.8 ± 7.9	0.41 ± 0.74	72.4
Kodiak	2023-2024	-3.4 ± 4.9	4.2 ± 3.6	0.5 ± 4.2	9.5 ± 4.6	18.4 ± 6.4	0.61 ± 1.19	110.7
Kodiak	2024-2025	-1.1 ± 3.6	5.9 ± 2.7	2.7 ± 3.0	10.2 ± 5.2	18.8 ± 7.4	0.76 ± 1.17	134.1